NOTICE

AVIS

Canada

UNIVERSITY OF ALBERTA

CRANIOFACIAL RELATIONSHIPS AND TMJ LOADING

BY

RAYMOND TONY MAH

A THESIS SUBMITTED TO THE FACULTY OF GRADUATE STUDIES AND RESEARCH IN PARTIAL FULFILLMENT OF THE REQUIREMENTS FOR THE DEGREE OF MASTERS OF SCIENCE

IN

MECHANICAL ENGINEERING

DEPARTMENT OF MECHANICAL ENGINEERING

EDMONTON, ALBERTA, CANADA

SPRING 1992

Canadä

UNIVERSITY OF ALBERTA

RELEASE FORM

NAME OF AUTHOR: RAYMOND TONY MAH
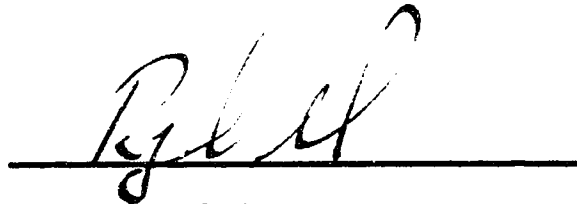
TITLE OF THESIS: CRANIOFACIAL RELATIONSHIPS AND TMJ LOADING

DEGREE: MASTERS OF SCIENCE IN MECHANICAL ENGINEERING

YEAR THIS DEGREE GRANTED: 1992

PERMISSION IS HEREBY GRANTED TO THE UNIVERSITY OF ALBERTA TO REPRODUCE SINGLE COPIES OF THIS THESIS AND TO LEND OR SELL SUCH COPIES FOR PRIVATE, SCHOLARLY OR SCIENTIFIC RESEARCH PURPOSES ONLY.

THE AUTHOR RESERVES ALL OTHER PUBLICATION AND OTHER RIGHTS IN ASSOCIATION WITH THE COPYRIGHT IN THE THESIS, AND EXCEPT AS HEREINBEFORE PROVIDED NEITHER THE THESIS NOR ANY SUBSTANTIAL PORTION THEREOF MAY BE PRINTED OR OTHERWISE REPRODUCED IN ANY MATERIAL FORM WHATEVER WITHOUT THE AUTHOR'S PRIOR WRITTEN PERMISSION.
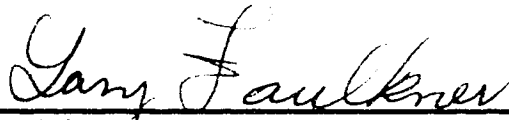
APT. 80, 1055 E. EVELYN AVENUE
SUNNYVALE, CA, USA
94086

DATE: APRIL 10, 1992
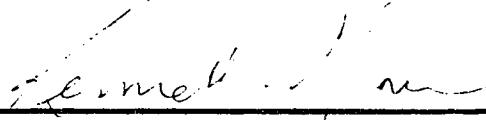
University of Alberta

Faculty of Graduate Studies and Research
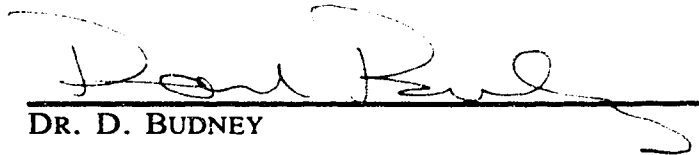
The undersigned certify that they have read, and recommend to the Faculty of Graduate Studies and Research for acceptance, a thesis entitled **Craniofacial Relationships and TMJ Loading** submitted by **Raymond Tony Mah** in partial fulfillment of the requirements for the degree of **Masters of Science in Mechanical Engineering**.

_____
Dr. M.G. Faulkner

_____
Dr. K. Glover

_____
Dr. D. Budney

DATE: April 10, 1992

To my Mom and Dad

ABSTRACT

The purpose of this investigation was to compare several numerical models of the human temporomandibular joint loading and then use these to analyze the mechanical effects of craniofacial morphologies on TMJ loading. Data from sixty-eight previously digitized human skulls were used to obtain the three dimensional spatial information needed for the study.

The majority of the models used forms of biological optimizing criteria with linear programming to predict the muscular tensions for each skull. The pragmatic model, however, assumed that experimental findings of the relative muscle forces would be constant for each skull. Although the models varied in technique, the results did not differ significantly. All models showed that the balancing condyle is loaded heavier than the working side and the sum of the joint loads is about 110% of the total occlusal force. The optimized models permitted full muscle saturation which did lead to erroneous results. They also showed that the maximum bite and contralateral joint loads were abnormally higher than previous clinical studies have shown. The pragmatic model tended to equalized the joint loads whereas the linear programming models loaded the balancing joint up to five times higher than the working temporomandibular joint.

When linearly correlated to the facial classifications, the results from these models showed poor results. Products of correlation, R^2, were on average less than 10%. There were slight indications that individuals with long chins and "square faced" individuals (viewed laterally) had lower resultant joint loads than the norm while at the same time being able to generate slightly higher bite forces.

ACKNOWLEDGMENTS

TABLE OF CONTENTS

TABLE OF CONTENTS

TABLE OF CONTENTS

LIST OF TABLES

LIST OF FIGURES

LIST OF FIGURES

PAGE

INTRODUCTION AND
LITERATURE REVIEW

1.1 Introduction

Due to its versatile movement, diverse functions and anatomical complexity, the temporomandibular joint (TMJ) is one of the most complex joint in the human body. It forms a major part of the masticatory system which can be regarded as the primary stage of the digestive system and incorporates a variety of functions including speech. Loads imposed on the mandible and dentition can cover a large range. It is believed that difficulties arise when the TMJ is abnormally loaded and the functional capacities of the joint tissues exceed their ability to adapt. The large number of TMJ dysfunctions seen clinically has prompted researchers to further define and understand the characteristics of the joint in normal and abnormal situations.

1.2 Dysfunction of the TMJ and Its Research Motivations

The temporomandibular joint has been of increasing interest to dental and engineering researchers as the complex problems associated with the function of the jaw are being

1

increasingly revealed. The majority of temporomandibular joint pain cases can be characterized as **Pain Dysfunction Syndrome** and are usually characteristic of younger patients. **Osteoarthritis**, a degenerative joint disease, is another complication which alters the function of the TMJ. This condition, which generally affects an older age group, degrades articular surfaces of a joint which subsequently leads to an uncontrolled remodelling of the underlying bone. TMJ crepitation, an grating uneven translatory motion of the mandible, is the most reliable clinical sign of osteoarthritis and has been found in nearly 25% of a Swedish population tested [Hansson and Milner, 1975]. While each case may not develop into complete TMJ dysfunction, there are a considerable number of individuals that do experience intense levels of debilitating joint and muscle pain associated with the masticatory system. Both pain dysfunction and osteoarthritis can be traced to repetitive overloading of the joint tissues [Ogus, 1979]. This biomechanical abuse of joints causes the articular tissues of the opposing bones to break down. The primary mechanical functions of these articular surfaces is to reduce the shear forces between the translating bones and to dissipate the existing joint loads over a larger area effectively reducing the localized stresses. When these tissues fail to perform their functions, local stresses in the underlying bone are raised inducing osseous tissue (bone) remodelling.

It is commonly believed that certain individuals may be more prone than others to pain dysfunction syndrome based on facial shape. Clinically, there is an assumed relationship between craniofacial form and masticatory function which represents the

basis for many clinical treatment rationales. Validity of this assumption however has yet to be thoroughly tested. The ability to predic the type(s) of facial morphologies which may be more susceptible to damaging of the joint tissues would be of great value. Both empirical clinical research and mathematical modelling can assist each other in determining if a relationship truly exists.

A brief review of both experimental work and mathematical modelling shows very diverse research approaches which attempt to unravel the complexities of the human temporomandibular joint.

1.3   Literature Review

There has been considerable recent interest in determining whether it is the form or the function of the TMJ that causes dysfunction. Does the shape of the facial region lead to unsuitable loading conditions or is the way people chew that is the major factor in the health of the temporomandibular joint tissues? The last decade has seen several advances in attempting to answer these questions. This section reviews the recent history of methods used to determine the TMJ loading characteristics.

1.3.1   Theories of TMJ Loading

Until relatively recently, many researchers strongly believed that the TMJ was an unloaded joint [eg. Robinson, 1946; Tattersall, 1973; Wilson, 1920]. This was commonly held since the condyle (ball shaped portion of the jaw joint) sits in a socket shaped cavity called the glenoid fossa which separates the joint cavity from the cranial vault through a very thin portion of bone. Because of its frailty, early investigators

concluded that it could support no significant loading. It was believed that the bite force was generated by the muscles pulling to create one resultant muscle vector that would be equal and opposite to the occlusal force. This would, in effect, alleviate the need for balancing forces provided by the joint. From these postulations, it appeared entirely possible that the temporomandibular joint was an unloaded joint.

This theory, however, has been strongly challenged by several researchers who utilized both experiment and by numerical modelling [eg. Barbenel, 1972, 1974; Gingerich, 1979; Gysi, 1921; Hay, 1985; Hylander, 1975, 1979; Kang, 1989; Koolstra, Van Eijden, Weijs, Naeije, 1988; Nickel, McLachlan, Smith, 1988; Osborn, Baragar, 1985; Ralph, Caputo, 1975; Smith, McLachlan, McCall, 1986; Standlee, Caputo, Ralph, 1989; Throckmorton, G.S., Throckmorton, L.S., 1985[1], 1985[2]]. They reasoned, and showed, that the joint load reacts through a curved portion of the cranial base called the articular eminence rather than the thin glenoid fossa. The eminence is comprised of a thicker dense bone capable of withstanding larger loads. *In vitro* experiments with adult and adolescent *Macaca fascicularis* and *Macaca mulatta* (monkeys) to determine mandibular bone strain (rosette strain gauges placed on the condylar neck) showed that the TMJ is compressively loaded during the power stroke of mastication, incision of food, and during isometric (nonmoving) molar and incisor biting [Hylander, 1979]. These stress patterns have been visually shown on a *photoelastic resin mandible* under normal loading conditions during an analysis called photoelastic stress analysis [Ralph

et al., 1975]. Methods such as these have proved useful in understanding the ways in which loads in the human jaw are carried and transmitted.

The joint loading directions may be as important as their magnitudes. The glycosaminoglycan content of articular discs removed from patients with TMJ dysfunction was investigated [Blaustein, Scapino, 1986; Scapino, 1983] since the compressive stiffness of articular cartilage is related to this content. It was found that where the retrodiscal tissues and posterior band of the capsule met there was significant remodelling to an abnormal loading situation. They only had a small sample (9 discs) but this research does suggest that the posterosuperiorly directed TMJ loads on the disc may lead to joint dysfunction. Due to the difficulties of measuring the TMJ loading directions accurately, numerical modelling is presently being utilized for this task.

1.3.2 Modelling the Temporomandibular Joint

There are several types of mathematical models to determine the occlusal and joint loads but different methodologies do not allow easy comparisons. Numerically modelling the TMJ requires several assumptions concerning how the jaw will function during mastication. Simple two dimensional models [Barbenel, 1972, 1974; Smith, 1978] have helped to understand the lever mechanics of the jaw but do not describe its full function. Forceful unilateral occlusion (biting on one side) is the most common chewing scenario; therefore, the mandible must be treated as a truly three dimensional entity.

Current researchers have employed several sophisticated three dimensional models to calculate the joint loads based on skeletal information. According to some biological

optimizing criteria, there is the prediction that the muscles will act to: 1) minimize the sum of the total muscle forces[1] [Osborn et al., 1985]; 2) minimize the total TMJ load [Smith et al., 1986]; 3) minimize the maximum relative muscle force[2] [Koolstra et al., 1988]; 4) minimize the muscular stress in the maximum stressed muscle[3] [An, Kwak, Chao, Morrey, 1984; Kang, 1989]. Other approaches have instead used predetermined muscle forces to achieve the necessary bite forces [Faulkner, Hatcher, Hay, 1987; McEvoy, 1989]. Experimental muscle data was used to provide relative muscle tensions based on the occlusal position studied. Due to the intrinsic complexity of the TMJ, all of these models must intentionally limit the forces generated to be within biological boundaries.

1.3.3 Biological Limitations

Muscular and skeletal limits to these models are supplied by experimental *in vivo* data. Electrodes placed on the skin surface or injected into the belly of the muscle to be investigated can estimate its electrical activity. This technique, called electromyography or **EMG**, demonstrates that the greater the muscle activity, the greater the generated muscle force [eg. Pruim, DeJongh, Ten Bosch, 1978; Kawazoe, Kotani, Hamada, 1979]. An example of a skeletal constraint was a study of mandibular strength [Hylander, 1975]. The required force to bend and break the mandibular neck on an average skull was 610

---

[1]Based on a *total energy use* criterion

[2]*Relative muscle force* is defined as the muscle force, F_i, relative to its predetermine maximum, F_{max_i}

[3]*Muscular stress* is the muscle force, F_i, divided the muscle's physiological crossectional area, $PCSA_i$, the muscle's power producing area

N. Occlusal limitations [Pruim et al., 1978] have been determined using bite force transducers. It has not yet been possible to entirely formulate a numerical model or technique that predicts the function of the TMJ without using biological constraints.

1.3.4 Facial Considerations

Correlations between dental and facial characteristics are widely used as diagnostic tools in various dental treatment rationales. Clinically, there is anecdotal evidence that patients with short mandibles (ANB angles greater than 5° - see Chapter 2) present proportionally more problems associated with their TMJs. There was also some evidence of this predisposition to higher loads shown in the investigation of the 68 skulls by McEvoy [1989].

Facial classifications such as cephalometric[s] reference planes have been shown to be inappropriate when attempting to imply functional traits [Iwasaki, 1987]. Long and short facial height ratios[ss] were correlated with results from a TMJ model minimizing total joint load [Iwasaki, 1987]. The results showed that for given biting conditions, the jaw mechanics for the two groups showed very little difference. This result is somewhat at odds with commonly held beliefs. The following includes an additional attempt to assist with answering this question.

---

[s]Radiographic analysis of reference planes and occlusal structures

[ss]Ratio based on *Lower Anterior Facial Height* (distance between Menton and Anterior Nasal Spine) over the *Total Anterior Facial Height* (distance between Nasion and Menton), see Chapter 2 for landmark explanations

1.4   A Guide to the Thesis

The chapters to follow have three main objectives. Chapter 2 describes the anatomy of the temporomandibular joint and its associated structures along with an explanation of some of the facial classifications presently used as clinical treatment tools. These classifications for the 68 skull sample are cross correlated to determine whether the schemes are related. Chapter 3 examines recent numerical modelling techniques of the TMJ. These models are compared using data obtained from a single skull which allows differentiation of only the methods themselves. Chapter 4 combines Chapters 2 and 3 by correlating the facial classifications with the results from each of the models to determine if facial morphology can be used in clinical practice. Finally, Chapter 5 discusses the conclusions to be drawn from the findings as well as it addresses areas which merit further investigation.

ANATOMY OF THE TMJ AND CRANIOFACIAL MORPHOLOGY

2.1   Introduction

This chapter will attempt to explain the medical terminology and anatomy relevant to the numerical modelling of the TMJ. In addition, a comprehensive description of existing classification schemes will be done to segregate cranial morphologies. These classifications can then be used to look for mechanical differences between facial and skeletal types.

2.1   Basic Terminology

A standardized and universally accepted terminology in anatomy allows the identification and description of structures from various other parts of the body to relate the position of these named structures to the rest of the body in a consistent manner. For this purpose the skull is separated into various anatomical reference planes (Figure 2.1). The **midsagittal** or median plane separates the skull vertically into right and left halves. Any plane parallel to this is termed a parasagittal plane. The **coronal** plane is a vertical
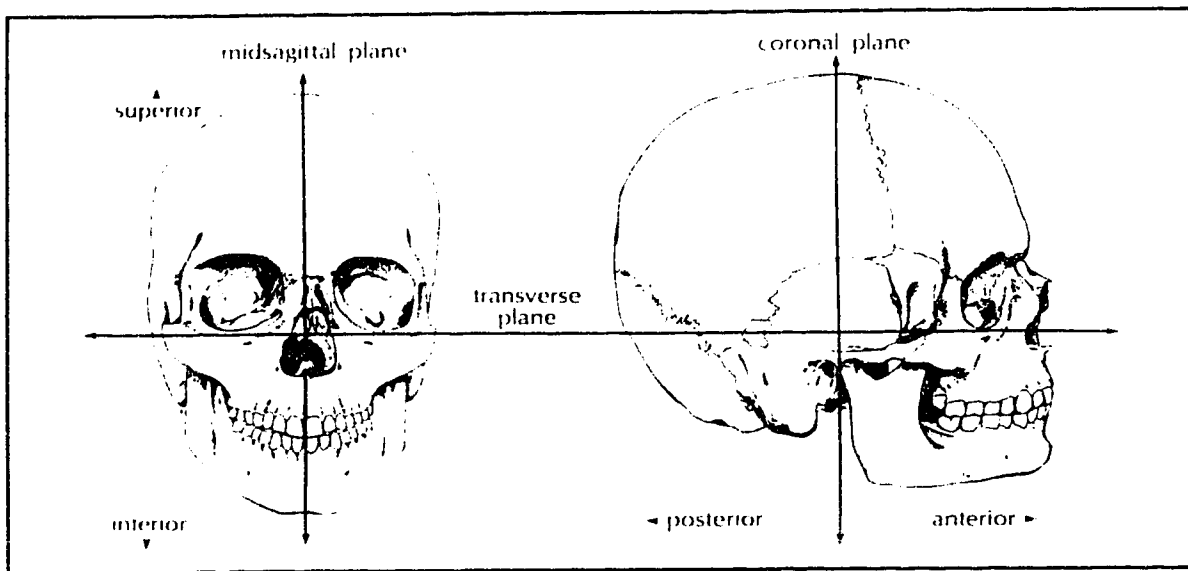
Figure 2.1 Anatomical Reference Planes

plane perpendicular to the sagittal plane. A transverse plane or horizontal plane is any

plane at right angles to both coronal and sagittal planes.

Related to these planes are the following paired descriptive terms:

1) Superior - toward the top of the head
   Inferior   - towards the chin

2) Medial   - toward the midsagittal plane
   Lateral   - away from the midsagittal plane

3) Anterior   - toward the front of the head
   Posterior - towards the back of the head

These terms will be used extensively when discussing TMJ loading directions.

When referring to the dentition, special terms are employed. Figure 2.2 shows a

superior view of the mandible relating some of the terminology associated with the teeth.

Lingual represents a position closer to the tongue while *buccal* would be toward the

cheek and lips. A *mesial* direction is toward the incisors (front teeth) and *distal* towards

the molar region.
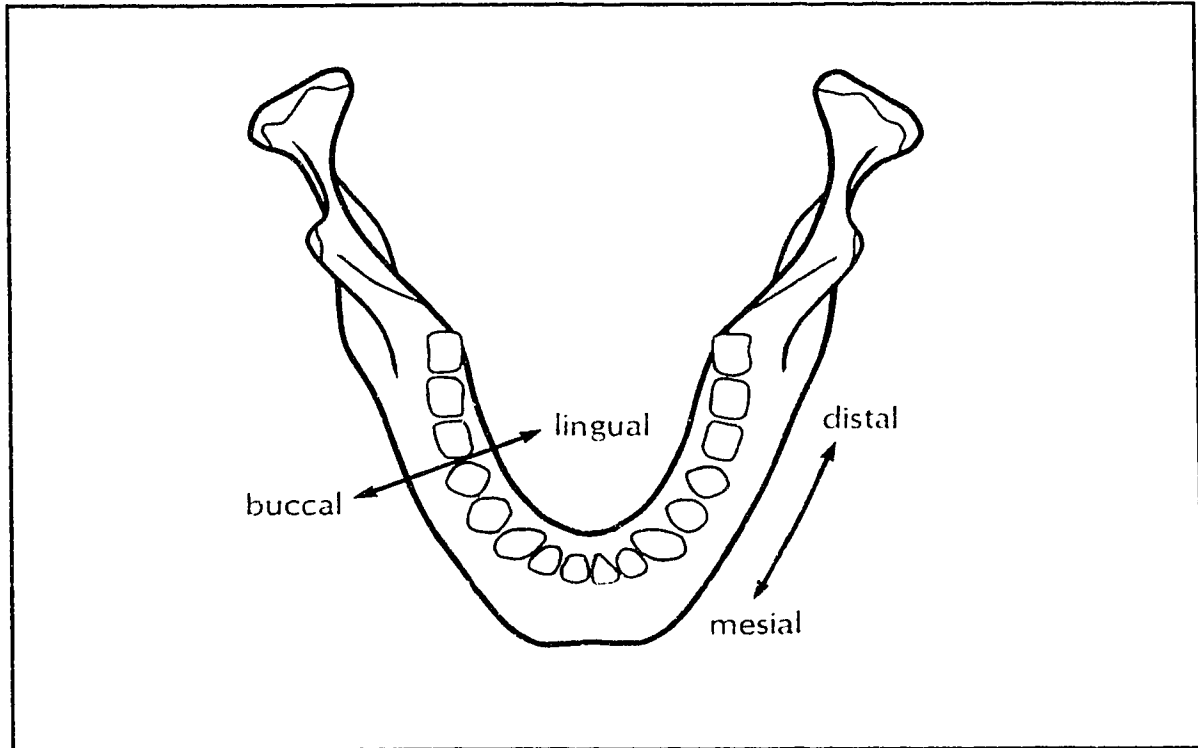
Figure 2.2 Occlusal Reference Directions

Other terms describing anatomical positioning are:

1) Superficial   - closer to the skin surface
   Deep   - further from the skin surface

2) Ipsilateral - the same or *working* side of the body
   Contralateral - the opposite or *balancing* side of the body

These terms will be used extensively to 1) describe muscles and 2) discuss

craniomandibular joint loading characteristics.

2.3 Functional Anatomy of the Skull

To understand the biomechanics of the temporomandibular joint it is important to discuss the form and function of the entire masticatory (chewing) apparatus which is primarily composed of osseous (bone), muscular, and connective (ligament) tissues as well as dentition. Each of these components and their corresponding relationships is be discussed in the following sections to explain the mechanical nature of the human temporomandibular joint.

2.3.1 Skeletal Anatomy

The human skull is comprised of several relatively rigidly connected bones which supply structural support and muscle attachment sites as well as surfaces for joint articulation for the masticatory system (Figure 2.3). All skeletal bone consists of an outer dense bone called cortical bone while internally consisting of a softer network of trabecular bone. The cortical bone can take large loads while the main structural purpose of the trabecular bone is to transfer and distribute the loads evenly.

The **temporal** bone is one of the most versatile bones in the skull because it provides the articular surfaces of the TMJ, located on the anterior aspect of the glenoid fossa, as well as partially supporting attachments for the temporalis and masseter muscles. The **parietal, frontal,** and **zygomatic** bones provide the remaining attachment sites for these muscles.

The **sphenoid** bone lies in the middle of the cranial fossa (base of the cranium). This bone articulates with nearly all the other bones of the skull and its foremost function in

the masticatory system is to provide the inserts for the pterygoid muscles (discussed in Section 2.3.2).

The **maxilla** (upper jaw) and the **mandible** (lower jaw) incorporate the dentition
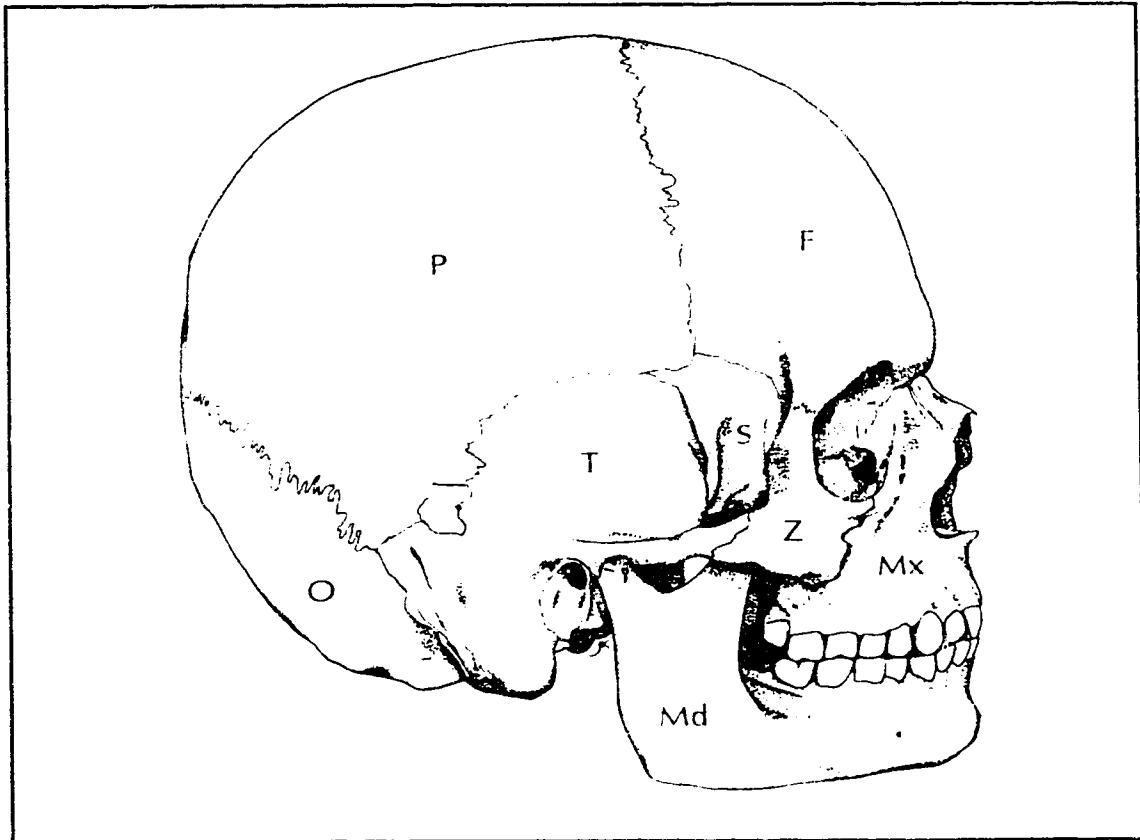
Figure 2.3 Lateral View of the Skull showing the bones of the skull: (F) Frontal, (Md) Mandible, (Mx) Maxilla, (P) Parietal, (O) Occipital, (S) Sphenoid, (T) Temporal, (Z) Zygomatic

and their primary function is to support these teeth and the occlusal loads imposed on them. The teeth are supported in the boney sockets by **periodontal ligaments** (multi-dimensional fibrous network limiting movement by torsion, tension or compression) that join the root surface to the underlying bone. During forceful occlusal contact, the forces

are transferred from the dentition by these ligaments to the thin socket of cortical bone then into the inner network of trabecular bone.

The mandible is comprised of the **body** and the **ramus**. The body of the mandible supports the dentition while the ramus accommodates the insertion sites for the primary muscles of mastication (refer to section 2.3.2 for details), the **coronoid process**, and the **condyle**. These can be seen in a simple lateral view of the mandible (Figure 2.4).

The medial perspective shows the **mandibular foramen** (opening for major nerves and blood vessels), the **gonion**, and the **sigmoid notch** while the cut section reveals the cortical and trabecular bone. A superior view of the mandible displays the lower dental arch consisting of the following dentition (single side, front to back):

1) Central Incisor, **CI**
2) Lateral Incisor, **LI**
3) Canine, **C**
4) 1st Premolar, **PM1**
5) 2nd Premolar, **PM2**
6) 1st Molar, **M1**
7) 2nd Molar, **M2**
8) 3rd Molar (Wisdom tooth), **M3**

where the first three represent anterior teeth and the remaining are termed posterior teeth. Occlusal loading in the molar region, (particularly M1), will be the only region investigated since it is occlusion in this region that results in the most frequent and demanding loads on the TMJ. The posterior view of the mandibular ramus (lower right, Figure 2.4) shows the head and neck of the condyle. Notice that the head is often cylindrical in shape being expanded mediolaterally but narrow anterioposteriorly. Its long axis is not quite in the transverse (horizontal) plane but is directed somewhat
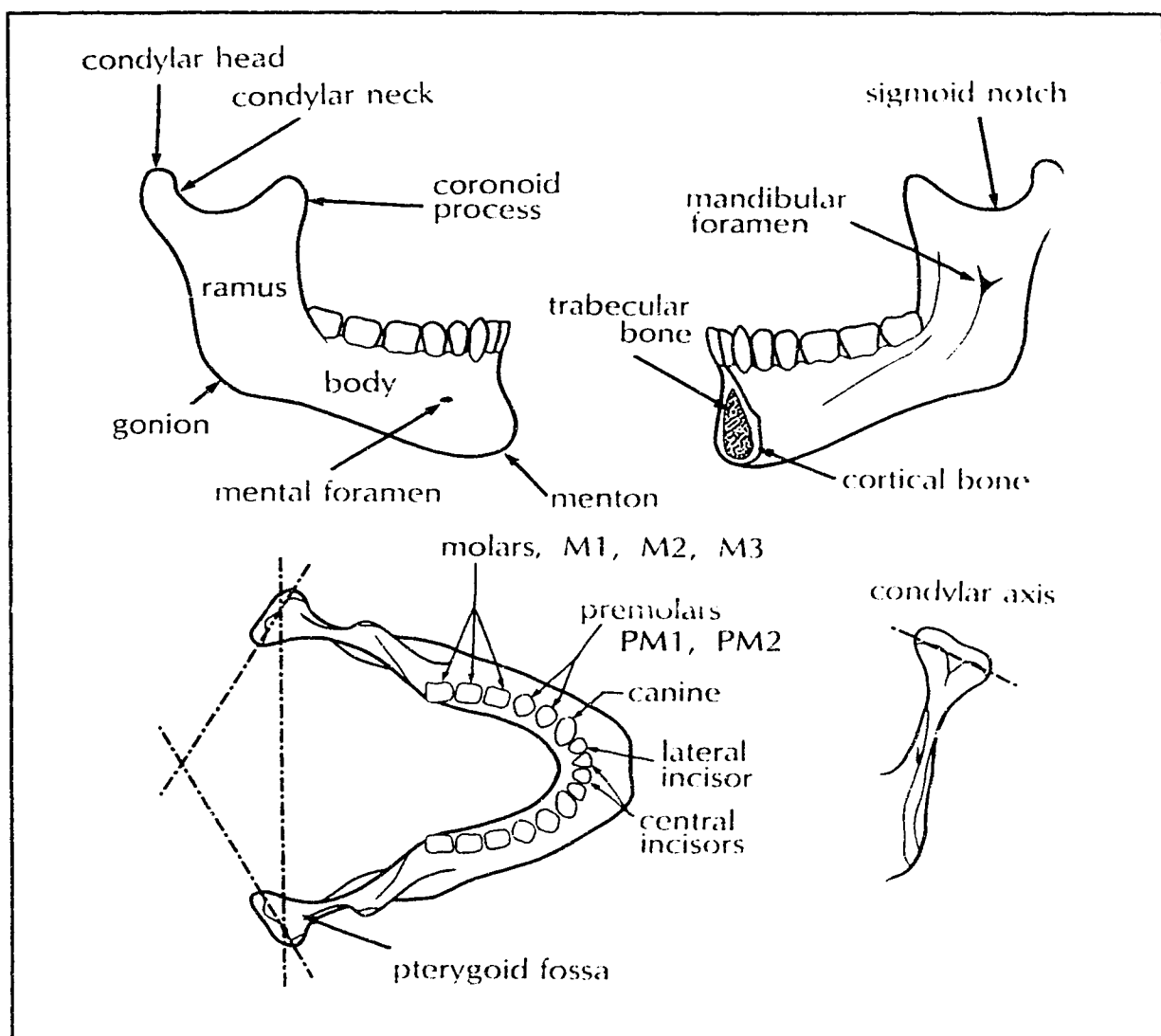
Figure 2.4 Lateral (upper left), Medial (upper right), and Superior (lower left) views of the mandible. Also shown (lower right) is the posterior border of the ramus, condylar neck and head of the mandible.

medioposteriorly. The superior and anterior surfaces of the condyle are covered with fibrocartilage or fibrous connective tissue and articulate with the articular surfaces of the anterior glenoid fossa.

2.3.2 Musculature

Movements of the jaw are brought about by the muscles of mastication which are of different sizes and shapes therefore enabling different activation resultants. For example, *longitudinal* or *strap* muscles (long rectangular shaped muscles) are designed to operate over a large range of extension. When activated, they can easily be modelled mechanically as a single force vector acting from an origin (the least movable of two muscle attachment points, on the skull) to an insertion (muscle attachment point that moves, on the mandible). A more complicated muscle would be a *fan shaped* muscle with its typical fan shaped origin while its insertion can be represented as a point. This type of muscle does not have the range of motion of a longitudinal muscle but its fan shape provides more control-type properties as it is able to activate various portions of the fan at differing levels. These types of muscles are best modelled by dividing it into sections. The primary muscles of mastication are listed as follows:

1) Temporalis
2) Deep Masseter
3) Superficial Masseter
4) Medial Pterygoid
5) Lateral Pterygoid

The fan shaped **temporalis** muscle originates from the lateral surfaces of the parietal, temporal, and frontal bones and inserts onto the anterior, superior, and posterior medial borders of the coronoid process (Figure 2.5). Its muscle fibers converge and pass between the lateral surface of the skull and the posterior root of the zygomatic arch.
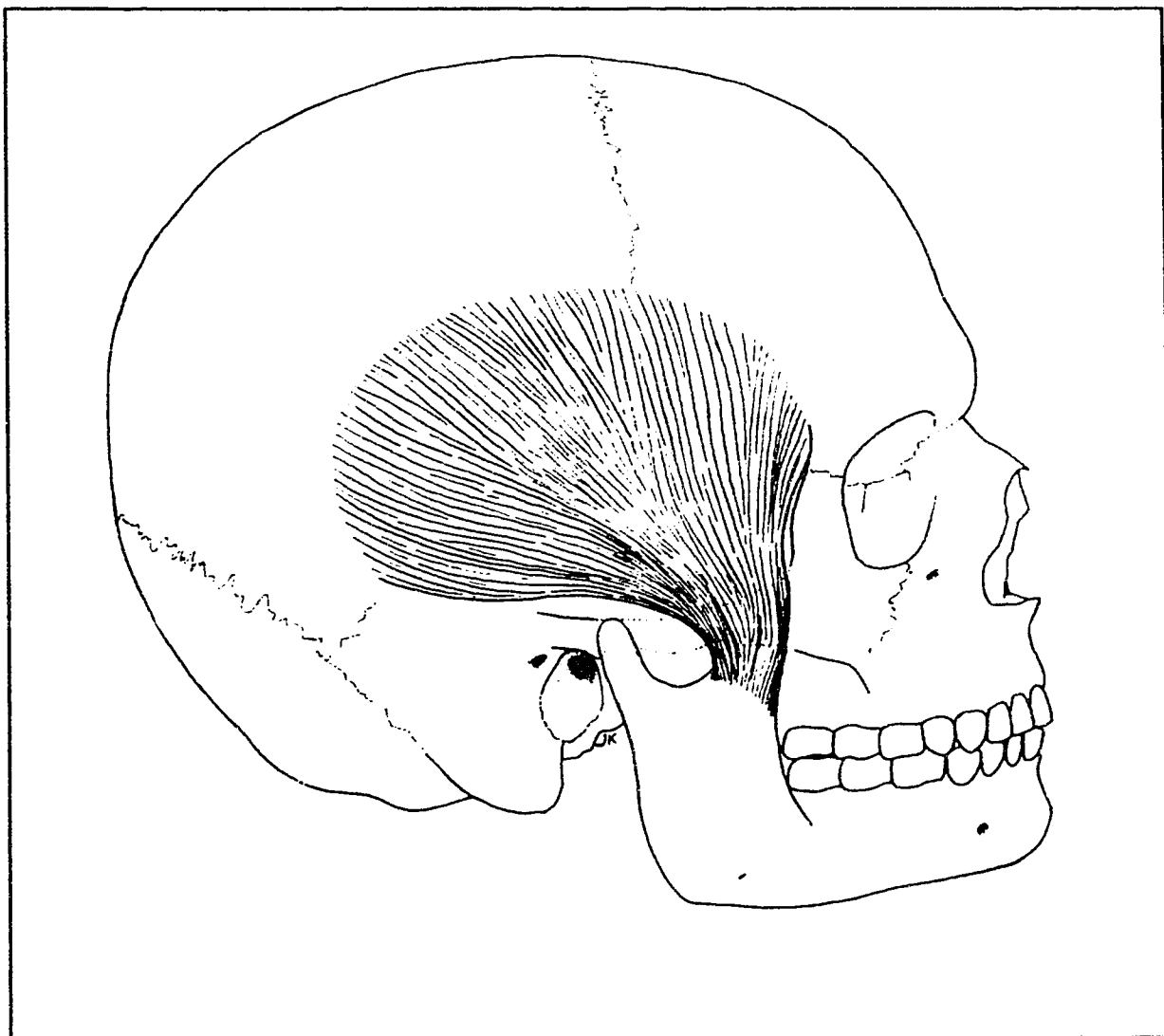
Figure 2.5 Temporalis Muscle

The **deep** and **superficial masseter** muscles are examples of longitudinal muscles. They both originate at the lower anterior portion of the zygomatic arch and insert on the lateral external surface of the mandibular ramus (Figure 2.6). The superficial masseter lies closer to the skin and originates more anterior than the deep masseter. The **medial pterygoid**, a longitudinal muscle, originates from the medial surface of the lateral
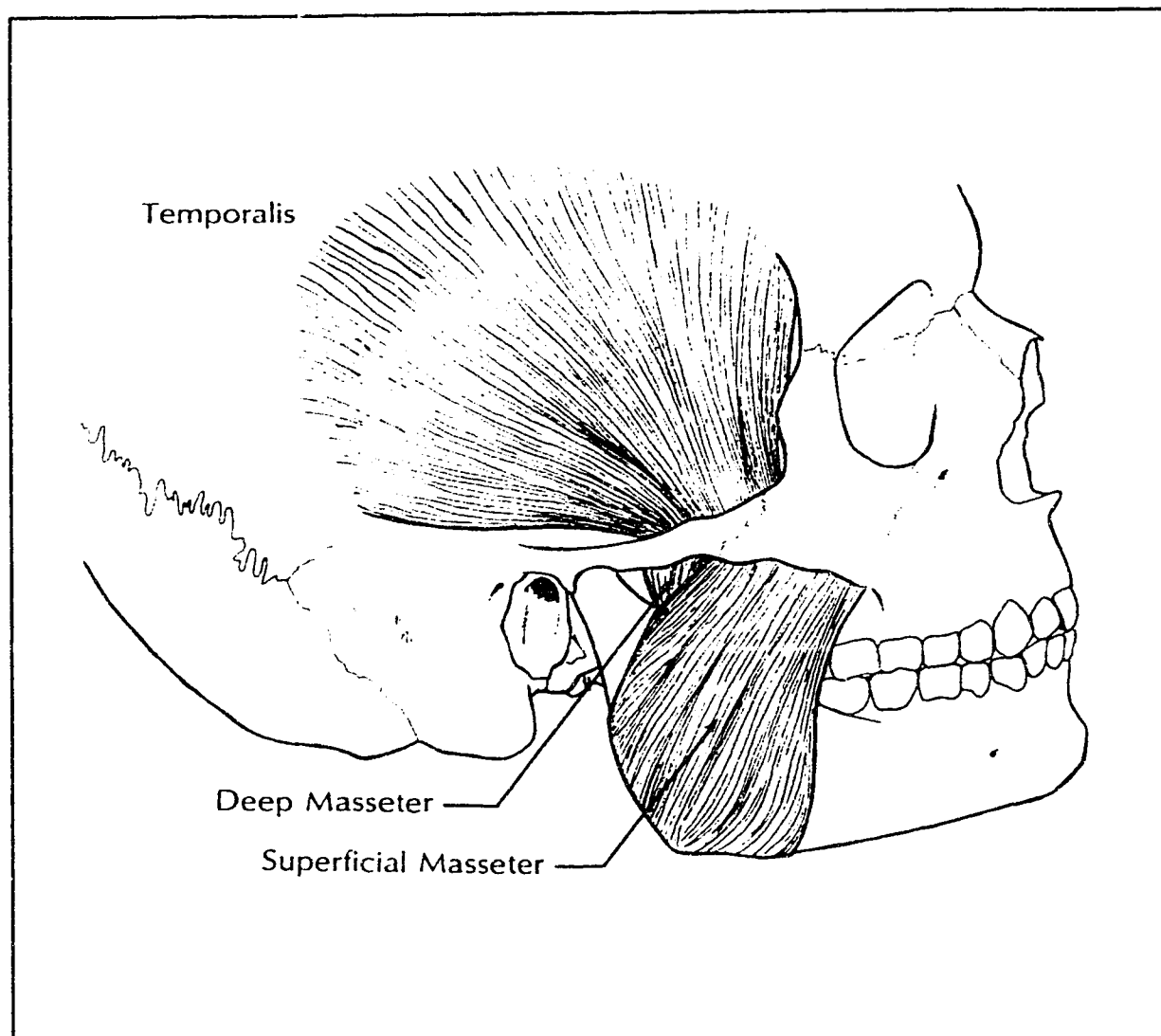
Figure 2.6 Deep and Superficial Masseters with the Temporalis Muscle

pterygoid plate located on the sphenoid bone and inserts on the medial side of the gonial angle and ramus up to the mandibular foramen (Figure 2.7). This muscle represents the medial side counterpart of the masseter muscles and its direction in the sagittal plane is approximately between the masseters.
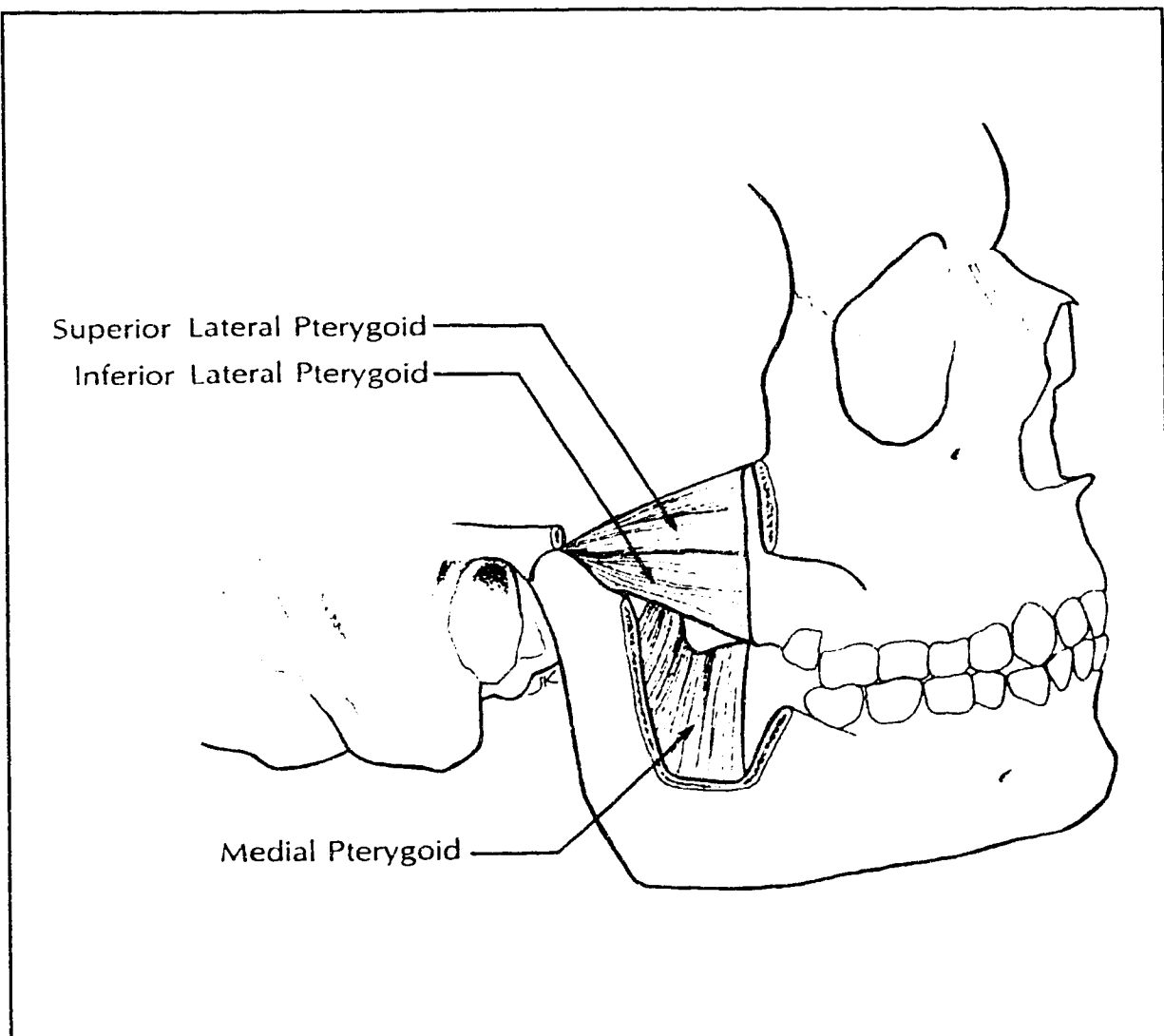
Figure 2.7 Medial and Lateral Pterygoid Muscles

The **lateral pterygoid** muscle is subdivided into two distinct bellies; the smaller superior and the larger inferior belly. The superior head is attached to the greater wing of the sphenoid bone while the inferior (lower) head originates from the lateral surface of the lateral pterygoid plate of the sphenoid bone (Figure 2.7). From these origins, the fibers run posterior and laterally to be inserted by a short tendon into the pterygoid fossa

on the anterior surface of the condylar neck (inferior head insertion) and into the anterior aspect of the articular capsule and hence into the disc of the TMJ (superior head insertion). The superior head is activated only upon opening and aids translation of the articular capsule and condyle. During forceful occlusal contact, the inferior head is active and exerts a stabilizing force holding the condyle against the articular eminence (anterior portion of the glenoid fossa) [McNamara, 1970].

2.3.3 Temporomandibular Joint

The temporomandibular joint (TMJ) is the only joint used in modelling of the masticatory system and is unique to all other joints in the body because it is a bilateral synovial joint capable of complex movements in all three dimensions. The TMJ is formed between the anterior portions of the glenoid fossa of the temporal bone (*temporo*)
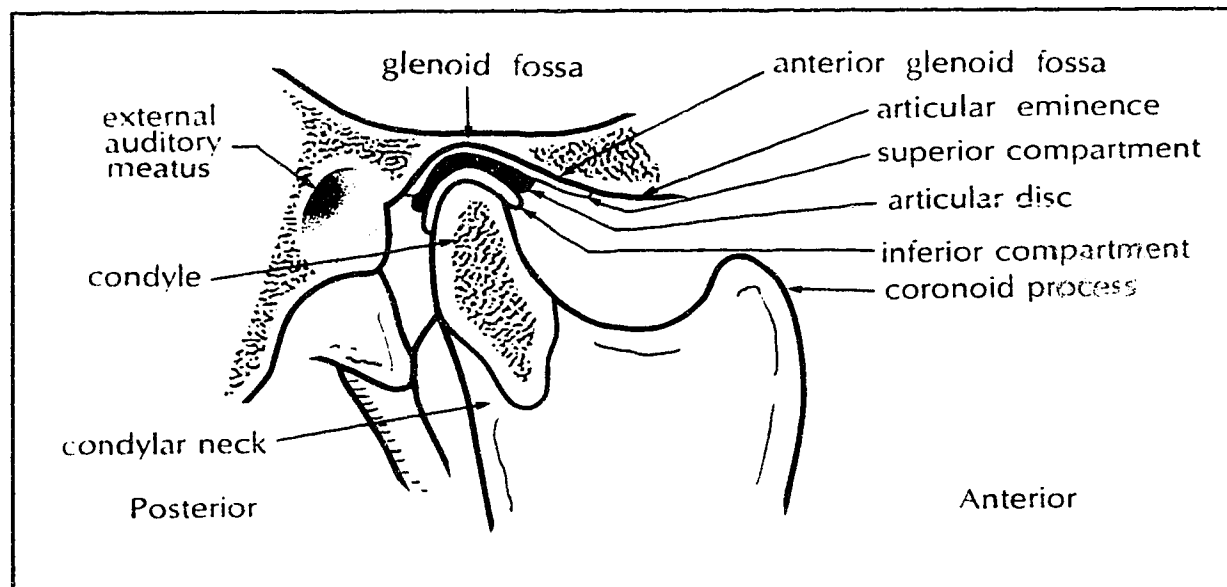
Figure 2.8 Sagittal section of the Lateral Pole of the Temporomandibular Joint

and the condyle of the mandible (*mandibular*), hence the name *temporomandibular*. The joint includes the condylar process, the articular disc, the articular eminence, the glenoid fossa, and the retrodiscal tissues (Figure 2.8).

The articular disc is a biconcave plate of fibrocartilage when coupled with the retrodiscal tissue completely divides the joint cavity into upper and lower compartments. Lubrication, nutrition, and protection of these joint surfaces is provided by the **synovial fluid** secreted by the capsule lining (synovium) which also removes the waste products of metabolism. The joint and associated structures are encapsulated by the **capsular** and **lateral ligaments** and are complimented by the **sphenomandibular** and **stylomandibular ligaments** which act to stabilize and control the movements of the mandible within tolerable limits. Occasionally, during dysfunction, the two compartments communicate by perforating the articular disc and/or the retrodiscal tissues.

The condyle can be translated forward towards the eminence, rotated in the sagittal plane, and/or rotated in the transverse plane independently leading to the complex functional morphology of the joint. The mobility of this joint makes it unique within the body but also means that the conditions which lead to dysfunctions can be rather complicated.

2.4   Craniofacial Morphology

Once familiar with the bony anatomy of the cranium and face, the morphology or facial shape can be assessed. It is hypothesized that certain differences in facial form may lead to variations of the resultant joint loadings. Some classification schemes have

been used extensively and are universally accepted methods for segregating skulls. These techniques as well as some new measures are introduced to identify mechanical differences between skulls.

2.4.1 Landmark Identification

A brief discussion of the major landmarks used in a morphological analysis of the human skull is necessary to describe variations in skeletal type. Because of symmetry (asymmetric skulls were not sampled), only a lateral cephalogram (x-ray) was used to differentiate facial morphologies. Figure 2.9 shows a lateral cephalogram tracing of the major radiological landmarks used in this investigation. The following is a brief listing of each anatomical landmark and plane of reference shown in Figure 2.9.

N, *Nasion*	-	The most anterior point on the frontonasial suture on the midsagittal plane.
S, *Sella turcica*	-	Geometric center of the pituitary fossa located by visual inspection.
Or, *Orbitale*	-	Most inferior border of the orbit (eye socket).
Po, *Porion*	-	Most superior border of the external auditory meatus (outer ear canal).
ANS, *Anterior Nasal Spine*	-	The anterior tip of the sharp bony process of the maxilla at the lower margin of the anterior nasal opening.
A, *Subspinale*	-	The most posterior midline point in the concavity between the ANS and the maxillary incisors.
B, *Supramentale*	-	The most posterior midline point in the concavity of the mandible between the most superior point on the alveolar bone overlying the lower incisors and the most anterior point of the chin (Pogonion).
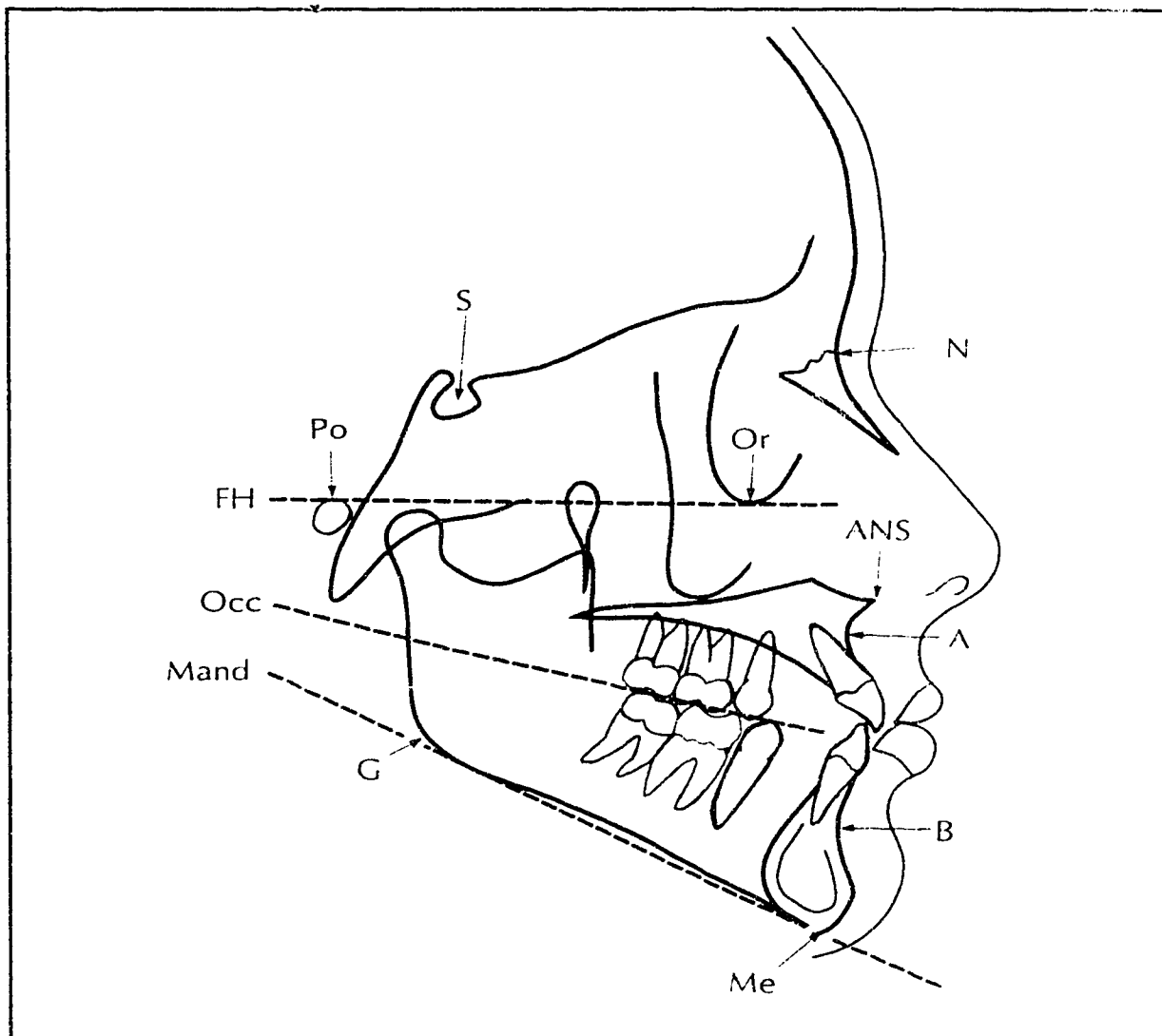
Figure 2.9 Lateral Cephalogram Tracing showing landmarks: (A) Subspinale, (ANS) Anterior Nasal Spine, (B) Supramentale, (G) Gonion, (Me) Menton, (N) Nasion, (Or) Orbitale, (Po) Porion, (S) Sella turcica. Also shown at the major anatomical planes: (FH) Frankfort Horizontal, (Mand) Mandibular, (Occ) Functional Occlusal Plane.

| G, *Gonion* | - | A point on the curvature of the mandible located by *bisecting* the angle formed by lines tangent to the posterior border of the ramus and the **Mandibular plane**. |

Me, *Menton*	-	The most inferior point on the symphysis of the mandible (parallel to line created by **Po** and **Or**).
FH, *Frankfort Horizontal*	-	Plane developed by a line joining the **Po** and the **Or**.
Occ, *Functional Occlusal Plane*	-	Plane developed by joining the central fossae of the first premolar (**PM1**) and the first molar (**M1**).
Mand, *Mandibular Plane*	-	Plane tangent to the inferior border of the mandible passing through **Me**.

2.4.2 Classification Schemes

Using these anatomical landmarks, there are numerous ways of classifying the 68 skulls sampled for this investigation. The following is a list of the various methods used:

1) ANB Classification
2) Facial Index and Facial Length Ratio
3) Wit's Appraisal
4) Plane Angles
5) Mandibular Triangle

A discussion of these schemes follows.

2.4.2.1 ANB Classification

In the 1890's, Edward H. Angle created a terminology to effectively differentiate anterior-posterior dental relationships. This system is only unidimensional but has provided dental personnel with a means of assessing the interdental relationship between the maxilla and the mandible. Angle hypothesized that the maxillary M1 was rarely misplaced, and using this tooth as the benchmark, various combinations of mandibular teeth interdigitation are possible. For example, in a Class I occlusion (considered normal occlusion) the mesial lingual (forward and towards the tongue) cusp of the maxillary first

molar is in line with the central fossa of the mandibular M1. A Class II molar relationship has the mandibular M1 at least one half a tooth width distal to the Class I relation. A Class III relationship would see the mandibular M1 more than one half a tooth width mesial to the Class I case.

This system was later expanded to describe the maxilla-mandible skeletal relationship [Reidel, 1952]. The anterior cranial base is defined as a line joining the sella turcica (S) and the nasion (N) which is called the SN line It depicts the anterior cranial base which is a significant landmark for assessment of facial to cranial relationships. Projecting this line inferiorly from the nasion to intersect the A point would form the SNA angle which relates the anterior-posterior relative position of the maxilla to the anterior cranial base. Similarly, the lines from S to N and N to B point would construct the SNB angle which relates the anterior-posterior relative position of the mandible to the anterior cranial base (Figure 2.10). The resultant angle ANB (SNA minus SNB) is used to determine the relationship of the maxilla to the mandible. The following classifications were made:

1) Class I $0° \leq ANB \leq +5°$
2) Class II $ANB > +5°$
3) Class III $ANB < 0°$

The limits of each of these classes are arguable, so the study will attempt to show the spectrum of ANB values individually rather than in these predetermined groups. Figure 2.10 shows the ANB angle of Skull 1 to be $9.0°$, an extreme Class II case.
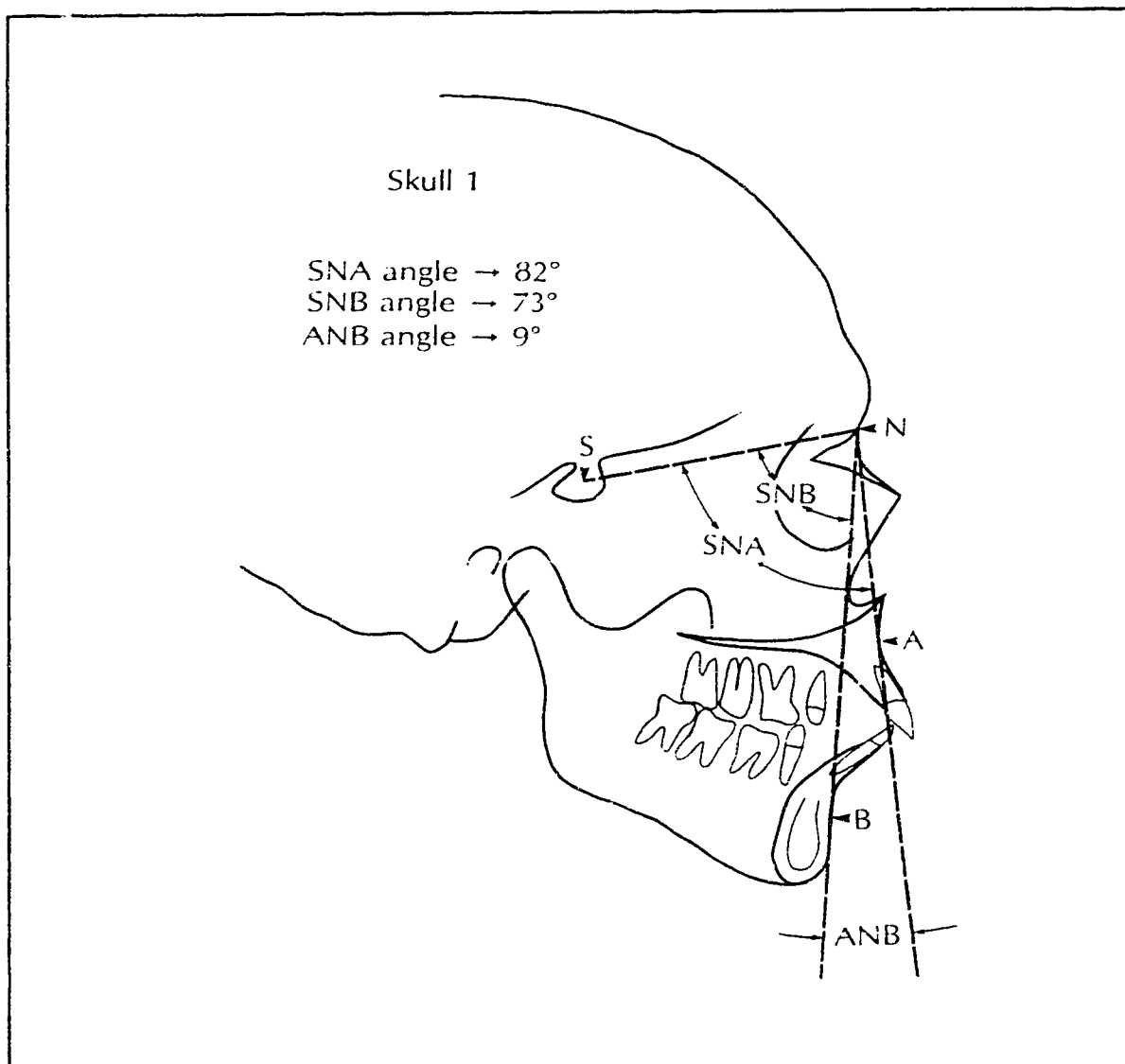
Figure 2.10 ANB Classification Scheme

2.4.2.2   Facial Index and Facial Length Ratio

Facial Index (FI), used as a predictor of mandibular growth, is defined as the proportion between the posterior and anterior facial heights calculated as

$$FI = \left[\frac{(Sella - Gonion)_{distance}}{(Nasion - Menton)_{distance}} \right] \times 100\% \qquad 2.1$$

and is written in percentage [Rakosi, 1982]. Figure 2.11 illustrates how anterior and posterior facial heights are measured. This technique for craniofacial measurements is no longer unidimensional as was the Angle's Classification. The facial height ratio is used to determine whether a laterally *squarer* face (FI close to 100%) will have significantly different joint loading characteristics than a *divergent* face (FI close to 50%).

With these data points already attained, it was suggested that the ratio of facial lengths also be tested which would give the Facial Length Ratio (**FLR**). This ratio is defined as the ratio between the superior distance, defined as the distance from the sella turcica (S) to the nasion (N), and inferior distance, defined as the distance from the gonion (G) to the menton (Me) (Figure 2.11) and is calculated by

$$FLR = \left[\frac{(Sella - Nasion)_{distance}}{(Gonion - Menton)_{distance}} \right] \times 100\% \qquad 2.2$$

and is also written in percentage form. Skull 1 (cephalogram trace - Figure 2.11) had a FLR of 109% which illustrates that the cranial base (superior length) is substantially longer than the inferior facial length (mandibular body length).
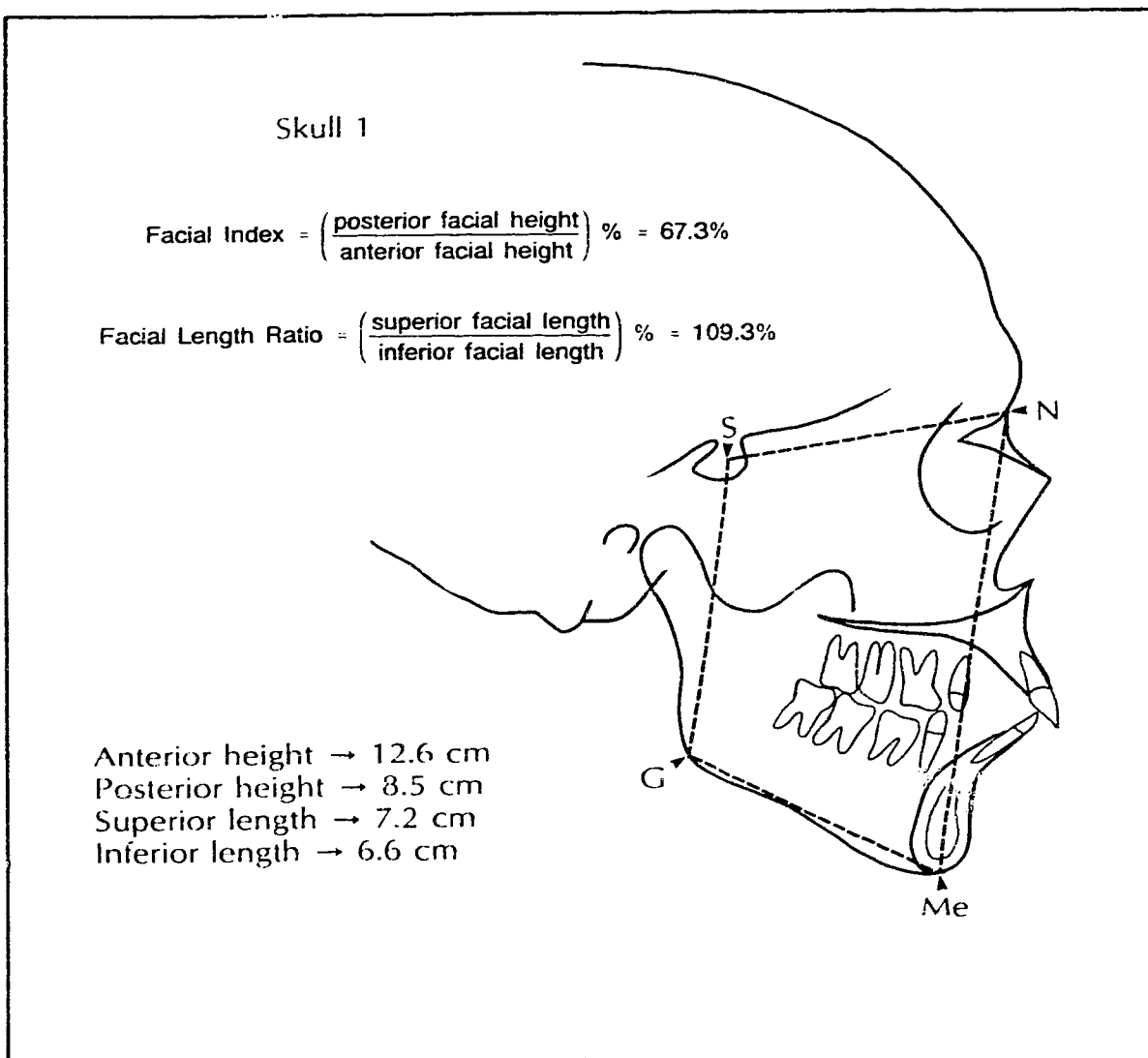
Figure 2.11   Facial Index and Facial Length Ratio

2.4.2.3   Gonial Angle

The angle formed by the posterior border of the ramus and the mandibular plane is denoted the **Gonial Angle** or **Angle of the Mandible**. It is hypothesized that if this angle is large, the muscles are not able to pull as effectively as a case where this angle is closer to 90°. The distance from the muscles to the intercondylar axis would be

lessened if this angle were great therefore reducing the jaw's effective moment arm. This is not a standard measure of facial morphology. It considers only the mandible and as a result, the dentition and superior-anterior facial structures are omitted. Figure 2.12 shows the measurement of gonial angle on Skull 1 as being 127.4°.

2.4.2.4   Wit's Appraisal

With the exception of the original Angle's classification, none of the above measures are concerned with the occlusal plane. Wit's appraisal uses an occlusal plane measurement to identify instances in which the ANB measurement, in particular, does not accurately reflect the extent of anteroposterior jaw dysplasia (dysharmony). In addition, this procedure also stresses the relationship of the jaws (upper and lower) to each other and to the cranial base.

To obtain this measurement, refer to Figure 2.12 which illustrates that a similar procedure to Angle's ANB measurement is made. The A and B point must be used to make this measurement. Ao is the point on the functional occlusal plane perpendicular to the A point while Bo is the point on the functional occlusal plane perpendicular to the B point. The total distance between these points is termed the Ao-Bo distance and is 8.22 mm for Skull 1 of the study (see Figure 2.12). Jacobson [1975] investigated the technique and showed that in some situations severity of jaw disharmony could be clearly seen whereas using the standard ANB measurement it was not evident. A negative reading meant that the Bo point was anterior to the Ao point.
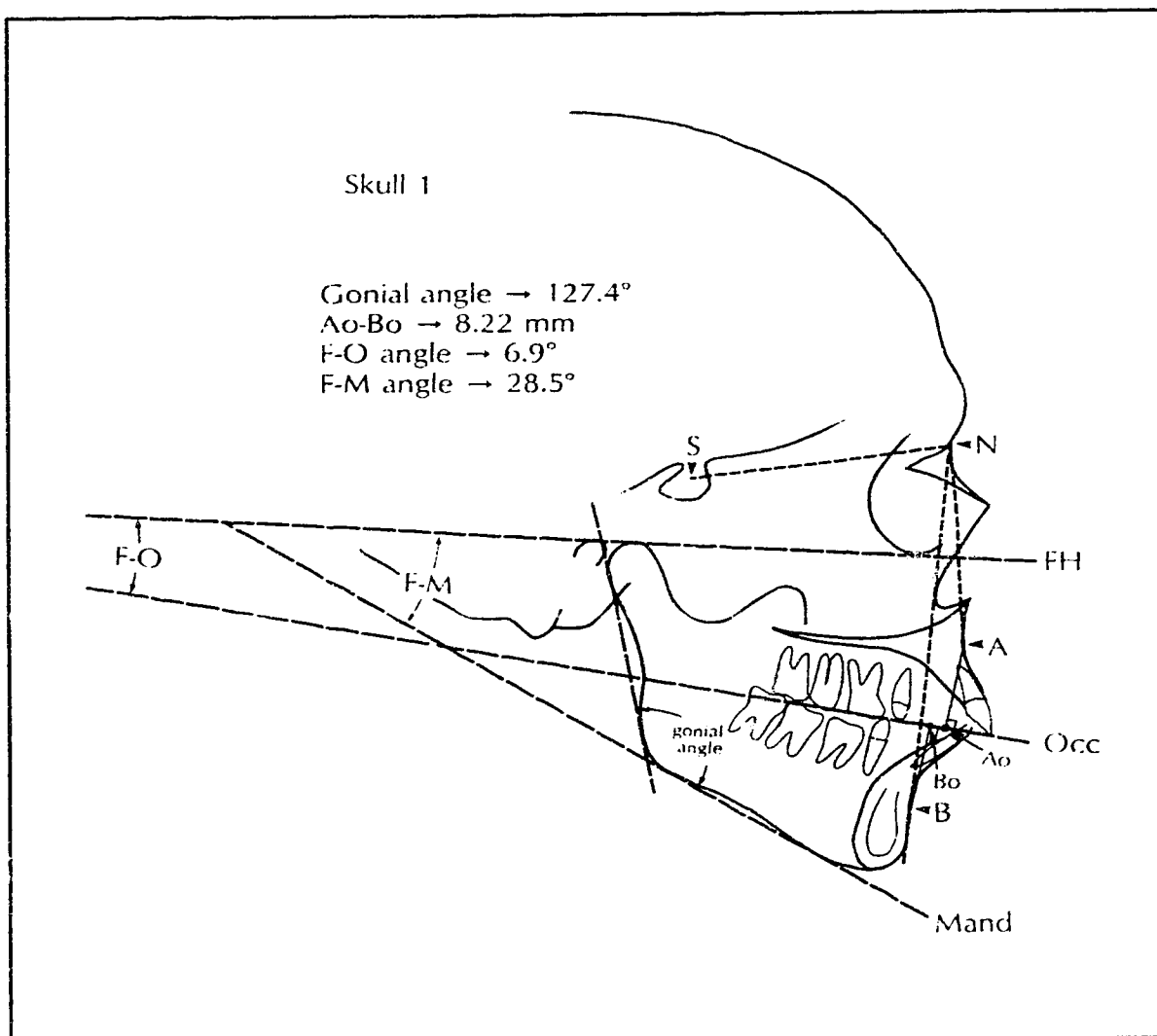
Figure 2.12 Gonial Angle, Wit's Appraisal and Plane Angle Measurements (Skull 1)

2.4.2.5 Reference Planes

Other methods of facial measurements involve the relative angles between significant facial planes in the lateral x-ray. This biomechanical investigation will be concerned with the Frankfort Horizontal (FH) Plane, the Functional Occlusal (Occ) Plane, and the

Mandibular (Mand) Plane. The angle each of the latter two planes make with the FH plane will be recorded for each skull in a similar method as shown in Figure 2.12. The steepness of each of these planes with reference to the FH plane may prove to discern differences in joint loading. A large angle may lead to a divergent face (as in FI discussion) which may have significantly different joint loading patterns as compared to the opposite style face. These angles will be termed the **F-O** and **F-M** (FH to Occ and Mand Planes respectively) angles. For Skull 1 (Figure 2.12), these measurements were 6.9° and 28.5° for the F-O and F-M angles respectively.

2.4.2.6   Mandibular Triangle

Because the mandible and maxilla are related significantly through occlusion and do not function independently of one another, the form each takes must be influenced by the other. For this reason, examining *only* the mandible may disclose information about the entire craniofacial morphology and TMJ loading patterns. A previously untried alternate approach was taken to formulate a classification scheme based on the geometrical relationships of two major muscle attachment locations and a TMJ loading point on the mandible.

These three points (Figure 2.13), which create a triangle located on the ramus of the mandible, are fixed by the joint and muscle force locations which are important in the loading of the jaw,. The *condylar loading point*, measured as the centroid of the wear facets on the condyle of the mandible, depicts the first point. The *gonion* is located near the insertion points of the deep and superficial masseters as well as the medial pterygoid
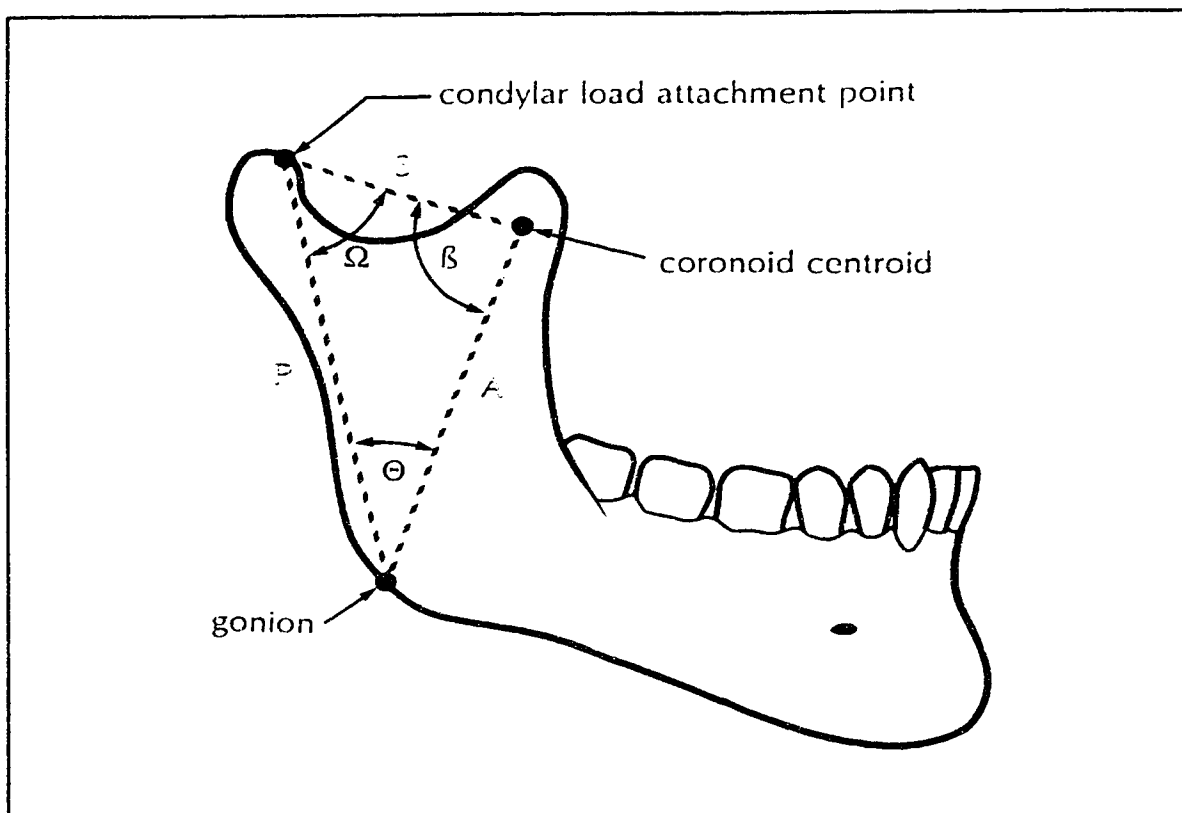
Figure 2.13 The **Mandibular Triangle** created by the three
Critical Mandibular Loading Points

muscle and therefore was chosen as an appropriate landmark for the second point of the triangle. The medial surface of the *coronoid process* is the area of insert for the temporalis muscle. Because this muscle contributes a major portion of the total muscular tension, the center of this coronoid insertion area marks the third and final point to complete the triangle. It is felt that these points represent the three most important loading points (omitting bite force locale) on the mandible.

In order to accommodate different sizes of skulls and mandibles, a normalization scheme was used. The three sides of the triangle are termed the superior (S), posterior

(P) and anterior (A)sides. Normalization of each side's length was achieved by dividing the length by the perimeter of the same triangle expressed as a percentage (A/Per., S/Per., P/Per). The angles between each of these sides were also noted:

Ω - Angle between superior and posterior side
ß - Angle between superior and anterior side
Θ - Angle between posterior and anterior side

Each skull contains two triangles, one per side. The lengths of each triangle (S, P, A) were averaged to create one representative triangle to be normalized.

It was conjectured that a skull with a large Θ angle and/or a relatively long superior length will supply the anterior muscles (namely the temporalis) with a mechanical advantage over skulls with lower normalized values during mastication. The ramus height, characterized by P and A from the triangle, may also suggest some pattern during this study. From a mechanical viewpoint, this normalized triangle may provide some insight into the calculated craniofacial loading patterns which the models discussed below generate.

2.5 Craniofacial Summary

The following table gives the mean, minimum, maximum, and standard deviation of each skull classification investigated. The skull series chosen were, as mentioned earlier, the same samples used by McEvoy [1989] in his investigation of facial morphological significance considering TMJ loading and will also be used in the following chapters.

Table 2.1 Summarized Morphological Data for Skull Series attained from the
Universities of Alberta and Pacifica
(Sample Size = 68)

Classification Scheme	Mean	Minimum	Maximum	Standard Deviation
ANB Angle, °	3.66	-10	11.5	4.11
Facial Index, FI, %	67.6	56.5	78.7	4.83
Facial Length Ratio, FLR, %	89.6	75.7	109.3	7.57
Gonial Angle, °	119.8	106.2	139.3	7.24
Ao-Bo Distance, mm	2.51	-15.3	10.4	4.69
Frankfort-Occlusal Plane Angle, F-O, °	4.03	0.55	11.5	2.47
Frankfort-Mandibular Plane Angle, F-M, °	21.8	9.19	36.6	5.60
Normalized Superior Length, S/Per, %	22.2	12.6	28.1	2.57
Normalized Posterior Length, P/Per, %	41.0	38.3	46.4	1.44
Normalized Anterior Length, A/Per, %	36.8	32.1	42.2	2.11
Superior-Posterior Angle, Ω, °	63.1	49.3	83.4	7.03
Superior-Anterior Angle, ß, °	84.4	72.7	114.7	7.41
Anterior-Posterior Angle, Θ, °	32.5	14.4	44.3	4.95

2.6 Craniofacial Correlations

Table 2.2 shows a compilation of the products of correlation made of each of the
craniofacial morphological schemes examined. Each method previously discussed was
correlated with the others to determine if there was a linear relationship between each
classification. The product of correlation, R^2, indicates the percent variation in the data

Table 2.2 The Products of Correlation, R^2, for Morphological Classification Scheme Comparison
(values given in percent)

	ANB	FI	FLR	Gonial	Ao-Bo	F-O	F-M	S/Per	P/Per	A/Per	Ω	β
FI	1.2											
FLR	12.4	23.1										
Gonial	0.8	42.3	36.1									
Ao-Bo	55.8	0.5	17.2	0.0								
F-O	0.0	1.4	0.4	0.0	0.4							
F-M	5.8	62.9	21.3	39.4	1.8	0.6						
S/Per	7.5	1.7	8.7	11.4	0.6	0.8	0.3					
P/Per	4.0	1.6	10.6	0.2	7.2	0.5	0.0	30.4				
A/Per	22.0	0.4	1.6	14.0	7.8	0.3	0.0	65.6	0.2			
Ω	23.2	0.1	0.2	8.50	14.4	0.1	0.0	14.2	29.2	69.2		
β	10.7	0.3	6.4	0.5	11.6	0.1	0.2	7.7	87.8	10.6	61.3	
θ	4.3	2.3	10.6	10.3	0.1	0.7	0.0	97.9	41.8	53.4	7.5	14.8

Legend:

ANB	- E.H. , ie's ANB Angle (SNA - SNB)	
FI	- Facial Index (Facial Height Ratio)	
FLR	- Facial Length Ratio	
Gonial	- Gonial Angle	
Ao-Bo	- Wit's Appraisal (Occlusal Plane distance)	
F-O	- Angle between Frankfort Horizontal and Occlusal Plane	
F-M	- Angle between Frankfort Horizontal and Mandibular Plane	

S/Per	- Superior Length / Perimeter	
P/Per	- Posterior Length / Perimeter	
A/Per	- Anterior Length / Perimeter	
Ω	- Omega (Angle between Sup. and Post. Sides)	
β	- Beta (Angle between Sup. and Ant. Sides)	
θ	- Theta (Angle between Post. and Ant. Sides)	

which is accounted for by the assumed relationship. It may prove useful in discovering the significant morphological patterns in TMJ loading.

The highest product of correlation, R^2, was found to be 97.9% between Θ and the S/Per ratio of the mandibular triangle. This is not surprising since Θ opposes the superior side of the triangle. From trigonometry, the **Cosine Law** is given by

$$S^2 = A^2 + P^2 - 2AP\cos\theta \qquad\qquad 2.3$$

(refer to Figure 2.13 for the triangle) which relates the length of side S to the remaining lengths, A and P, and its opposing angle, Θ. *Normalizing* this law by dividing the length of each side by the perimeter of the triangle gives the following relationship:

$$\left(\frac{S}{Per}\right)^2 = \left(\frac{A}{Per}\right)^2 + \left(\frac{P}{Per}\right)^2 - 2\left(\frac{AP}{Per^2}\right)\cos\theta \; . \qquad\qquad 2.4$$

When $(S/Per)^2$ is linearly correlated with $\cos(\Theta)$ there is a near linear correlation since the product of correlation is 97.9% using the compilation of 68 skulls. This normalized length, S/Per, versus its opposite angle, Θ, proved to be nearly linear over the small range of angles investigated ($\Theta = 14°$ to $44°$ with a standard deviation of $5.0°$). Similarly, the remaining correlations of length versus opposing angle showed high linearity as a result of this normalized cosine law.

The relative lengths A/Per and S/Per of the mandibular triangles are not changing significantly which means the distance between the Gonion and condylar loading point as well as from the Gonion to the centroid of the Coronoid process appear to be constant for the sampled jaws. Only the distance between the joint load and the Coronoid process

varies. These high correlations, especially with Θ and S/Per, illustrate which components of the mandibular triangles are changing. This may lead to the ability of predicting which skulls are vulnerable to higher or misaligned joint loading conditions.

Not surprisingly, the ANB Classification scheme and Wit's Appraisal (Ao-Bo) compared well ($R^2=65.6\%$ correlation) since both measure similar aspects, jaw disharmony. A good relationship between the Facial Index and the Frankfort-Mandibular Plane Angle existed since both characterize the amount of facial *divergence* or *squareness*.

There were a number of poor correlations. The Frankfort-Occlusal Plane Angle demonstrated poor linearity with all other classification schemes indication that the dentition and occlusal plane are unstable methods of evaluating craniofacial morphology. These correlations portray the variability of human skulls. In most cases the relationships and comparisons were poor ($R^2<30\%$) showing the independence of each classification scheme. Complications arise when trying to determine which classification scheme(s) to use for predicting the loading characteristics of the human temporomandibular joint.

NUMERICAL MODELLING OF THE TEMPOROMANDIBULAR JOINT

3.1   Introduction

As stated above, the main purpose of the mechanical models developed for the TMJ is to evaluate the loading characteristics of the condyles during mastication. While there are many techniques used to determine the magnitude and direction of the condylar reactions, the approach used by various investigators was to calculate the condylar forces after the muscle and bite forces were determined by some means. Various models have been created to analyze temporomandibular joint function with each author using different muscle groupings and skull parameters to characterize their particular formulation. This makes it difficult to compare models except on the basis of the resultant condylar loads calculated.

This chapter introduces the major TMJ models and attempts to compare them on equal terms while discussing the primary concepts used in temporomandibular joint modelling. Four models are compared to determine the differences in modelling

philosophies. These include two general approaches to determining the muscle and bite forces applied. The first uses a biological optimizing criterion to estimate the muscle forces often employing linear programming to find forces subject to assigned constraints. The second assumes that measurement of physical parameters including muscle size and EMG activity allow reasonable estimates of muscle force.

Only one bite situation will be investigated. This allows differentiation of each model without clouding the problem with more variables. A single skull is initially used to determine the characteristics of each model. Results for the entire data set (68 skulls) are then compiled for each model.

3.2   Assumptions used in Numerical Modelling

Modelling the temporomandibular joint embodies many assumptions which can reduce the number of unknowns and potentially make the problem of determining the condylar joint reactions tractable. The cranioskeleton, muscles and ligaments of the cranioskeleton which affect TMJ function are used collectively to provide the forces necessary to chew a bolus of food. *In vivo* internal joint forces are difficult to measure directly. Also, the task of calculating these quantities is no simple matter. The large number of muscle and ligament forces usually render the problem statically indeterminate since the number of unknowns exceed the number of independent equations. This complex system must be simplified in some manner to estimate the unknown loads which may cause joint dysfunction. Electromyography, used in the determination of the relative muscle activation rates, has been employed to reduce the number of unknowns in the mechanical

system. Discretization of the muscles and skeleton is not obvious and it is easy to justify more than one technique of accomplishing this modelling. The method used in the current model development is outlined following a discussion of the assumptions made in various components of the system.

3.2.1 Osseous Tissue

The osseous tissues that vary in shape gives the bone various shapes and sizes thereby facilitating the ability to transfer loads evenly and prevent excessive loads which could result in either large scale fracture or local destruction of skeletal components. Because there are different boney elements comprising even a single bone, numerical modelling is difficult. If the bones are considered rigid bodies, the analysis can concentrate on the loading of the structure alone. Many authors have used this assumption in modelling the osseous tissue [eg. Barbenel, 1972, 1974; Pruim, DeJongh, Ten Bosch, 1980; Hylander, 1985; Osborn et al., 1985; Smith et al., 1986; Koolstra et al., 1988; McEvoy, 1989]. The assumption that the bones of the mandible and maxillary regions are rigid is used for all the models considered.

3.2.2 Musculature

Skeletal muscle can take diverse shape and form as introduced earlier in Chapter 2 and the forces each muscle can generate may also vary in magnitude. There are even differing muscle tissue fibers which are designed to perform specific functions based upon their need. The geometries, area and length, as well as the maximum force each individual muscle can develop are carefully considered. These geometric and force limits

are to be included in a computer simulation to provide an alliance between the numerical and biological TMJ systems.

While the insertion and origin of a muscle or muscle group are usually modelled as a single point, in reality these attachment points cover a distinct area of bone and are anchored to provide the forces necessary to cause movement or in the case of static TMJ modelling, occlusal contact forces. This anchoring causes bone scarring due to localized stresses in the bone structure. For modelling, each area centroid of a bone scar is used as the insertion and origin of that muscle. It is also assumed that the muscle force acts only on a straight line between the area centroids of the insert and origin of the muscle and, since muscles can only create tension, it acts in only the one prescribed direction. Fan shaped muscles must be considered more carefully than longitudinal strap muscles. To better approximate this form of muscle it is assumed to be originating from differing locations (origins) and inserting at the same one (the insertion point). This allows the model of the muscle to independently activate individual portions of the muscle rather than the entire muscle. The primary muscles of mastication are the masseter, the medial and lateral pterygoids, and the temporalis. All but the medial pterygoid were divided into smaller muscles to better approximate the biological system. The masseter was separated into its superficial and deep portions with their respective inserts and origins. The fan-shaped temporalis was sectioned into anterior, middle, and posterior parts. The lateral pterygoid has two distinct bellies. Only the inferior belly of the lateral pterygoid muscle is used in the computer models since it is the primary belly of this

muscle which is activated during forceful biting [eg. Grant, 1973; McNamara, 1970]. The superic. belly is activated during opening and is attached to the disc capsule rather than the pterygoid fossa on the condylar neck. For these reasons, the superior belly is assumed to be inactive during the occlusal phase of mastication.

This muscle segmentation allows more flexibility for activation than does a model with fewer groups. Classifying muscles in this manner creates more degrees of freedom allowing the models more adaptability.

3.2.3 Temporomandibular Joints

Condylar loads are applied to the mandible as a single vector. The load bearing portion of the mandibular condyle was determined from the centroids of the four digitized wear facets which are identified as scarred bone on the skull specimens. This point load is transferred to the skull via the centroid of the digitized region of the articular eminence. In reality, these loads are transferred over a distinct area of the articular surfaces of the temporal bones and mandibular condyles. A thin intervening film of synovial fluid separates the disc and articular surfaces and provides a near frictionless contact [Charnley, 1959]. This low friction fluid allows the articular surface of the mandible to move with respect to the eminentia with virtually no frictional forces. All the TMJ models to be investigated assume that the TMJ is a frictionless joint.

As a result, any shear force component which would act parallel to the interface of the articular surfaces during mastication is considered unlikely to occur in reality. Even

though the direction of the joint force during mastication is not known precisely, models which produce absurd angles can be discounted.

The temporomandibular joints, each having independent three dimensional components, contain a total of six unknown forces. Each of these must be determined in order to obtain the magnitude and direction of the resultant condylar loads. The *direction* of the condylar reaction is as important as its *magnitude* since misdirected condylar force may be a source of TMJ dysfunction. Any shear forces on the articular capsule and eminence may lead to degenerative joint break down and compromise the connective tissues.

To compare the joint loading directions given by the models with the actual case, the anterior aspect of each glenoid fossa was represented `` four data points. The digitization of these points (on a left fossa) is shown ..  `` re 3.1 where the specific locations chosen were selected to best represent th. ``ic` `ating surfaces. Points #2 and #4 depict the posterior and anterior borders of the articular eminence used during normal occlusion in an approximate sagittal plane. The line joining these two points represents the simplified anterior fossa which, in most cases, provides the facing for the condyle. In the sagittal plane, the ideal loading pattern would be one at which the condylar reaction acts perpendicular to the articular eminence. Figure 3.2 shows how the sagittal component of joint load misalignment is characterized. For an *ideal* load, the angle between the load and the anterior fossa would be $90°$ (perpendicular) to alleviate any shear forces which may result. The angle, α, will result in posterosuperiorly (backwards
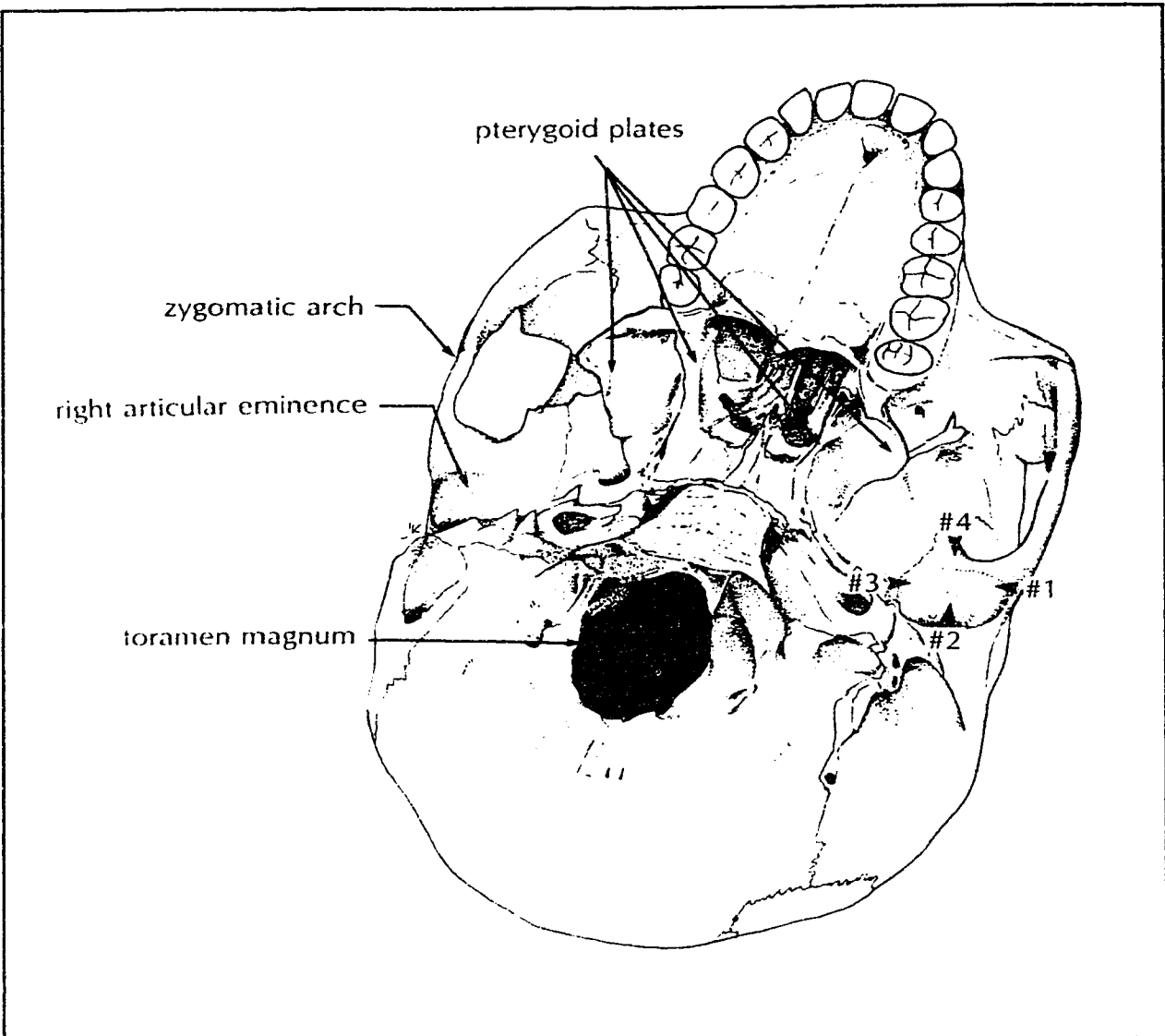
Figure 3.1 Inferior View of the Human Skull illustrating the Four Digitized
Locations of the Anterior Fossa

and upwards) directed shear forces when positive and vice versa when negative.

Figure 3.3 shows the convention used to distinguish the resultant condylar loading angles
of the models. Figure 3.3a illustrates how the sagittal component of the joint load is
directed. The angle in the Sagittal plane is shown as the Parasagittal Incline, Θ where
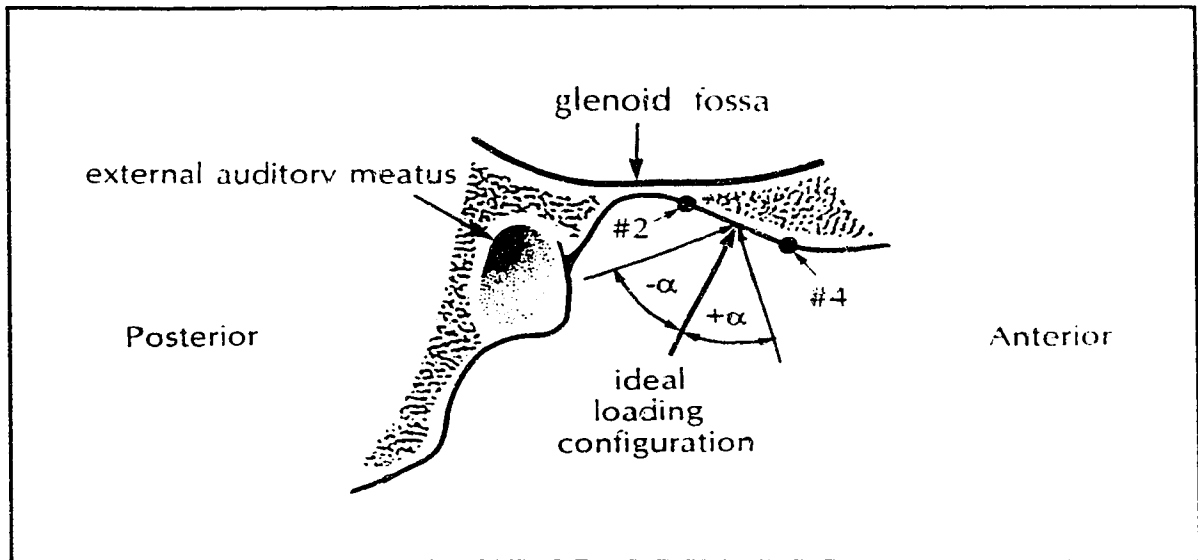
Figure 3.2 Ideal TMJ Loading Pattern in the Sagittal Plane

Θ = 0° represents a vertical joint load in this plane. If Θ were 90°, a horizontal posteriorly directed joint load would exist on the condyle. The mediolateral components are represented in Figure 3.3b. A positive mediolateral angle depicts a medially directed load (towards the center of the body). The medial border of the glenoid fossa of the temporal bone carries the medial TMJ load while the capsular and temporomandibular ligaments support the lateral load.

Osborn et al. [1985] and Koolstra et al. [1988] had previously constrained the joint load directions to act only on the midsagittal plane. In the current study, complete 3D modelling of the forces is considered and for effective model comparison, the resultant condylar loads will not be constrained in direction nor magnitude which will permit each condyle to be loaded in any direction.
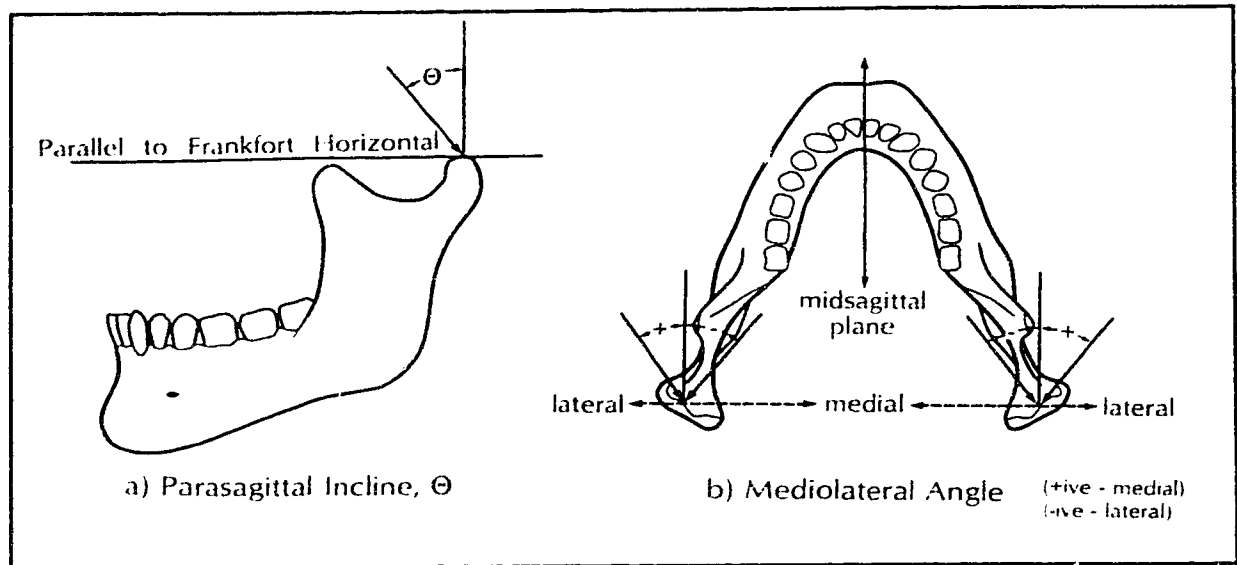
Figure 3.3 Temporomandibular Joint Load Conventions

3.2.4 Ligaments

There are numerous ligaments involved with a synovial joint to form the joint capsule and are designed to restrict the range of motion of the jaw. These ligaments do have load bearing capabilities during certain normal functions and mandibular movements but these tissues are assumed not to provide any substantial influence during static occlusion. The assumption was made that these connective tissue structures have no influence and can be neglected in the static force analysis. Other authors [Osborn et al., 1985; Smith, 1986; Koolstra et al., 1988] use this assumption when studying static occlusal mechanics. Models investigating motion of the mandible would undoubtedly use the ligaments as restraints.

3.3   Model Parameters

Of the existing models of the TMJ, each author had used a different skull which makes models comparing difficult. For this investigation, each model is compared to the same skull data and muscle data sets. This allows the evaluation of the methodologies of each technique to be done without consideration of the differences in the skulls. As discussed earlier, a full three dimensional model utilizing 14 muscle forces and unilateral biting is used as the foundation for these comparisons.

While each model has a different methodology, there are certain commonalities. The mandible and the cranioskeleton are both considered three dimensional rigid bodies. The jaw contacts the skull at three locations: the occlusal contact, and both condylar reaction points. The occlusal contact is the center fossa of the tooth to be investigated while the condylar force application points is located at the center of the wear facets on both condyles.

3.3.1   Spatial Data

As mentioned, the data representing the spatial orientation of 112 landmarks surveyed on seventy skulls was done by McEvoy [1989]. Incorporating a 2D digitizing tablet with a height gauge and pointer it was possible to digitize an entire skull within a cubic volume of 300 mm x 300 mm x 300 mm with a resolution of 0.025mm in each dimension. This system allowed a reliable and efficient method to determine the spatial orientation of the landmarks required for TMJ investigations. These landmarks, as well

as some found only in a radiographic cephalogram (eg. sella tur͏ ͏a), were then used in his comparison of facial morphology and TMJ loading characteristics.

Of the 112 digitized data points done by McEvoy [1989], 52 were used to investigate TMJ loading. Muscle origins on the cranioskeleton could be described with 14 coordinates while their respective inserts on the mandible only required 10. Three points were used to describe the temporalis origins from osseous scarring on the temporal, parietal, and frontal bones. All three divisions, anterior, middle, and posterior temporalis, inserted medially on the centroid of the coronoid process. Occlusal representation was achieved with 50 points. These described the maxillary dentition but only ten were required to locate the central cusps of the teeth. Four data points described the anterior aspect of each glenoid fossa and the condylar loading point was taken as the centroid of the region. This provided the condylar force application point when the mandible was mathematically placed in centric occlusion prior to loading. The remaining digitized points were landmarks to discern anatomical planes of interest used in coordinate references. More detail on the apparatus and procedure of the craniofacial digitization and landmark identification can be found in the thesis by McEvoy [1989].

3.3.2 Coordinate System

A cartesian coordinate system was chosen to describe the spatial relationships of the landmarks used for temporomandibular joint modelling. The origin was fixed on the intersection point between the Frankfort Horizontal plane and a line which extended superiorly from the anterior nasal spine. The positive Z-axis pointed superiorly from this

point while the Y-axis projected posteriorly parallel to the Sagittal plane. The X-axis

extended left, parallel to the Coronal and Frankfort planes, to complete the coordinate

system. The coordinate system is shown in Figure 3.4.
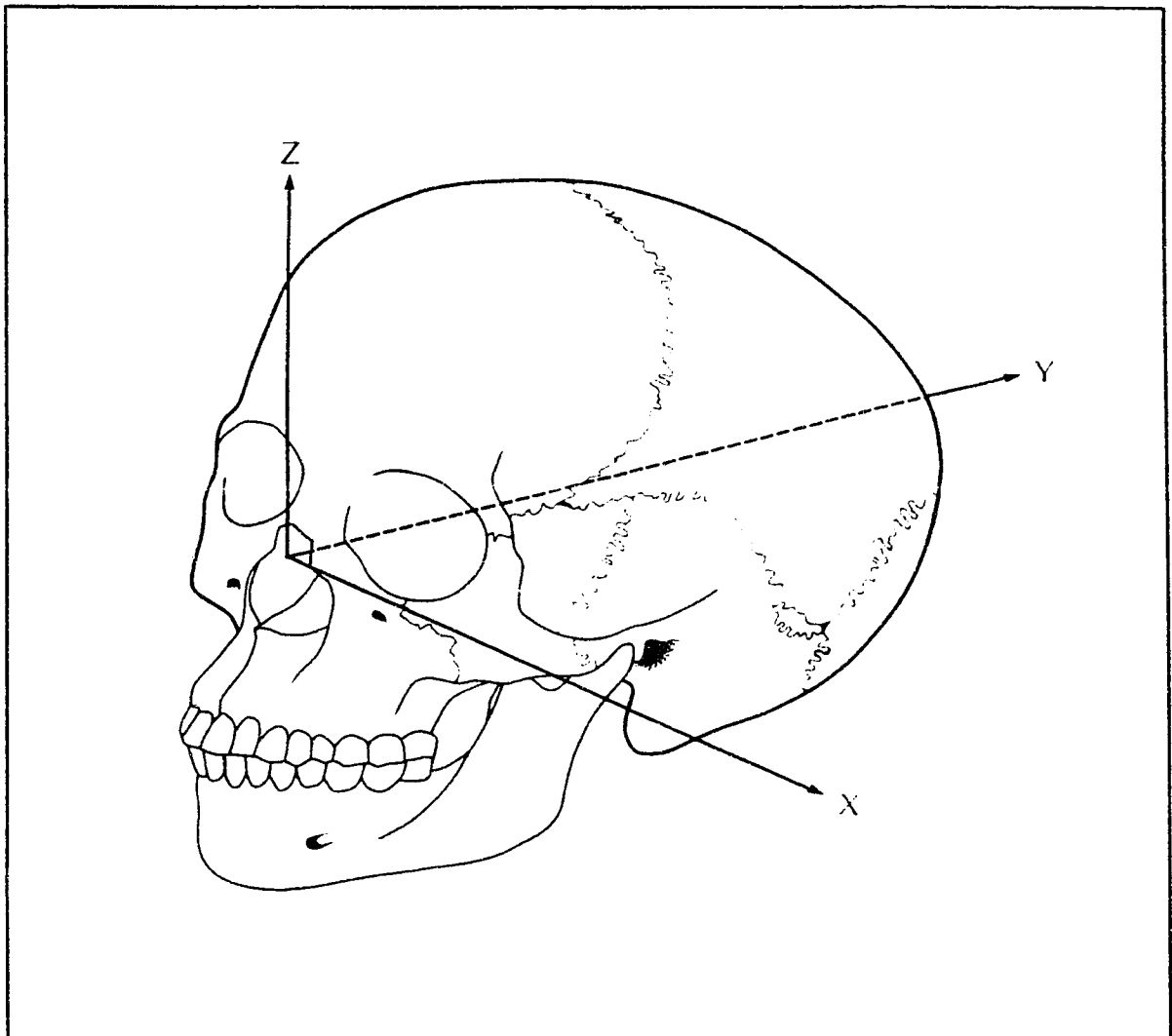
Figure 3.4 Coordinate System

3.3.3 Static Equilibrium

An analysis of the masticatory system must involve all forces applied to the mandible. From Newton's second law of motion, the total force acting on a body is linearly proportional to its acceleration. The force required to accelerate the mandible is assumed insignificant compared to the bite and muscle forces required to chew. As a result, the mandible is considered in static equilibrium during mastication. A three dimensional model includes six linear equations of equilibrium. The vectorial sum of the muscle forces, joint loads, and bite force along each axis must be equal to zero and the vector summation of the moments about each axis must also be equal to zero.

$$\sum_{i=1}^{n} Fx_{muscle_i} + \sum_{j=1}^{2} Fx_{joint_j} + Fx_{bite} = 0 \qquad \textbf{3.1}$$

$$\sum_{i=1}^{n} Fy_{muscle_i} + \sum_{j=1}^{2} Fy_{joint_j} + Fy_{bite} = 0 \qquad \textbf{3.2}$$

$$\sum_{i=1}^{n} Fz_{muscle_i} + \sum_{j=1}^{2} Fz_{joint_j} + Fz_{bite} = 0 \qquad \textbf{3.3}$$

Equations 3.1, 3.2, and 3.3 represent the sums of the forces in X, Y, and Z directions respectively. The index i depicts one muscle of a total of n muscles, 14 in this case. The two joint load components are added similarly.

The moment equations are treated in a similar fashion.

$$\sum_{i=1}^{n} Mx_{muscle_i} + \sum_{j=1}^{2} Mx_{joint_j} + Mx_{bite} = 0 \qquad 3.4$$

$$\sum_{i=1}^{n} My_{muscle_i} + \sum_{j=1}^{2} My_{joint_j} + My_{bite} = 0 \qquad 3.5$$

$$\sum_{i=1}^{n} Mz_{muscle_i} + \sum_{j=1}^{2} Mz_{joint_j} + Mz_{bite} = 0 \qquad 3.6$$

This set of equations has a unique solution only if the number of unknowns is equal to six. Assuming a specific bite force vector, there are 20 variables; 14 muscle magnitudes (eight predominant muscles of mastication were divided into 14 sections) and six condylar joint load components. As mentioned earlier, this characterizes a statically indeterminate problem since the number of unknowns, 20, outweighs the number of equations, six. In order to obtain a solution to this type of problem, other methodologies must be used. These include linear programming techniques and a pragmatic approach in which the muscle forces are assumed known *a priori*.

3.4   Models of the Temporomandibular Joint

Four models are considered, three using linear programming approaches and one using a pragmatic strategy. The linear programming models optimize the muscle function in a specified manner during static clenching. The bite force, placed at the occlusal location to be tested, is assumed to be the input while the model computes the resultant condylar loads and muscle forces. The pragmatic strategy determines the

condylar loads and bite force due to assumed muscle forces which have been inferred from experimental values of muscle cross-sectional area and EMG activity.

3.4.1 Introduction to Linear Programming of the TMJ

One of the major techniques used to determine muscle forces is linear programming. This method, along with various types of objective functions can create plausible muscle force combinations. This mathematical technique has been used primarily in business and military applications but has been used recently to optimize a specific feature of the masticatory system to determine the muscle forces and resultant joint loads.

As the word *linear* implies, the variables and equations used in a linear program are of the first degree. A linear program is characterized by a linear function, or commonly termed the objective function, of m variables which is to be maximized or minimized by a set of n linear constraints. A constraint may be an equality or an inequality which supplies another form of restriction on the linear variables.

A typical linear programming problem is stated as the following: Find all the values $x_i \geq 0$, $i = 1...,m$, that will minimize or maximize the objective function, $f(x_i)$

$$f(x_i) = \sum_{i=1}^{m} c_i x_i \, , \qquad \qquad 3.7$$

subject to the following linear constraints

$$\sum_{i=1}^{m} a_{ij} x_i \ (\leq, =, \geq) \ b_j \, , \qquad \qquad 3.8$$

for $j = 1,...,n$. Note that the constraints can be inequalities.

The x_i's are the physical variables, while the a_{ij} and b_i in the n constraints and c_i in the objective function are given constants for all the subscripts. Each x_i represents a variable and a possible solution in m-dimensional space.

Illustration of the method of linear programming can be easily achieved with a 2D model and graphical interpretation. Graphical analysis effectively describes the linear programming method even though this is not used in modelling the complex problem of the TMJ. Graphical interpretation can be accomplished with a two dimensional (two variables) problem whereas biomechanical modelling often includes many more variables to deal with. This form of analysis allows a description of how linear programming works in optimizing an objective function. An example is presented in Appendix A.

In multidimensional space created by a problem such as the multivariable modelling of the TMJ, it is not possible to visualize and interpret constraints and solutions using graphical techniques. However, the **Simplex Algorithm** was developed in the mid-fifties to obtain solutions for a variety of different applications. In what follows a Simplex algorithm, written by Morris [1990] will be utilized to optimize some component of the TMJ model based on each author's presumptions. Various different objective functions and constraints will be analyzed to determine the merits of each model when applied to the same muscle groups and skeletal parameters.

3.4.2 Minimization of Total Muscle Force

Osborn et al. [1985] presented one of the first three dimensional linear programming models of the TMJ. As mentioned earlier, a single human skull was used to do the

modelling. A symmetric bite force was placed in various occlusal positions on the mandible. The linear program predicted the muscle forces in which the objective function was to minimize the **total** muscle tension. The bite force (direction and magnitude) must act as the force initiator or the solution would be trivial (all muscle and joint loads equal to zero). Once this was done the resultant condylar joint reaction forces were calculated. Osborn's twenty-six muscle forces, 13 per side, were applied to the mandible as previously described. Due to the high degree of symmetry resulting from a bilateral bite and a near symmetrical skull, the more complicated 3D model was effectively turned into a simpler 2D representation in the midsagittal plane.

For this investigation, a full 3D model complete with unilateral occlusion also attempts to minimize the total muscle tension. The muscle groupings are different from Osborn and Baragar's set. Appendix B has a complete break down of how each muscle and muscle group were divided.

The linear programming model does the following:

Find all the positive muscle tensions, $F_{muscle_i} \geq 0$, $i = 1...14$, that will minimize the physiologically based objective function, $f(F_{muscle_i})$

$$f(F_{muscle_i}) = \sum_{i=1}^{14} F_{muscle_i}, \qquad\qquad 3.9$$

subject to the following linear constraints:

$$-\sum_{i=1}^{14} Fx_{muscle_i} - \sum_{j=1}^{2} Fx_{joint_j} = Fx_{bite} ,$$

3.10

$$-\sum_{i=1}^{14} Fy_{muscle_i} - \sum_{j=1}^{2} Fy_{joint_j} = Fy_{bite} ,$$

3.11

$$-\sum_{i=1}^{14} Fz_{muscle_i} - \sum_{j=1}^{2} Fz_{joint_j} = Fz_{bite} ,$$

3.12

$$-\sum_{i=1}^{14} Mx_{muscle_i} - \sum_{j=1}^{2} Mx_{joint_j} = Mx_{bite} ,$$

3.13

$$-\sum_{i=1}^{14} My_{muscle_i} - \sum_{j=1}^{2} My_{joint_j} = My_{bite} ,$$

3.14

$$-\sum_{i=1}^{14} Mz_{muscle_i} - \sum_{j=1}^{2} Mz_{joint_j} = Mz_{bite} ,$$

3.15

$$F_{muscle_i} \geq F_{saturation_i} ,$$

3.16

for $i = 1,...,14$. Equations 3.10 through 3.15 will be referred to as the static constraints. These are used in each of the models presented here. The bite force acts as the force originator while the remaining unknowns, muscle tension and joint loads, balance this in order to minimize the total muscle tension. The last constraint, Equation 3.16, provides a biological limit for each muscle. It is unrealistic to assume that a muscle can create infinite muscle tension. Pruim et al. [1980] determined the maximum tension each masticatory muscle could generate. The muscular data used in the linear programming aspects of this study are also presented in Appendix B.

Once the muscle directions are known, the bite force initiated, and the condylar reaction points are located, it is possible to allow the linear program to determine muscle recruitment levels. For comparison, a occlusal location was taken at the left first molar on the first skull in the skull series of 68. At small intervals (5-25 N), the bite force acting perpendicular to the occlusal plane was raised from zero to its maximum possible without overloading the muscles. The muscle activation pattern for this objective function, bite location, and skull are shown in Figure 3.5.
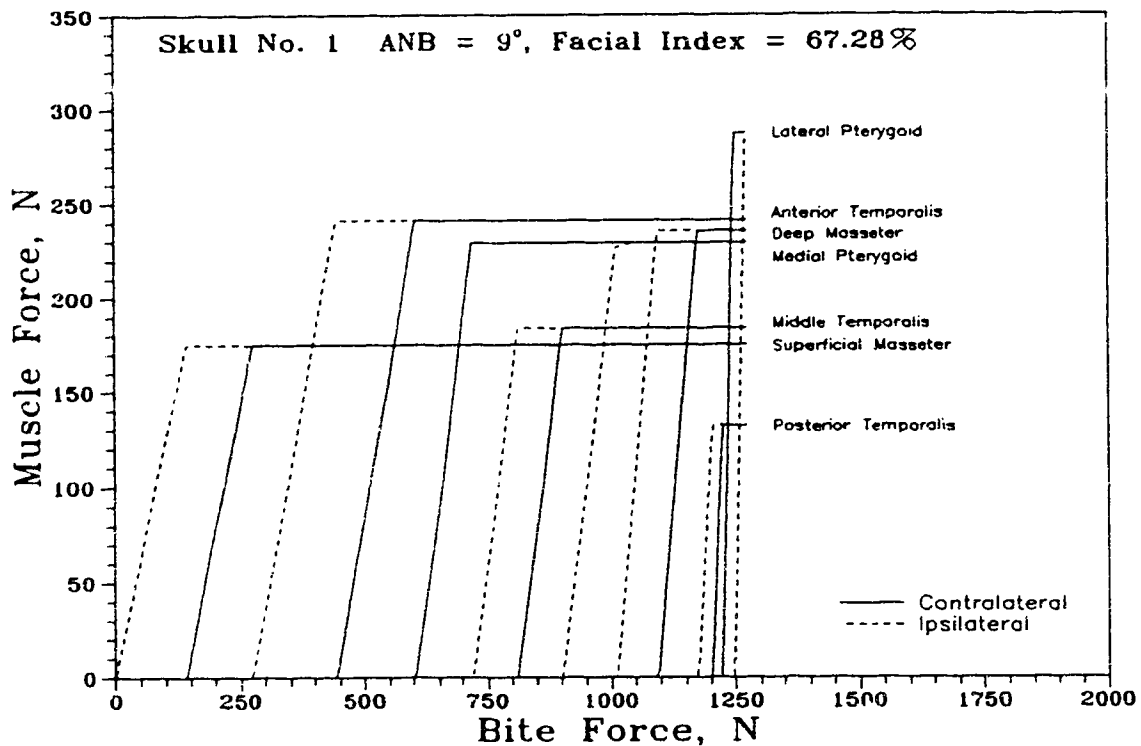
Figure 3.5 Muscle Recruitment for Minimizing Total Muscular Tension

This sequential recruitment pattern is indicative of the previous model presented by Osborn and Baragar. The muscles having the best moment advantage are those furthest

from the intercondylar axis, the axis through both poles of the condyles. This *rippling* effect is seen when these muscles are activated prior to those with shorter moment arms. This model suggests that there are two main types of muscles of mastication. *power* muscles and *control* muscles. The power muscles, usually the first to be activated in this model, are the masseters, medial pterygoid, and the anterior and middle portions of the temporalis. They tend to move the mandibular condyle along the articular eminence while the control muscles, posterior temporalis and the lateral pterygoid attempt to prevent this type of action. Their shorter moment arms are better at translating and stabilizing the condyle and articular capsule during forceful occlusion.

Previously, because of symmetry, the model Osborn and Baragar used did not distinguish between left and right muscle activation patterns. As shown here, many of the left muscles are activated prior to the right and the system appears to be operating as expected. Once a muscle is activated, it contracts to its prescribed saturation level at which time another muscle then begins its climb to maximum muscle tension. The model is saturated when all the muscles are fully tensioned at their predetermined maximum levels. This particular skull obtained a maximum bite force of 1271.5 N. This value is within the range that Pruim's test subjects bit on their first molars (range = 609 N - 1308 N) during his collection of maximum muscle tension data.

The joint load magnitudes from the same skull are shown in Figure 3.6. This peculiar pattern is a result of the sequential recruitment pattern of the muscles. The contralateral load seems to be consistently higher (after a certain level is reached) than
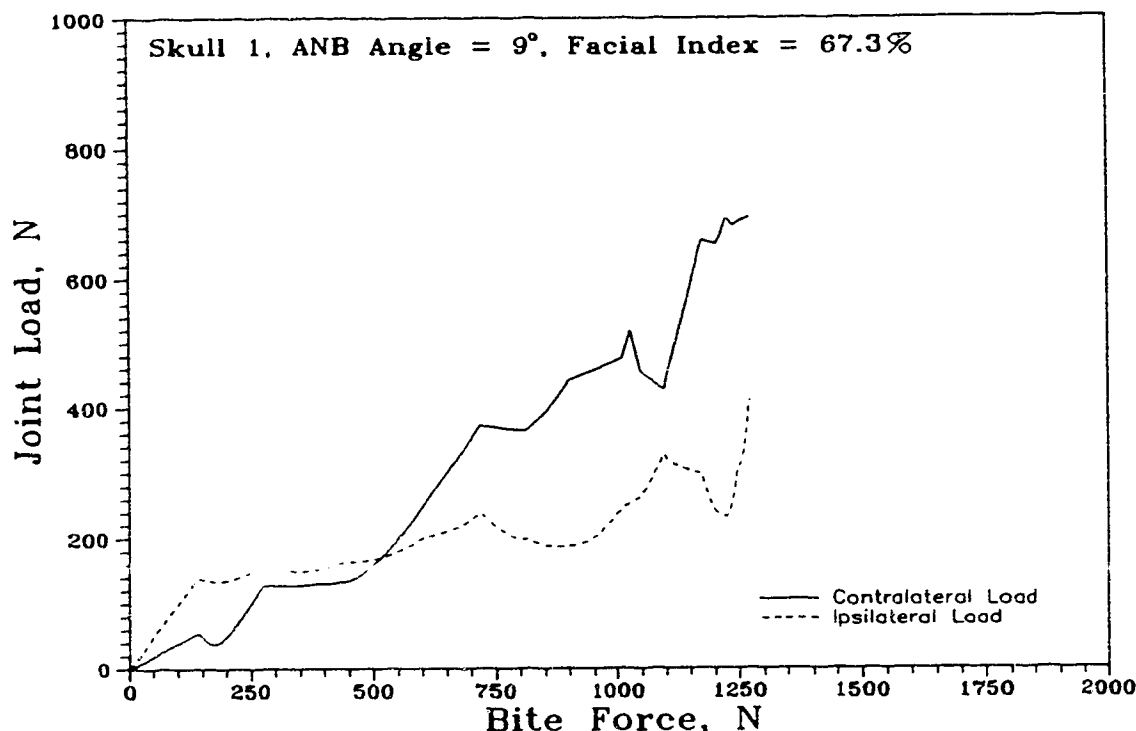
Figure 3.6 Resultant Joint Load Magnitudes for Minimizing Total Muscular Tension

the ipsilateral load. At full muscle usage, the balancing side joint load is 694 N while the working side joint load is 409 N. The result shows that for this skull the contralateral joint load is 1.7 times that of the ipsilateral. This correlates well with previous results given by Faulkner et al. [1987], Koolstra et al. [1988], and McEvoy [1989] since these investigators also found that the balancing side joint load magnitude was higher than the working side joint load. The maximum joint load, the contralateral, was 55% of the maximum bite load achieved by this skull while the ipsilateral load was 32% of the total bite load.

The resultant joint load angles for both joints are shown below in Figure 3.7.
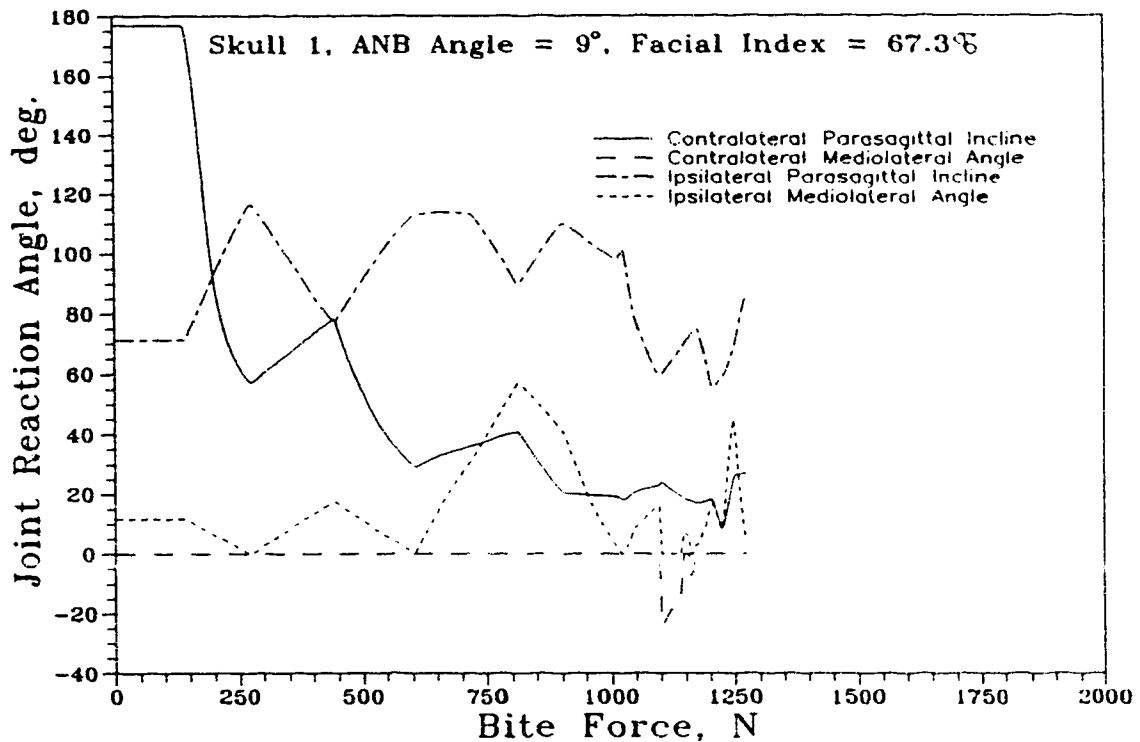
Figure 3.7 Resultant Joint Load Angles for Minimizing Total Muscular Tension

These are not as expected. At low bite forces, only the ipsilateral superficial masseter is activated. This generates a torquing of the mandible about the Y-axis which causes the ipsilateral joint to be loaded in compression and the contralateral joint is in tension-away from the condyle rather than towards it. This is seen in the TMJ loading directions in Figure 3.7. As the bite force grows, more muscles are recruited on both sides of the skull. This has the effect of providing compressive loads at both TMJs. At maximum muscular activation, the contralateral parasagittal load direction is 27.0° (from vertical) with no mediolateral component which is closer to the anticipated direction. The

ipsilateral load, while varying somewhat as the bite force increases, acts with a parasagittal incline of approximately 85° (nearly parallel to the FH plane). The mediolateral components for both joints are small during the entire bite force range and the directions a: just slightly out of the Sagittal Plane.

These uncommon joint loading directions are due to the rippling muscle activation pattern (sequential muscular recruitment rather than continuous) and is characteristic of this model. Osborn and Baragar's investigation constrained the joint load direction and this approach limited the unrealistic behavior. This was not done in the current application.

3.4.3 Minimizing Muscle Forces

J.H. Koolstra et al. [1988] presented a linear programming model to predict the maximum possible bite forces. One cadaver was used to derive the spatial relationships of the muscles and temporomandibular joint. Their three dimensional model investigated both unilateral and bilateral occlusal modes for differing bite and mandibular positions in which 16 muscle forces and 2 constrained (direction was constrained) joint loads were forecast based upon a model designed to minimize the *relative activity* of the most active muscle. Each muscle was determined to have its own characteristic saturation level (see Appendix B). For any given bite force, the ratio of that force, F_{muscle_i} relative to its saturation level, $F_{saturation_i}$ is termed the *relative activity*.

For this study, Koolstra's formulation would be to: Find all the positive muscle

tensions, $F_{muscle_i} \geq 0$, $i = 1,...,14$, that will minimize its relative activity; hence, the objective function would be:

$$f(F_{muscle_i}) = maximum \left[\frac{F_{muscle_i}}{F_{saturation_i}} \right], \qquad 3.17$$

for $i = 1,...,14$.

This objective function is not suitable for the Simplex Algorithm used in this investigation since the existing function (Equation 3.17) is discontinuous. This means that since each $F_{saturation_i}$ is an input variable and unchangeable once the optimization is initiated, more than one objective function would exist. The algorithm is allowed to change only the muscle tensions but the model may be rewritten to obtain the same goal. The *new* objective function would minimize the following:

$$f(F_{muscle_i}) = \mu_{global}, \qquad 3.18$$

where μ_{global} is the *global relative activity* of the muscles. This type of objective function requires additional constraints which are represented as

$$\left[\frac{F_{muscle_i}}{F_{saturation_i}} \right] - \mu_{global} \leq 0, \qquad 3.19$$

for $i = 1,...14$. *All* of the relative muscle activities must be less than or equal to μ_{global}. The remaining constraints, equations 3.10 through 3.16, describe the static constraints and the saturation limits of each muscle and are utilized again in this model increasing the total number of constraints to 34.

For this type of objective function, the muscle recruitment pattern is shown in Figure

3.8. (Skull #1 only). As the bite force acting perpendicular to the occlusal plane
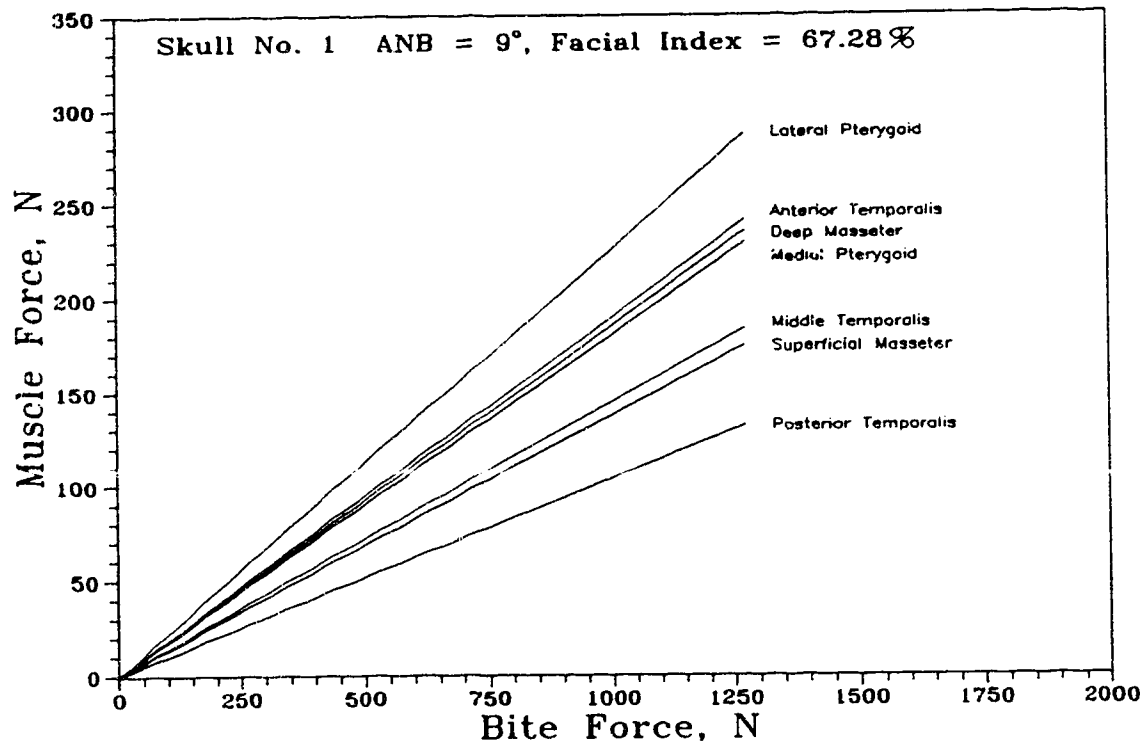
Figure 3.8 Muscle Recruitment Pattern for Minimizing *Relative* Muscle
Activity, μglobal

on the first left molar increases from zero to the maximum obtained with this skull

(1271.5 N), the muscles responded linearly and are simultaneously saturated at maximum

bite. Osborn and Baragar's formulation showed a different initial activation pattern but

converged to the same solution once all the muscle were required to saturate. As

determined by Koolstra, the entire system is linear which showed the maximum bite

force could be determined from Equation 3.20.

$$F_{\text{maximum bite}_i} = \frac{1}{\mu_{\text{global}}} F_{\text{bite}_i} \cdot \qquad\qquad 3.20$$

The present study however was not interested in only the maximum bite force but also the characteristics of each model during loading. The muscle recruitment order resulting from minimizing the global relative muscular activity correlates quite well with the experimental work of Van Eijden, Brugman, Weijs, Oosting, [1990] who measured EMG activation levels on seven test subjects. Using transducers to measure the bite force and direction, he related bite force and muscle activity as functions of magnitude, direction, and occlusal position. They concluded that the muscles of mastication would behave *linearly* irrespective of bite force location and direction when the bite was greater than 50 N and that for vertical unilateral occlusion, only a small difference between ipsilateral and contralateral muscle activities was noticed. Minimizing μ_{global} showed no difference between left and right muscle activations for this bite condition. The activity of the muscles relative to one another remains constant for the entire range and is similar for all the skulls tested since μ_{global} is a linear function of the bite force. These model characteristics are due to the joint loads being unconstrained in direction.

The magnitude of the loads on the temporomandibular joints are shown in Figure 3.9. This model is to be linear both with muscle tensions and again with respect to the joint loads. The resulting contralateral/ipsilateral load ratio at maximum bite force is 1.7 and is consistent throughout the entire range of bite force. This value at maximum bite force is identical to the model reformulated from Osborn and Baragar's hypothesis since
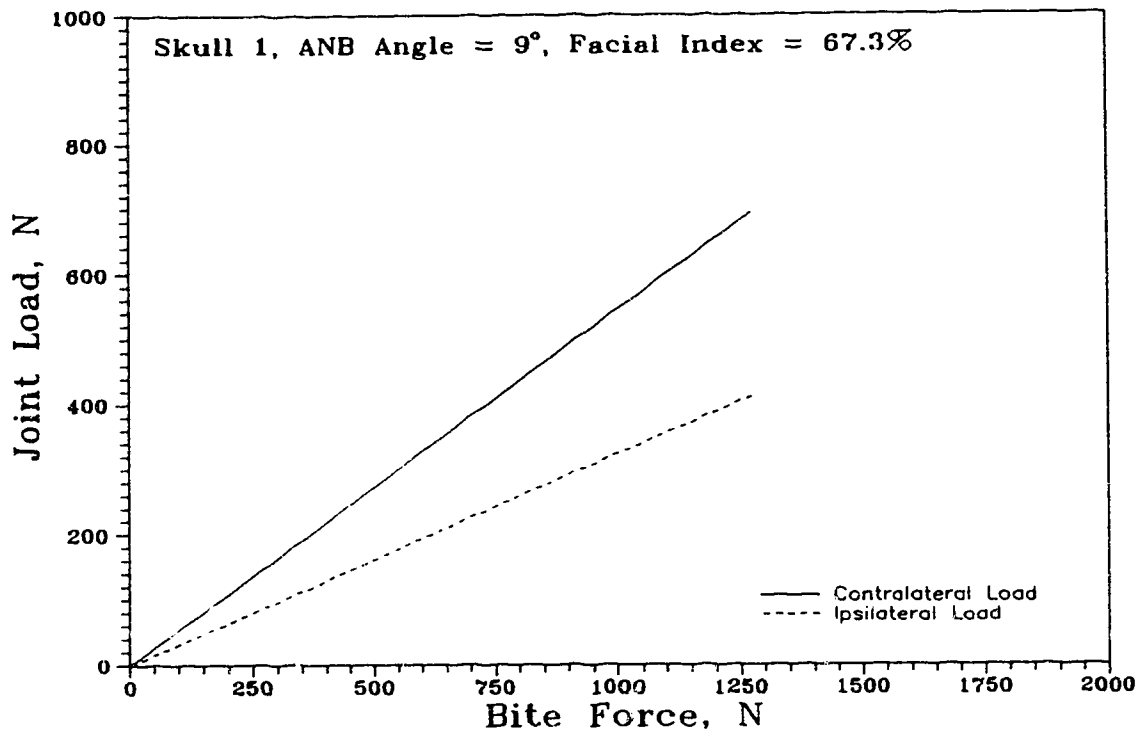
Figure 3.9 TMJ Load Magnitudes for Minimizing *Relative* Muscular Activity,
μglobal

both models allowed the entire muscle set to saturate.

The directions of the joint loads (refer to Figure 3.3 for conventions used) are demonstrated in Figure 3.10. In the sagittal plane not only were the magnitudes linear over the entire bite range but they also maintained the same loading angles with respect to the eminentia. The ipsilateral and contralateral joint loads were loaded at 84.8° and 27.0° respectively from the vertical Coronal plane. These sagittal components of joint loads were essentially constant in all the skulls investigated and showed no significant variations in directions over the entire bite load range. The mediolateral components of
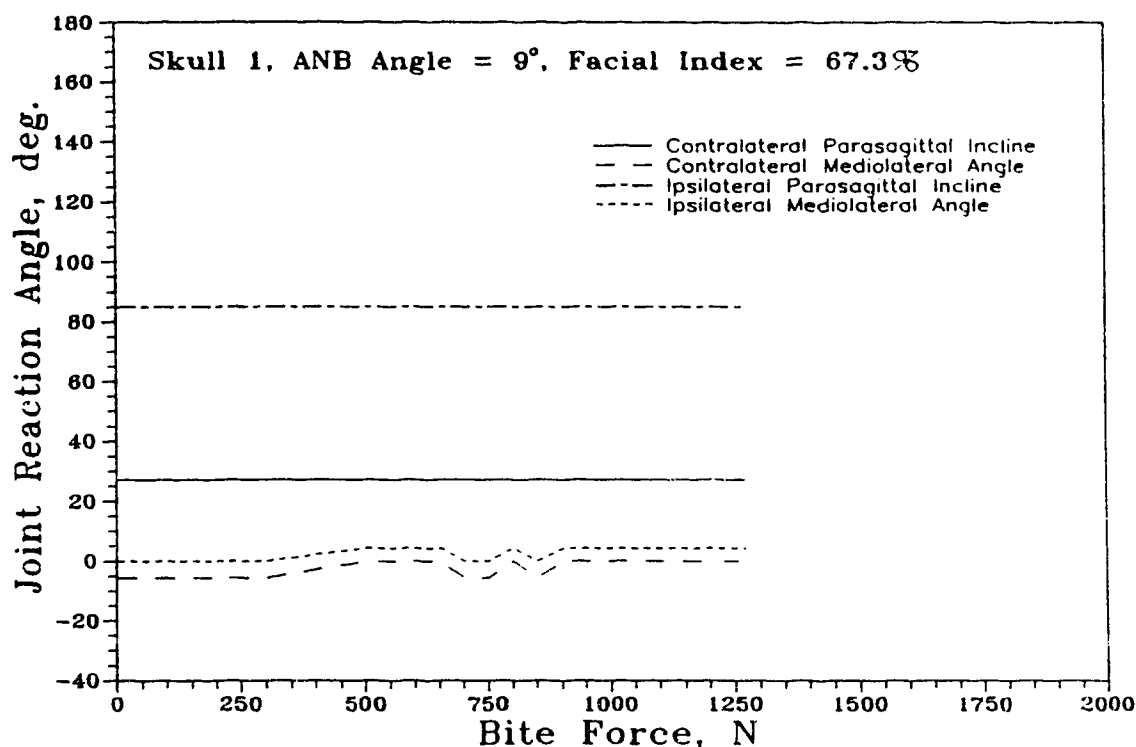
Figure 3.10 Joint Load Angles for Minimizing *Relative* Muscular Activity

the joint loads were only 2.3% of the maximum bite force achieved. From Figure 3.10 it is seen that these components shift irregularly from the condyles. The complexity of the muscular system and this objective function causes these minor anomalies in the model.

Minimizing the relative activity of the most active muscle when the joints are unconstrained leads to linear increases in muscle activation and joint loading as the bite force increases. No differences were found in the ipsilateral and contralateral muscle tensions for unilateral biting perpendicular to the occlusal plane. Unless a method of

constraining the joint loading direction is used, this linear symmetric behavior will be the muscle recruitment pattern for this objective function.

3.4.4 Minimizing the Stress in the Maximum Stressed Muscle

K. N. An et al. [1984] introduced a mathematical technique to solve the indeterminate problem of calculating the muscle and joint loads during flexion of the complex elbow joint. To obtain a unique solution, An et al. uses an optimization approach which minimizes an upper bound of muscular stress. This technique individualizes each muscle fiber by using muscle stress instead of muscle force since stress is measured on a per unit area basis. During the elbow investigation, this modified linear optimization model proved to be both mathematically and physiologically superior when compared to other linear and nonlinear optimization methods since convergence to a solution was almost always guaranteed and muscle coactivation occurred regularly.

An et al. suggested the proposed method, introduced only a 2D model, would be feasible for more sophisticated 3D modelling of joints. When applied to the temporomandibular joint, again the unilateral bite acted as the force initiator while the muscles worked together to *minimize* the upper bound of muscular stress. The muscular stress is defined as the ratio of muscle force, $Fmuscle_i$, to its predetermined physiological crossectional area, $PCSAmuscle_i$.

The objective function would be minimize the following:

$$f\,(F_{muscle_i}) \;=\; maximum \left[\frac{F_{muscle_i}}{PCSA_{muscle_i}}\right], \qquad\qquad 3.21$$

for i = 1,...,14. This is identical to the Koolstra et al., [1988] initial formulation with PCSAmuscle$_i$ replacing Fsaturation$_i$ in the denominator of the function. Again this objective function must be rewritten to accommodate the algorithm since each PCSAmuscle$_i$ is unchangeable and leads to multiple objective functions. The revised objective function would be to minimize the *global muscular stress* and is written

$$f\,(F_{muscle_i}) \;=\; \sigma_{global}. \qquad\qquad 3.22$$

This upper bound of muscular stress, σglobal, limits *all* the muscles since each must be less than or equal to this value. This leads to the additional constraints shown as

$$\left[\frac{F_{muscle_i}}{PCSA_{muscle_i}}\right] - \sigma_{global} \leq 0, \qquad\qquad 3.23$$

where the physiological crossectional area is considered to be directly related to muscle force. The remainder of the equations are the same as the Osborn and Koolstra reformulations which lead to a total of 34 constraints.

Minimizing global stress effectively attempts to minimize the individual force each muscle fiber exerts. In fact, from Figure 3.11, it is seen that the relative activation depends only upon the physiological crossectional area of each muscle since muscular stress increases linearly with bite force. This relationship holds true until some of the
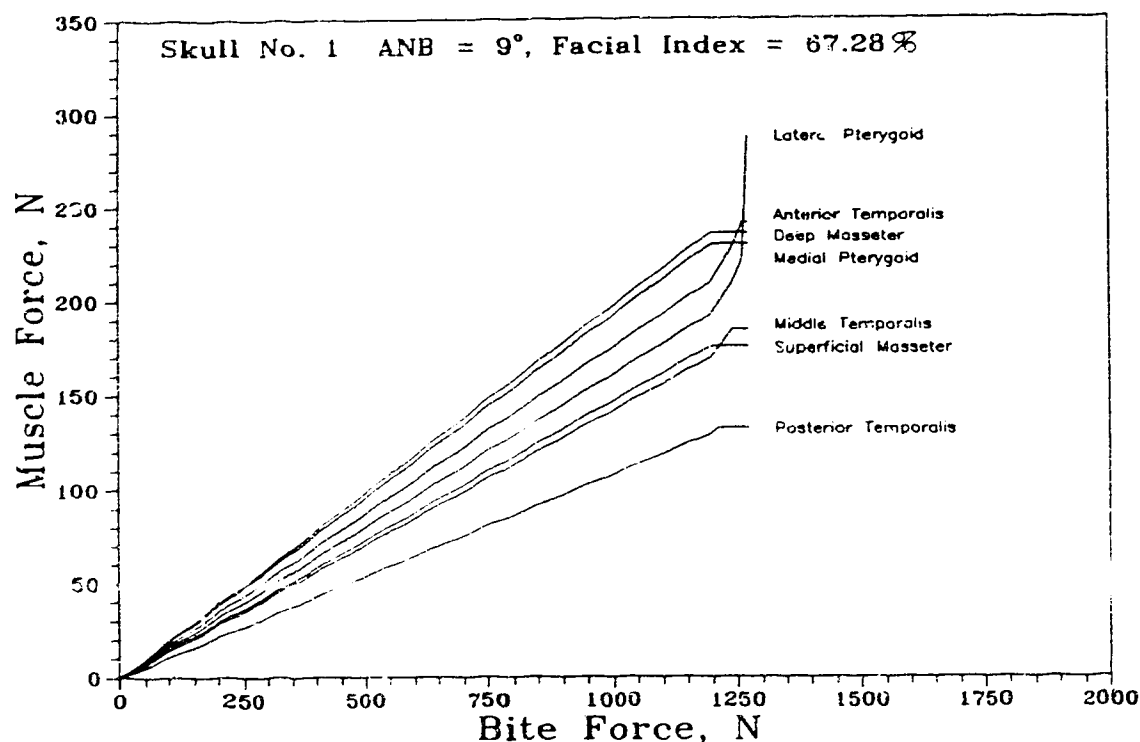
Figure 3.11 Muscle Recruitment Pattern for
Minimizing Global Stress, σ global

muscles, namely the posterior temporalis, masseter, and medial pterygoid, begin to saturate. The remaining muscles are permitted to maintain higher levels of stress as Pruim's work suggests (shown in Appendix B). The stresses of all the muscles are identical for *all* muscle groups until this threshold is reached. The muscle's initial relative activation depends on the physiological crossectional area of each muscle, ie. the muscle with the largest area (deep masseter) will be able to take the largest load. Again, all the muscles are able to contribute to the bite force and therefore reach the same saturation levels that the previous linear programming models reached (maximum bite

force of 1271.5 N). The joint loads are unconstrained which allows the model to maintain symmetrical ipsilateral and contralateral muscular stresses as was the case in the Koolstra model. The linear muscle activation shown here compares with the experimental work of Van Eijden et al., [1990], who showed that for a unilateral bite in the molar region, the working and balancing side muscles showed no significant differences in EMG activity. This model again showed right and left muscles having equal tension.

The joint loading patterns are shown in Figure 3.12. The initial joint loading of contralateral to ipsilateral is 1.9 and decreases to 1.7 at the end of the saturation phase. The ipsilateral joint load increases sharply once this phase is reached.

Each joint appears to be loaded in a stable manner in as much as their loading directions are constant again until the saturation range is approached. From Figure 3.13, the parasagittal inclines shift approximately five degrees between the bite force of 1250 and 1270 N. This 5° shift aligns the contralateral joint load closer to ideal (see Figures 3.2 - 3.3) but places the ipsilateral joint load in a more horizontal direction. The latter orientation generates shear forces which may be detrimental to the health of the posterior band of the articular disc. Most of the bite range (0 - 1250 N) show results similar to those of Koolstra's formulation in as much as the joint load directions are constant. Even the small shifts of the mediolateral components were present but appeared more jagged. Smaller steps in bite force could be attained with this model compared to the Koolstra case since convergence to a solution was more likely to occur with minimizing σ_{global}.
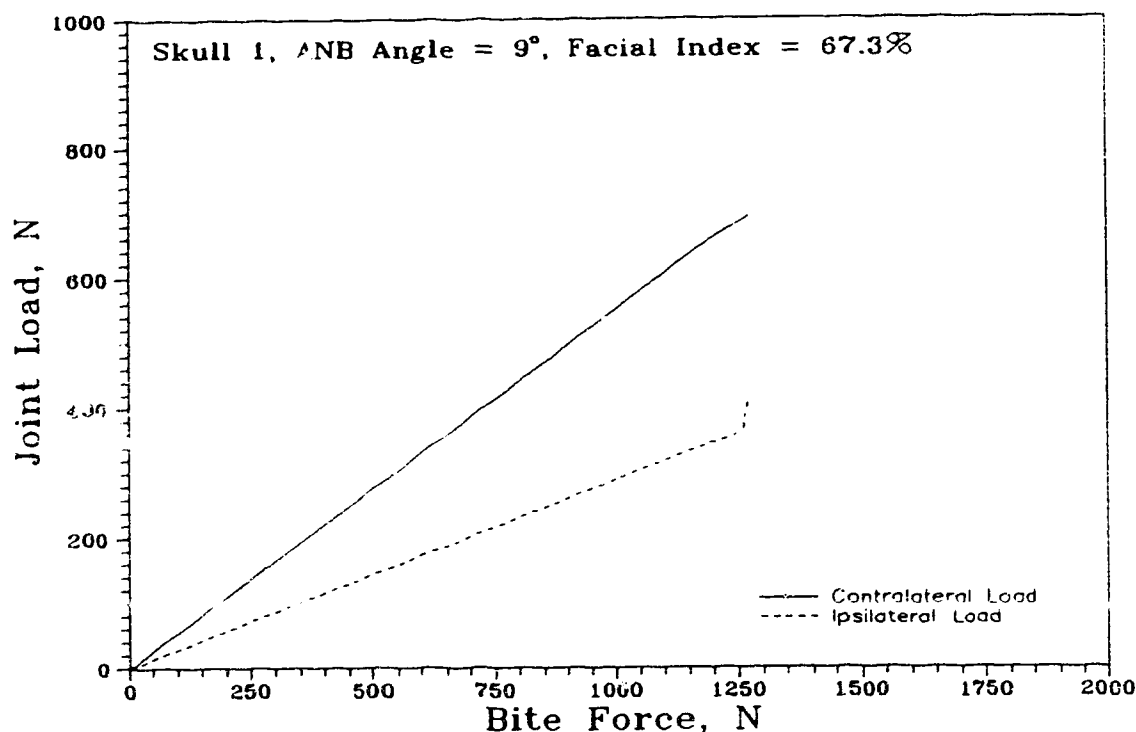
Figure 3.12 Joint Loading Pattern for Minimizing σ global

Formulation of An's elbow model for the TMJ illustrated results that compared to experimental work [Van Eijden et al., 1990]. Coactivation, muscular tension symmetry, and linearity of muscular response occurred in the experiments done on his elbow model. At maximum joint load. An's TMJ load magnitudes compared identically to both Osborn and Baragar's as well as Koolstra's application to the same problem once saturation of all the muscles was realized.
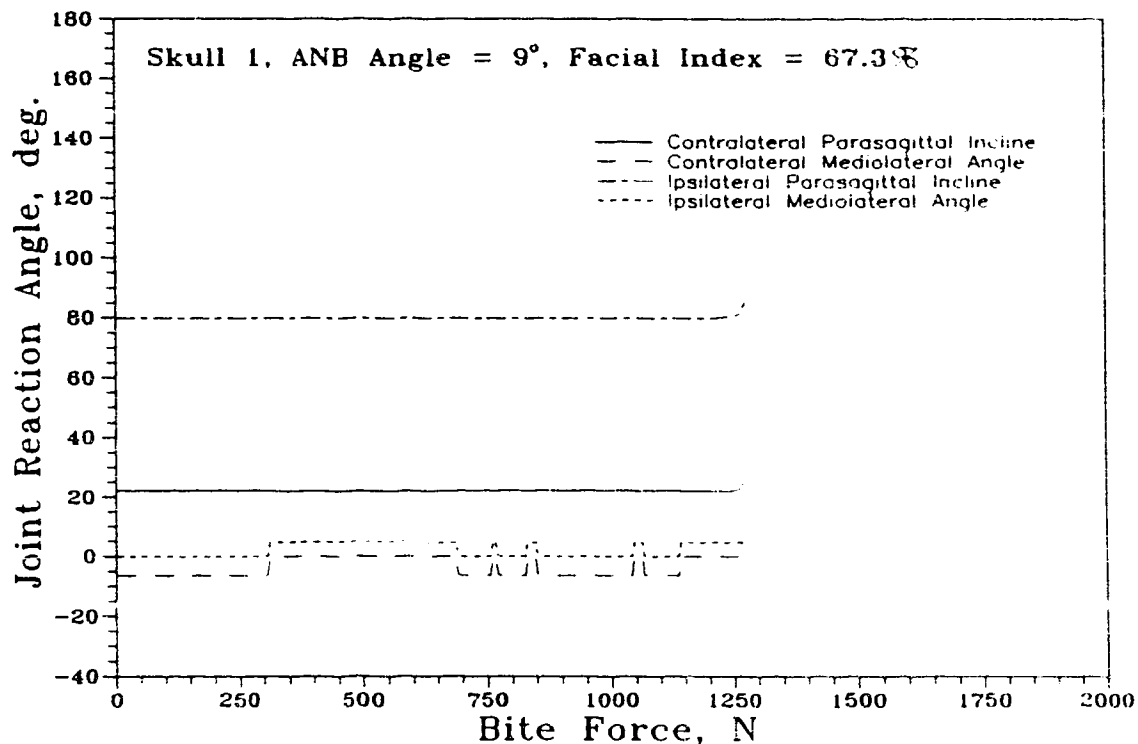
Figure 3.13 Joint Loading Directions for Minimizing σ global

3.4.5 Pragmatic Model

As an alternative to the use of some physiologically based objective function, Hay [1986] and McEvoy [1989] used estimates of the *relative* nature of muscle tensions to gain an understanding of the mechanics of the masticatory system. A combination of EMG information [Carlsöö, 1952; Møller, 1970; Mushimoto, Mitani, 1982; Pruim et al., 1978] and physiological crossectional areas of the muscles of mastication [Pruim et al., 1978; Schumacher, 1961] was used to predict the muscular tensions for a certain occlusal scenario.

Knowing the muscle magnitudes reduces the number of unknowns in the static model from 21 to seven. With the 14 muscles tensions given, there are seven remaining unknowns to determine; the bite force magnitude (bite force direction is an input variable) and the six components of joint load. The six equations of statics (Equations 3.1 - 3.6) are not adequate to solve the indeterminate problem; therefore, an additional assumption is used. This additional constraint divides the mediolateral joint load component evenly amongst the two joints (recall for the linear programs that all the mediolateral component was taken by *only* one of the two joints which lead to some irregularities in the models). This assumption has little effect on the result since the mediolateral components are small relative to the other components [Faulkner et al., 1987]. With seven equations and an equal number of unknowns, the problem could be solved.

For occlusion in the molar region, the relative muscle magnitudes used in this investigation of the pragmatic model are shown in Figure 3.14 [McEvoy, 1989]. The relative values of muscle tensions sum to 100 arbitrary load units. For example, the ipsilateral deep masseter would carry 13.7% of the entire muscular input. The bracketed terms are the actual muscle forces used in this study. The ipsilateral deep masseter is the only muscle that saturates during the normalization. From initial EMG examination [Carlsöö, 1952; Møller, 1970; Mushimoto et al., 1982; Pruim et al., 1978], asymmetry in muscular activation was supplied to the model. The ipsilateral supports 55% of the total muscular input while the contralateral side is required to carry the remaining 45%.
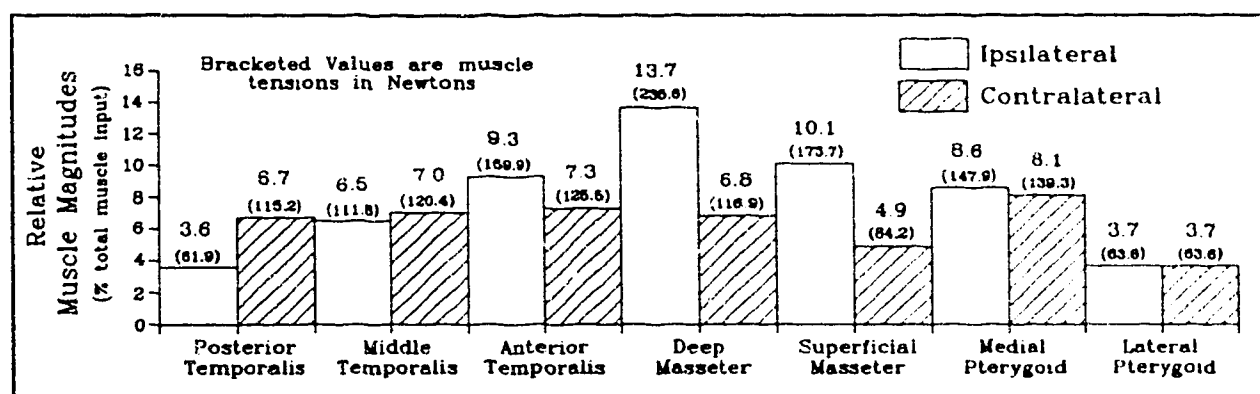
Figure 3.14 Relative Muscle Magnitudes based on EMG and Muscle Areas

Since these relative muscle forces are assumed constant during occlusion, it is obvious that there will be linear coactivation of all muscle groups which will be similar for the entire bite range.

The normalized muscular tensions cannot provide the same bite force as did the other models since only one (the ipsilateral deep masseter) of the 14 muscles can be assumed to be saturated. As a result, a bite force of only 819 N could be achieved with this skull which is a 36% drop from 1271 N achieved by all the linear programs due to a 42% drop in muscle tension.

This drop in total muscular input is also seen in the resultant joint loads. Figure 3.15 shows immediately that the contralateral/ipsilateral load ratio, now 1.1, has changed significantly from the linear programming models. With these predetermined muscle forces, the joints are loading the skull in a symmetrical fashion in as much as the magnitudes of the joint loads are concerned.

Figure 3.16 shows the joint reaction angles resulting from the static model. The
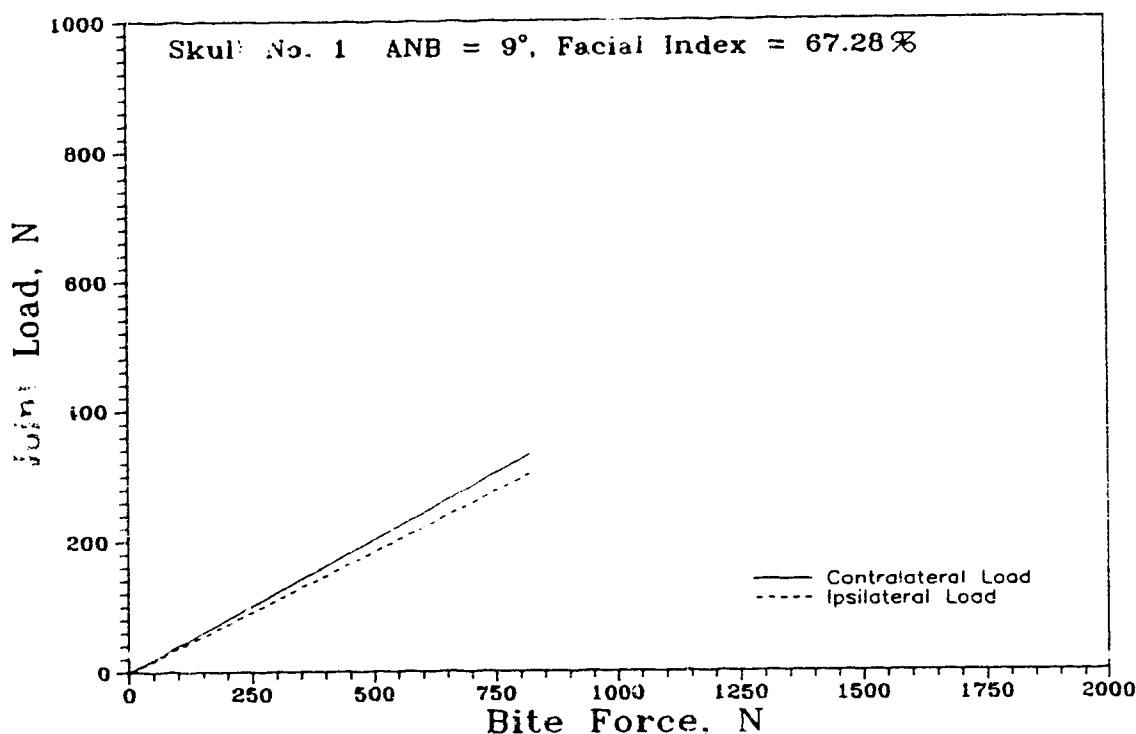
Figure 3.15 TMJ Load Magnitudes for Pragmatic Model

ipsilateral parasagittal incline was 54° while the contralateral incline was found to be 10°. Using the digitized region of the ipsilateral articular eminence in the sagittal plane and its respective joint loads is calculated to have a misalignment of -2.6° (see Figure 3.3 for alignment conventions). This is to be expected since the digitized region *may not* include the point at which the contralateral load is actually applied. As a result on the ipsilateral side, this particular model aligns this joint load in a way which nearly eliminates the shear component of the joint load. Comparison of the joint loading angles between the various models and the measured values will only be done with the ipsilateral joints since the digitized region of the articular eminence describes the area
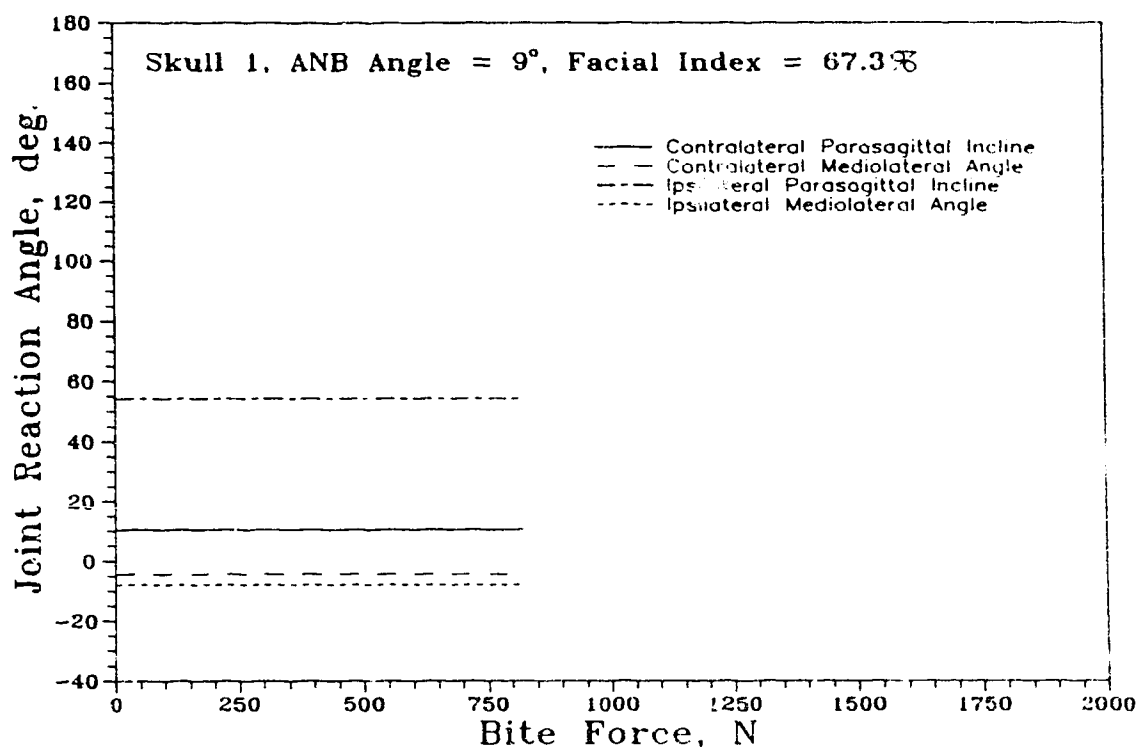
Figure 3.16 Joint Loading Angles for Pragmatic Investigation

where this joint will react. During unilateral occlusion, the lower jaw performs a small lateral excursion towards the ipsilateral side in order to align the cusps of the upper and lower teeth for chewing. For a left excursion, there is a medial and anterior shift of the right condyle while the left condyle moves laterally. This motion is termed the *Bennett movement*. Since the contralateral condyle shifts anteriorly, it articulates with the glenoid fossa along its inferior curved portion. The contact point where the eminence and the condyle communicate is difficult to determine, therefore, checking the predicted load application angle was not accomplished.

When the skulls were screened for digitization, symmetry was a major concern. For this reason the mediolateral components (24 N per joint at maximum bite) are small. They do not cause the overall TMJ reaction to stray significantly from the sagittal plane on either side.

This pragmatic evaluation derives one resultant muscle vector per skull regardless of occlusal location and bite angulation. This model would break down if, for example, significant bite angulations were investigated without further researching muscle EMG data for these occlusal modes. As a result, only bites nearly perpendicular to the occlusal plane can be investigated and this was done to discern skull morphological differences by McEvoy [1989].

3.5 Summary of Temporomandibular Joint Modelling

Of the four models considered, three used linear programming tactics and one used a pragmatic strategy to determine the joint loading characteristics (magnitude and direction) of one skull for a single occlusal mode (a vertical bite on the first left molar).

Each of the linear programming models allowed full muscular activation (all muscles could saturate if required) and, since any particular muscle was able to contribute to the bite force, eventually the entire set of masticatory muscles saturated. Once this state was reached, all the models gave identical results (see Figure 3.17) As mentioned, all the muscles have saturated and their relative exertions based upon 100% total muscle input are very different from the pragmatic model's results (see Figure 3.14). Figure 3.17 also illustrates the symmetric force contribution of the muscle pairs during forceful occlusal

contact. Coincidentally, the largest TMJ loads were also realized with the linear

programming approaches when the maximum bite force was attained. It is this condition,

full muscle activation, that will be used to analyze the set of 68 skulls.
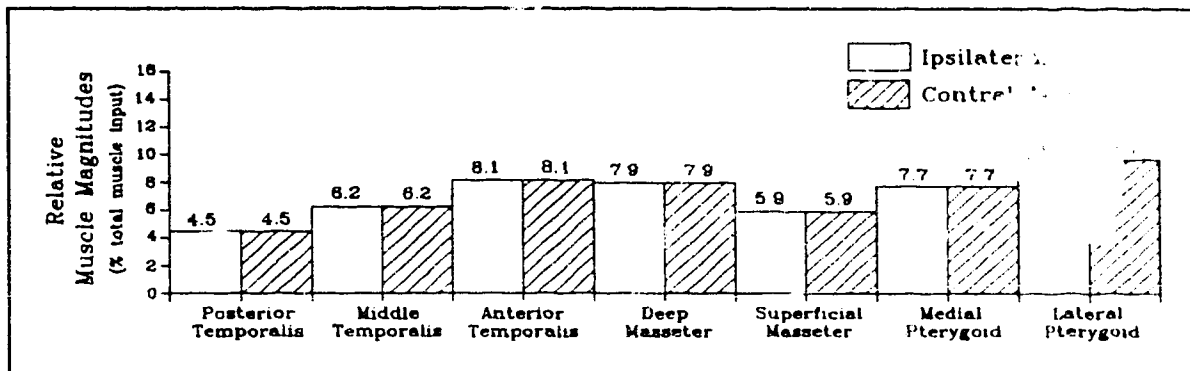
Figure 3.17 Linear Programming Muscle Activation at Maximum Bite Force

In analyzing each of the skulls for each of the linear programming models, no

significant differences were noticed in muscular activation patterns. Occasionally, the

muscle recruitment pattern of Osborn and Baragar's model would indicate muscle

recruitment in a different order but ultimately would saturate the entire set of muscles.

The shift in recruitment order had only minor effects on joint load magnitudes and

directions over the range of bite forces. Minimizing the global relative muscular activity,

μglobal (Koolsi et al.), and the global muscular stress, σglobal (An et al.), produced

consistently linear results in activation patterns and joint loading for all skulls

investigated.

Table 3.1 gives the averages, range, and standard deviations of the loads determined

by the two different types of models when applied to the total sample of 68 skulls (all

linear programs converge to the same solution) and can also be graphically interpreted

in Figure 3.18. The C/I Ratio is the ratio of loads between the contralateral and ipsilateral TMJs.

Because the muscle input is higher for the linear programming results than the pragmatic approach, larger occlusal forces are generated and consequently loading which may detrimental to the contralateral TMJ was noticed for all the skulls investigated. Hyiander [1975] found that a force of 610 N could break a condylar neck of a mandible. The ipsilateral load is considerably lower than all the contralateral loads since the minimum C/I ratio found was 1.4 for these linear models. The pragmatic method did not result in as large a load for either of the joints (maximum joint load = 505 N).

Table 3.1 Temporomandibular Joint Modelling
Resultant Load Summary
(68 Skulls)

	Linear Programming Models				Pragmatic Model			
	Bite Force (N)	Ipsilateral Load (N)	Contralateral Load (N)	C/I Ratio	Bite Force (N)	Ipsilateral Load (N)	Contralateral Load (N)	C/I Ratio
Average	1011	344	737	2.1	645	333	387	1.2
Minimum	659	138	652	1.4	418	249	332	0.93
Maximum	1347	610	862	4.8	831	505	469	1.56
Standard Deviation	105	71	50	0.58	67	37	30	0.13

This latter approach lowered the contralateral TMJ loads profoundly without changing the ipsilateral joint load average significantly. This was evident when the C/I ratio was halved by the latter model. The shading in Figure 3.18 shows that the standard deviations are higher for the linear programming models than the pragmatic strategy. The pragmatic model does not allow the muscle forces to vary relative to one another

therefore there is less overall variability. *Normalizing* the average joint loads as a percentage of the total bite force was done (see Figure 3.19). The average total joint loads are 107% and 112% of the bite force for the linear and pragmatic approaches
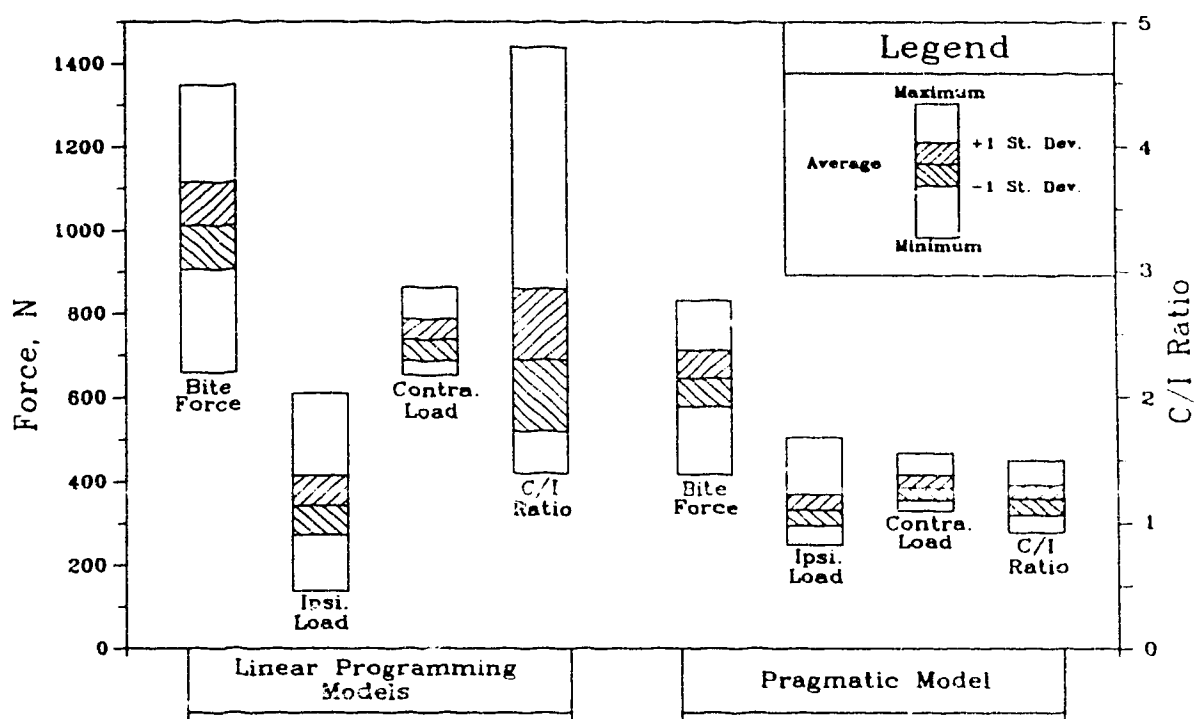
Figure 3.18 Graphical Summary of Occlusal and TMJ Loading from the Linear Programming and Pragmatic Modelling

respectively. This means that the models are not significantly different in total load transferred to the skull via the joints. The predominant difference is in the separation of the joints loads. The linear programming showed that the contralateral TMJ was loaded more than twice as much as the ipsilateral while the pragmatic approach allowed the joints to be loaded in a much more symmetric fashion with the contralateral joint being only 20% larger than the ipsilateral.
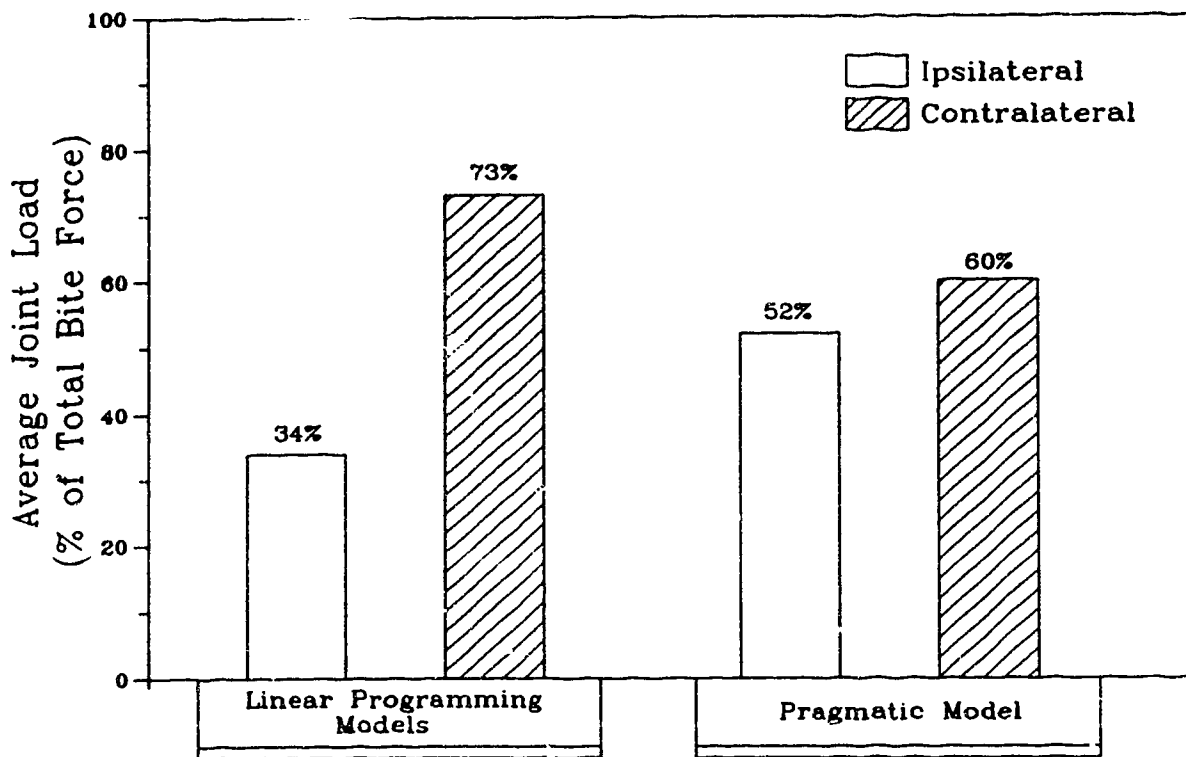
Figure 3.19 Average Normalized Condylar Joint Loads for the TMJ Models

By not constraining the temporomandibular joint loading directions, the opportunity for full muscle usage was available and achieved by **each** of the linear programming models. Each muscle was geometrically positioned so that it could (neglecting efficiency) generate additional occlusal force and in effect allowed every muscle to saturate. This lead to high joint loads with substantial misalignment when utilizing each optimizing criterion. The pragmatic approach had significantly lower and symmetrical (C/I ratio average 1.2) joint loads, albeit lower muscle tension. Theoretically, this approach can only be utilized when EMG data collected is for the specific occlusion mode to be investigated.

CORRELATION OF CRANIOFACIAL MORPHOLOGY AND TMJ LOADING

4.1 Introduction

Using the models developed for determining the temporomandibular joint reactions and bite forces along with the classification schemes outlined, it is possible to investigate whether the models show significant differences related to craniofacial morphology. In this chapter, an attempt is made to *linearly* correlate the loads obtained from the models with the numerous classifications schemes.

For simplicity, only bite forces acting perpendicular to the occlusal plane at the first left molar are used as the occlusal loading situation for these correlations even though this can limit the study of the human masticatory system [Koolstra et al., 1988]. By analyzing what is believed to be one of the most demanding loading conditions of the TMJ, static molar occlusion, approximately the highest TMJ loads are effectively being applied.

For each of the model types, the following variables are analyzed and correlated with the facial classification schemes:

i) Ipsilateral Load
ii) Contralateral Load
iii) Occlusal Force
iv) Misalignment of TMJ Load

The fourth variable shown is calculated by determining the angle between the resultant ipsilateral load and the approximated articular eminence. These loading results are the dependant variables in the correlations to follow.

4.2 Statistical Comparisons

The primary purpose of correlation analysis is to measure the strength of the relationship between the variables, in this case, between the facial morphology of a particular skull and its TMJ loading characteristics. The coefficient of linear correlation, R, is a measure of the strength of *linear* relationship between these variables. Squaring the correlation coefficient gives the product of correlation or coefficient of determination, R^2, indicating the proportion of the variation of the y's that can be attributed to the linear relationship with x. An example of perfect linear correlation is a situation where all the data would fall on a straight line. In contrast, if this *best-fit* line were horizontal or vertical, there is zero correlation showing that the variables are actually independent.

4.2.1 Pragmatic Model Correlations

Utilizing a vertical bite force perpendicular to the occlusal plane, the joint reactions can be determined from the predefined muscle tensions for each individual skull as was done in Chapter 3. The classifications schemes, introduced in Chapter 2, are used to

determine whether significant cause-and-effect relationships exist between these classes and the loading of the joints in the 68 skulls studied.

Table 4.1 tabulates the products of correlation for the comparisons made from the pragmatic TMJ model results and the 13 different facial classifications. The first three rows correlate actual loading results (eg. ipsilateral TMJ load) with the classes. Row 4 correlates the classes with the misalignment angle, α (see Figure 3.2). The sign of R^2 has been included to denote the *slope* of the resulting linear correlation with the independent variable (facial classification type). The arbitrarily shaded areas represent the R^2 values of less than 5.0% which can be considered truly insignificant. This group accounts for 33 of the 52 correlations. Row 5 gives the value of the facial classification which would result in perfect TMJ loading (i.e. zero shear forces), as predicted by the pragmatic model. For example, an **ANB** angle of -1.2° would theoretically align the TMJ loads with no shear component on the articular tissues. The shaded terms in this row represent predicted values which are out of the range of the 68 skulls tested. An example of this is the prediction of an **F-O** angle of 506°. This shows that the line was practically horizontal (no correlation).

Comparison of the ANB angles with the joint loading resultants has previously been done [McEvoy, 1989] but the skulls were classified as being in one of three groups to simplify results (see Chapter 2 for these groupings). His results showed that individuals with retrusive chins (Group II **ANB** $\geq$ 5.0°), displayed moderately higher temporomandibular joint loads with higher levels of joint misalignment while at the same

Table 4.1 The Products of Correlation[s] between Facial Classification Schemes and Results from the Pragmatic Model (Rows 1-4) with the Facial Classification Predictions for Zero Shear on the TMJ (Row 5) Shaded values represent R^2 values > 5% (Rows 1-4) and Values out of the range investigated (Row 5)

	ANB	FI	FLR	Gonial	Ao-Bo	F-O	F-M	S/Per	P/Per	A/Per	Ω	β	θ
Ipsilateral Load	+0.3	-3.2	-6.9	+0.0	-1.2	-4.1	+3.3	-28.5	+24.0	+8.7	-0.5	+17.4	-28.6
Contralateral Load	+1.1	-0.7	-0.1	+0.7	-2.9	-3.0	+0.9	-0.0	+5.6	-2.3	-8.9	+9.1	-0.1
Occlusal Load	-0.3	+13.3	+1.0	-2.4	+7.4	+9.5	-12.8	+8.5	-7.2	-2.6	+0.2	-5.6	+8.7
Ipsilateral Misalignment	+5.4	-1.2	-11.0	+3.9	-0.3	-0.0	+2.3	+0.1	-0.1	-0.0	+0.0	-0.1	+0.1
Zero-shear Prediction	-1.20	79.3	83.4	110	23.9	506	2.10	4.30	50.3	72.8	15.9	-130	-10.0

Legend:

ANB	- E.H. Angle's ANB Angle (SNA - SNB)
FI	- Facial Index (Facial Height Ratio)
FLR	- Facial Length Ratio
Gonial	- Gonial Angle
Ao-Bo	- Wit's Appraisal (Occlusal Plane distance)
F-O	- Angle between Frankfort Horizontal and Occlusal Plane
F-M	- Angle between Frankfort Horizontal and Mandibular Plane

S/Per	- Superior Length / Perimeter
P/Per	- Posterior Length / Perimeter
A/Per	- Anterior Length / Perimeter
Ω	- Omega (Angle between Sup. and Post. Sides)
β	- Beta (Angle between Sup. and Ant. Sides)
θ	- Theta (Angle between Post. and Ant. Sides)

[s]R^2 values given in percentage

time generating less occlusal force than the other groups. The same correlation illustrated that larger ANB angles resulted in higher TMJ loading. These same skulls could not produce as high occlusal forces as did skulls with protrusive chins. In the current correlation, the influence of ANB angle on the loading of the skull is relatively small. The correlation of ANB angle with the misalignment of the ipsilateral TMJ load and the articular eminence was very small ($R^2=5.4\%$) for the skull sample with the optimum ANB angle being $-1.2°$ (optimum meaning zero shear at the ipsilateral joint).

Facial Index, which measures the degree of facial divergence in the sagittal plane, implying that a low value of FI represents a divergent face while a large FI results in a squarer face. From Table 4.1 it is seen that squarer faces have lower TMJ loads (both condylar loads have a negative slope with increasing FI) while at the same time being able to generate slightly higher bite forces. In fact, the predicted FI with the best alignment characteristics would be one with a value of 79.3% which is a relatively square face.

The linear correlations of the magnitudes of the joint loads and the misalignment of the ipsilateral TMJ load were poor. The highest product of correlation came when comparing the bite force with FI in which 13.3% of the change in bite force can be explained by the variation in facial indices (Figure 4.1). The figure shows that while there is significant scatter in the results, there is a trend showing that a skull having large Facial Index is also able to bite harder.
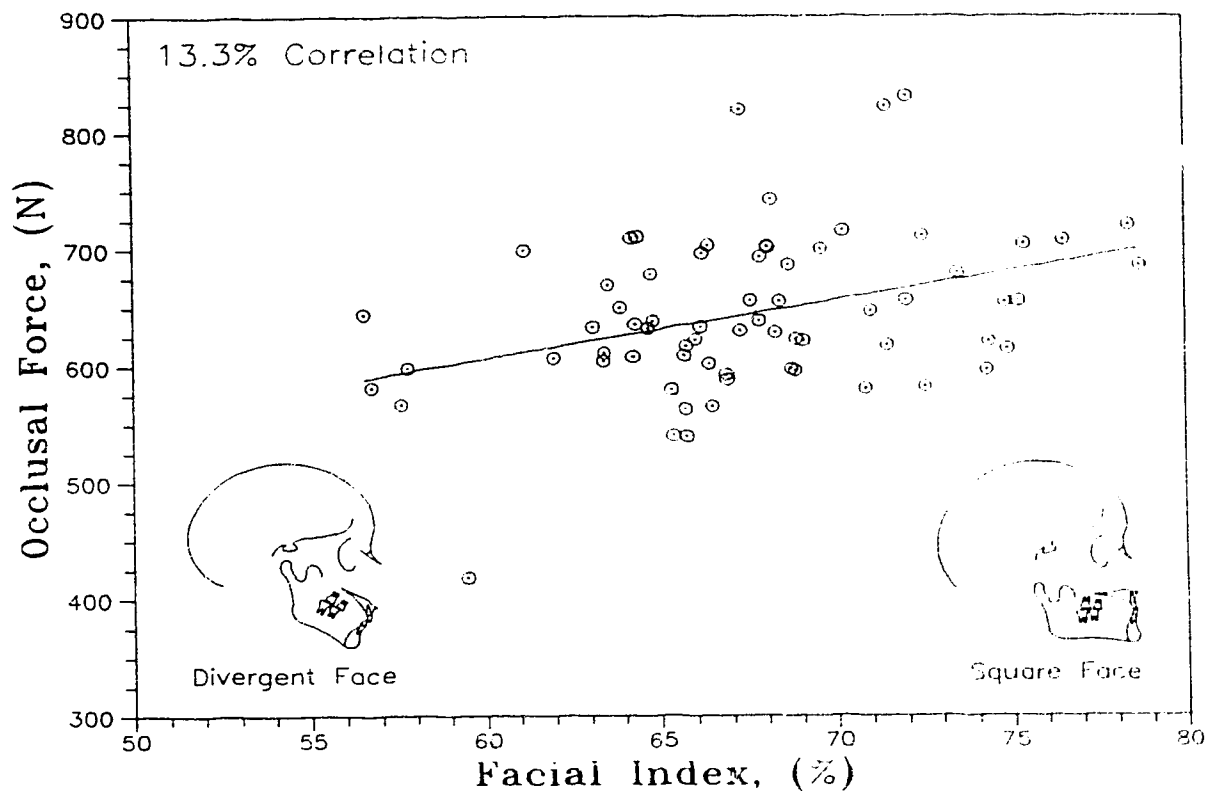
Figure 4.1 Linear Correlation of Facial Index and the Resultant Occlusal Force from the Pragmatic Model (sample size = 68)

The inclusion of the FLR for each skull, was motivated by the belief that there would be a mechanical relevance to the length of an individual's facial structures. The bottom row of Table 4.1 indicates that an FLR of 83.4% is predicted to have the best aligned loading configuration of the ipsilateral TMJ.

Using the Gonial angle as a basis for characterizing morphology proved futile since it showed virtually no correlation to the predictions of the pragmatic model. There was no R^2 over 4.0% strongly suggesting that these are independent variables. It was speculated earlier that FI and Gonial angle would give similar results since they

correlated well together with each other ($R^2=42.3\%$) but this was not the case. There were slight trends in the linear approximations indicating that lower TMJ loads and higher bite loads would be achieved on people with smaller gonial angles.

The Ao-Bo distance correlated best with the occlusal load generated by the model and showed trends that opposed the **ANB** angle results. As the **Ao-Bo** distance increases, lower joint loads and higher bite forces are predicted. These trends, which are opposite to those using **ANB**, can be rationalized by the fact that neither correlation is very strong.

The reference plane angles **F-O** and **F-M** did not correlate with each other very well ($R^2=0.6\%$) but did show similarities to the results from the pragmatic model. When the angles were compared to the occlusal force, correlation coefficients of 9.5% and 12.8% for F-O and F-M were attained respectively; however, they showed opposite trends. The analysis showed the TMJ loads increasing and the bite load decreasing as the F-M angle opens. The F-O angle was an even poorer measure indicating again that using the occlusal plane as a landmark plane can lead to difficulties.

The mandibular triangle showed the best results overall because 12 out of the 24 correlations gave R^2 values of greater than 5.0%. The normalized values, S/Per, A/Per, P/Per, Ω, ß, and Θ, from an averaged (right and left) mandibular triangle were also correlated with the results from the pragmatic model. The highest linearity was achieved with S/Per, P/Per, and Θ having R^2 values of 28.5%, 24.0%, and 28.6% respectively.

These were attained when correlated to the ipsilateral TMJ load.   Figure 4.2 shows an

example of the relatively high level of linearity obtained with these correlations.   With
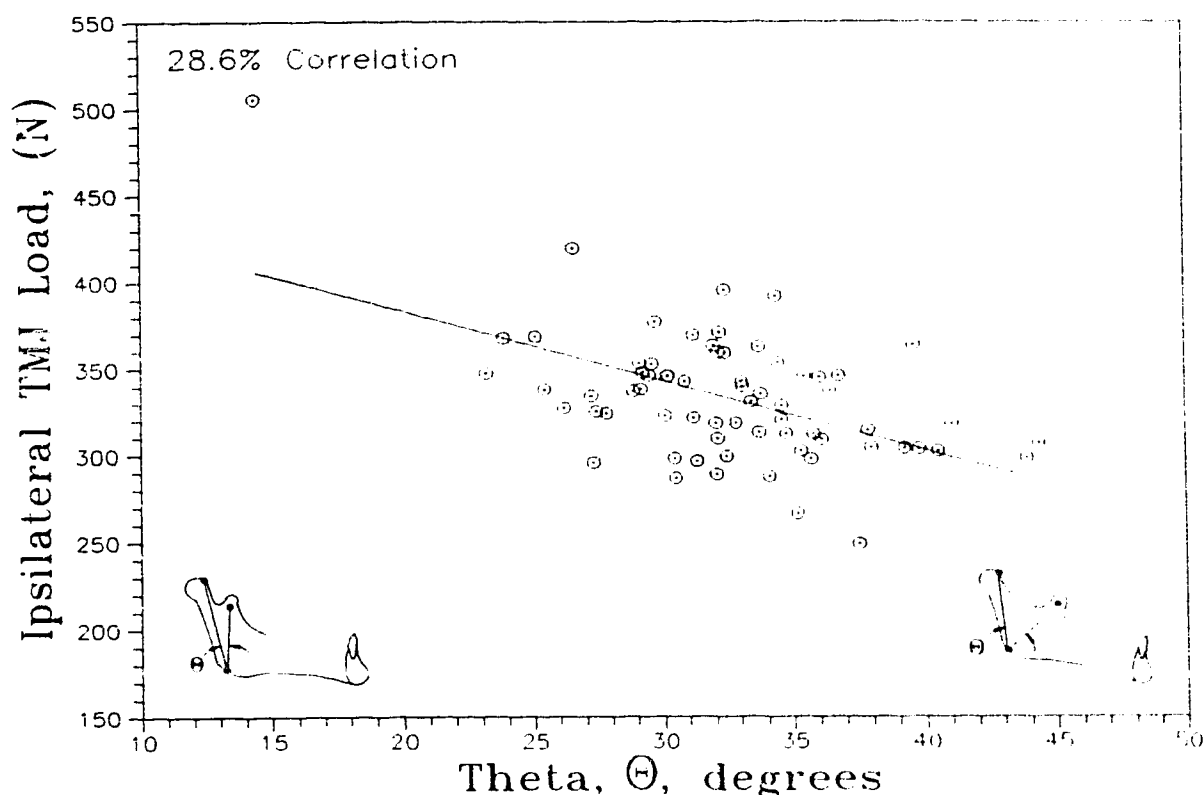
Figure 4.2 Linear Correlation of Theta, Θ, and the Resultant Ipsilateral TMJ Load from the Pragmatic Model (sample size = 68)

28.6% of the variations in ipsilateral load explained by corresponding differences among

Θ it r_n be seen that for a mandible with a small Θ greater ipsilateral loads are realized

indicating that Θ best describes this TMJ loading parameter.   In contrast, jaws with a

large Θ exhibit lower ipsilateral joint loads.   A similar result is also seen by the

comparison with the superior side of the triangle.   As the distance between the condyle

and the coronoid process closes, higher loads are predicted for the working side. Unfortunately, this correlation does not carry over to the balancing side. The correlation with the contralateral load shows more effect when compared to by the posterior side of the triangle ($R^2 = 5.6\%$). Higher TMJ loads and lower bite forces are generated for skulls with larger posterior mandibular heights.

The mandibular triangle does give slightly better results than the other indices but is harder to visualize than, for example, the ANB angle. In summary however, correlations of the pragmatic model predictions with various facial type descriptors are poor. Slight trends do indicate that squarer faced individuals with long protrusive chins are able to generate higher occlusal forces with subsequent lower temporomandibular joint loads. These general findings are seen for the ANB angle, FI, FLR, Gonial angle, and F-O angle investigations.

4.2.2 Linear Programming Model Correlations

Each linear program investigated gave similar results, hence the correlations between these models and the facial classification schemes can be simplified. By allowing all the muscles to saturate, as did each of the linear models, maximum joint and occlusal forces for each skull can be correlated to these differing facial types.

Table 4.2 shows, as did Table 4.1, poor correlations are present for all the combinations. Thirty-four of the 52 correlations gave less than 5% correlation and only one of the 13 predictions for zero shear were within the range of values investigated.

Table 4.2 The Products of Correlation[a] between Facial Classification Schemes and Results from the Linear Programming Models (Rows 1-4) with the Facial Classification Predictions for Zero Shear on the TMJ (Row 5) Shaded values represent R^2 values < 5% (Rows 1-4) and Values out of the range investigated (Row 5)

	ANB	FI	FLR	Gonial	Ao-Bo	F-O	F-M	S/Per	P/Per	A/Per	Ω	β	θ
Ipsilateral Load	+0.0	+0.8	-10.7	-4.6	+0.3	-0.0	-1.1	-15.6	+10.2	+6.2	-0.1	+7.5	-14.2
Contralateral Load	+3.2	+0.4	-0.1	-0.5	-0.2	-0.9	-0.2	-0.9	+3.9	-0.1	-2.8	+5.0	-0.9
Occlusal Load	-0.4	+13.4	+0.4	-3.1	+6.6	+8.9	-13.1	+7.2	-6.3	-2.1	+0.3	-5.4	+7.4
Ipsilateral Misalignment	+7.0	-3.4	+6.5	+3.1	-1.3	+0.0	-6.1	-1.9	+0.0	+2.6	+2.2	-0.3	-1.6
Zero-shear Prediction	23.4	33.8	129	172	-49.8	175	51	-1.38	227	54	127	95.3	-14.86

Legend:

ANB — E.H. Angle's ANB Angle (SNA - SNB)
FI — Facial Index (Facial Height Ratio)
FLR — Facial Length Ratio
Gonial — Gonial Angle
Ao-Bo — Wit's Appraisal (Occlusal Plane distance)
F-O — Angle between Frankfort Horizontal and Occlusal Plane
F-M — Angle between Frankfort Horizontal and Mandibular Plane

S/Per — Superior Length / Perimeter
P/Per — Posterior Length / Perimeter
A/Per — Anterior Length / Perimeter
Ω — Omega (Angle between Sup. and Post. Sides)
β — Beta (Angle between Sup. and Ant. Sides)
θ — Theta (Angle between Post. and Ant. Sides)

[a] R^2 values given in percentage

Although nearly all the products of correlation are halved from the pragmatic model's, similar trends are seen. Squarer faced individuals with long chins are able to generate higher occlusal forces with subsequent lower temporomandibular joint loads. These results are seen with **ANB**, **FI**, **Ao-Bo**, and **F-M** classifications. The mandibular triangle indicates that as the triangle gets narrower and taller, lower TMJ loads are seen while at the same time being able to generate larger occlusal forces.

Both type of models presented gave poor correlations while investigating significance of facial morphology. The pragmatic model demonstrated a slightly higher correlation than the linear programming models but both showed similar trends. The mandibular triangle showed that tall narrow triangles exhibit low TMJ loads and high bite force capabilities. Many of the other classifications showed that square faces (laterally) and long chins could bite harder while simultaneously yielding lower TMJ loads. It is important to realize, however, that the majority of these correlations are poor.

CONCLUSIONS AND FUTURE
RESEARCH CONSIDERATIONS

5.1   Final Discussion

Three major topics were studied during the course of this thesis. The first looked at various facial classifications and tested the independence of each. Current numerical models of the TMJ were compared using three dimensional data from one skull to isolate the characteristics of each model. These two themes were joined in Chapter 4 when an attempt was made to discern any possible relationships between facial morphology and TMJ loads.

Thirteen different types of facial classifications were compared with each other using data collected from 68 skulls to test the dependence of each method. Many of these were standard clinical techniques used in orthodontics. In contrast, the mandibular triangle approached the problem of morphological classification from a mechanical viewpoint. An inherent problem with the mandibular triangle is that the type of morphologies it characterizes is not as easily seen as with the ANB and F-O angles.

A large number of poor correlations were seen. The worst case being that of the Frankfort-Occlusal Plane angle. This trend indicates that the dentition can be considered essentially independent of all other facial classifications. The mandibular triangle showed independence from the other techniques since its correlations were poor when compared to the other more familiar techniques. In contrast, the **ANB** angle correlated well with the **Ao-Bo** distance (Wit's Appraisal). This was not surprising since both clinically measure jaw dysplasia. Another good relationship was that of the **FI** and **F-M** angle. Apparently, both indicate the amount of lateral facial squareness of an individual.

Chapter 3 compared various types of numerical modelling procedures recently used to investigate the loading characteristics of the TMJ. One skull was used with a single bite scenario to isolate the characteristics of each model. This comparison gave two major types of results. The linear programs allowed the all muscles to fully saturate at maximum bite force (one result for all these models) while the pragmatic model used predefined ratios for the muscular activations and hence gave different results. Because the joint loading directions or magnitudes were not constrained, it allowed the muscles to fully saturate in the case of the linear programs. The results obtained from these major types of models did correlate with previous studies in as much as they yielded similar muscle recruitment patterns. The contralateral TMJ load was found to be higher than the ipsilateral load in most of the skulls. The linear programs gave abnormally high contralateral loads, even enough to break a condyle. For this reason, it is believed that total muscle saturation in these models is an unlikely scenario. Present constraint

techniques are inadequate in characterizing the TMJ loads. Linear programs allowing muscular freedom will lead to identical solutions.

In an attempt to find individuals potentially at the risk of abnormal TMJ loadings, a correlation between various facial classifications and numerical models was done. The resulting correlation was inadequate since the majority of the present classifications were unable to predict which facial groups were at risk. The results showed that the new mandibular triangle classification could predict the loading of the mandible slightly better than the classical measurements. Characterizing facial morphology based solely on the mandible makes mechanical sense but can be more difficult to visualize than the more commonly used methods (eg. ANB and FI).

Slight trends did indicate, however, that square faces (visualized laterally) and longer chinned individuals are able to bite harder while at the same time inducing lower loads of the temporomandibular joint. Mandibles with tall and thin mandibular triangles tend to exhibit these same traits.

5.2   Areas for Further Development

An attempt was made to formulate a new facial classification on a mechanical basis. Since mastication is a mechanical function, more work must be done from this viewpoint to isolate the population that may be susceptible to abnormal TMJ loading. Data from the maxillary region coupled with the mandibular triangle may lead to a more accurate means of predicting facial deficiencies concerning TMJ loading.

The ideal model of the jaw would be one that could accurately predict the muscle activation levels. Investigating the macroscopic electrical response of the muscles of mastication would give a more realistic representation of the muscle tensions and their respective attachment points. Once achieved, an objective function other than the ones chosen for this investigation must be able to predict the muscle tensions on a macroscopic scale. This function would allow the model more adaptability and versatility. With continued use of numerical modelling, recent biological data provides the link between the physical and mathematical systems. There is a need for more data on material properties and limitations of various body tissues and more experimental research to develop techniques for validating many of these models. Perhaps using a combination of linear and nonlinear programming, a compromise between the muscle activations and joint loads can be met.

A statistical method must be standardized to analyze these biological studies. Only linear correlations were attempted in this investigation due to the lack of other justified methods.

LITERATURE SEARCH OF
TMJ PHYSIOLOGY AND MODELLING

An, K.N.; Kwak, B.M.; Chao, E.Y.; Morrey, B.F. *"Determination of Muscle and Joint Forces: A New Technique to Solve the Indeterminate Problem"* JOURNAL OF BIOMECHANICAL ENGINEERING Vol. 106(1984):pp. 364-367

Barbenel, J.C. *"The Biomechanics of the Temporomandibular Joint: a Theoretical Study"* JOURNAL OF BIOMECHANICS Vol. 5(1972):pp. 251-256

Barbenel, J.C. *"The Mechanics of the Temporomandibular Joint: a Theoretical and Electromyographical Study"* JOURNAL OF ORAL REHABILITATION Vol. 1(1974):pp. 19-27

Blaustein D.I.; Scapino R.P. *"Remodelling of the Temporomandibular Joint Disk and Posterior Attachment in Disc Displacement Specimens in Relation to Glycosaminoglycan Content"* PLASTIC AND RECONSTRUCTIVE SURGERY Vol. 78(1986):pp. 756-764

Carlsöö, S. *"Nervous Coordination and Mechanical Function of the Mandibular Elevators"* ACTA ODONTOL SCAND. Vol. 10(1952):Suppl. 11

Charnley, J. *"The lubrication of animal joints"* PROCEEDINGS OF A SYMPOSIUM ON BIOMECHANICS Institution of Mechanical Engineers, London, (1959)

Faulkner, M.G.; Hatcher, D.C.; Hay, A.S. *"A Three-Dimensional Investigation of Temporomandibular Joint Loading"* JOURNAL OF BIOMECHANICS Vol. 20(1987):pp. 997-1002

Gingerich, P. *"The Human Mandible: Lever, Link, or Both?"* AMERICAN JOURNAL OF PHYSICAL ANTHROPOLOGY Vol. 51(1979):pp. 135-138

Grant, P. *"Biomechanical Significance of the Instantaneous Center of Rotation: The Human Temporomandibular Joint"* JOURNAL OF BIOMECHANICS Vol. 6(1973):pp. 109-113

Gysi, A. *"Studies on the Leverage Problems of the Mandible"* THE DENTAL DIGEST Vol. 27(1921):pp. 74-84, 144-150, 203-208

Hansson, T.; Milner, M.; *"A study of the occurrence of symptoms of diseases of the temporomandibular joint, masticatory musculature, and related structures"* JOURNAL OF ORAL REHABILITATION 2(1975): pp. 313-324

Hay, A.S. *"A Mechanical Analysis of the Temporomandibular Joint"* M.Sc. Thesis, University of Alberta, 1985

Hylander, W. *"The Human Mandible: Lever or Link"* AMERICAN JOURNAL OF PHYSICAL ANTHROPOLOGY Vol. 43(1975): pp. 227-242

Hylander, W. *"An Experimental Analysis of Temporomandibular Joint Reaction Force in Macaques"* AMERICAN JOURNAL OF PHYSICAL ANTHROPOLOGY Vol. 51(1979): pp 433-456

Hylander, W. *"Mandibular Function and Temporomandibular Joint Loading"* TEMPOROMANDIBULAR JOINT DISORDERS, MONO. , Center for Human Growth and Development, University of Michigan, (1985)

Iwasaki, L.R. *"A Three Dimensional Analysis of Isometric Biting in Long and Short Facial Types"* M.Sc. Thesis, University of Manitoba, 1987

Jacobson, A. *"The 'Wits' appraisal of jaw disharmony"* AMERICAN JOURNAL OF ORTHODONTICS Vol. 67(1975):pp. 125

Kang, Q. *"Biomechanics of the Human Temporomandibular Joint"* Ph. D. Thesis, Lehigh University, (1989)

Kawazoe, Y.; Kotani, H.; Hamada, T. *"Relation Between Integrated Electromyographic Activity and Biting Force During Voluntary Isometric Contraction in Human Masticatory Muscles"* JOURNAL OF DENTAL RESEARCH Vol. 58(1979):pp. 1440-1449

Koolstra, J.H.; Van Eijden, T.M.G.J. Weijs, W.A.; Naeije, M.; *A Three Dimensional Mathematical Model of the Human Masticatory System Predicting Maximum Possible Bite Forces"* JOURNAL OF BIOMECHANICS Vol. 21(1988): pp. 563-576

McEvoy, S.P. *"Effects of Facial Morphology on TMJ Loading"* M.Sc. Thesis, University of Alberta, 1989

McNamara, J. Jr. *"The Independent Functions of the Two Heads of the Lateral Pterygoid Muscle"* AMERICAN JOURNAL OF ANATOMY Vol. 138(1970):pp. 197-206

Møller, E. *"Computer Analysis of Electromyographic Data in Clinical Studies of Oral Function"* SCAND. JOURNAL OF DENTAL RESEARCH Vol. 78(1970):pp. 411-416

Morris, A.H. *"Linear Programming Simplex Algorithm"* NAVAL SERVICE WARFARE CENTER (NSWC) LIBRARY OF MATHEMATIC SUBROUTINES, (1990)

Mushimoto, E.; Mitani, H. *"Bilateral Coordination Pattern of Masticatory Muscle Activities During Chewing in Normal Subjects"* THE JOURNAL OF PROSTHETIC DENTISTRY Vol. 48(1982):pp. 191-197

Nickel, J.C.; McLachlan, K.R.; Smith, D.M. *"Eminence Development of the Postnatal Human Temporomandibular Joint"* JOURNAL OF DENTAL RESEARCH Vol. 67(1988):pp. 896-902

Ogus, H. *"Degenerative Disease of the Temporomandibular Joint in Young Persons"* BRITISH JOURNAL OF ORAL SURGERY Vol. 17(1979):pp. 17-26

Osborn, J.W.; Baragar, F.A. *".Predicted Pattern of Human Muscle Activity During Clenching Derived from a Computer Assisted Model: Symmetric Vertical Bite Forces"* JOURNAL OF BIOMECHANICS Vol. 18(1985):pp. 599-612

Pruim, G.J.; De Jongh, H.J.; Ten Bosch, J.J. *"Jaw Muscle EMG-Activity and Static Loading of the Mandible"* JOURNAL OF BIOMECHANICS Vol. 11(1978):pp. 389-395

Pruim, G.J.; De Jongh, H.J.; Ten Bosch, J.J. *"Forces Acting on the Mandible During Bilateral Static Bite at Different Bite Force Levels"* JOURNAL OF BIOMECHANICS Vol. 13(1980):pp. 755-763

Ralph, J.; Caputo, A. "Analysis of Stress Patterns in the Human Mandible" JOURNAL OF DENTAL RESEARCH Vol. 54(1975):pp. 814-821

...si, T. "Anterior and Posterior Face Height" AN ATLAS AND MANUAL OF CEPHALOMETRIC RADIOGRAPHY (1982) Sect. 2.12:pp. 65

Riedel, R.A. "The relation of maxillary structures to cranium in malocclusion and in normal occlusion" JOURNAL OF ANGLE ORTHODONTICS Vol. 22(1952):pp. 142-145

Robinson, M. "The Temporomandibular Joint: Theory of Reflex Controlled Non-Lever Action of the Mandible" JOURNAL OF AMERICAN DENTAL ASSOCIATION Vol. 33(1946):pp. 1260-1271

Scapino, R.P. "Histopathology associated with malposition of the human temporomandibular joint disc" JOURNAL OF ORAL SURGERY Vol. 55(1983):pp. 382-397

Schumacher, G.H. "Funktionelle Morphologie der Kaumuskulatur" VEB GUSTAV FISCHER VERLAG. JENA, (1961)

Smith D.M.; McLachlan K.R., McCall W.D. Jr. "A Numerical Model of Temporomandibular Joint Loading" JOURNAL OF DENTAL RESEARCH Vol. 65(1986):pp. 1046-1053

Smith R. J. "Mandibular Biomechanics and Temporomandibular Joint Function in Primates" AMERICAN JOURNAL OF PHYSICAL ANTHROPOLOGY Vol. 49(1978):pp. 341-350

Standlee, J.; Caputo, A.; Ralph, J. "The Condyle as a Stress-Distributing Component of the Temporomandibular Joint" JOURNAL OF ORAL REHABILITATION Vol. 8(1981):pp. 391-400

Tattersall, I. "Cranial Anatomy of Archaeolemurinae (Lemuroidea Primates)" ANTHROP. PAP. AMER. MUS. NAT. HIST. Vol. 52(1973):pp. 1-110

Throckmorton, G.S.; Throckmorton, L.S. "Quantitative Calculations of Temporomandibular Joint Reaction Forces - 1. The Importance of the Magnitude of the Jaw Muscle Forces" JOURNAL OF BIOMECHANICS Vol. 18(1985[1]):pp. 445-452

Throckmorton, G.S.; Throckmorton, L.S. *"Quantitative Calculations of Temporomandibular Joint Reaction Forces - II. The Importance of the Direction of the Jaw Muscle Forces"* JOURNAL OF BIOMECHANICS Vol. 18(1985^2):pp. 453-461

Van Eijden, T.M.G.J.; Brugman, P.; Weijs, W.A.; Oosting, J.; *"Coactivation of Jaw Muscle Recruitment Order and Level as a Function of Bite Force Direction and Magnitude"* JOURNAL OF BIOMECHANICS Vol. 23(1990):pp. 475-485

Wilson, G. *"The Anatomy and Physics of the Temporomandibular Joint"* JOURNAL OF THE NATIONAL DENTAL ASSOCIATION Vol. 7(1920):pp. 414-420

GRAPHICAL INTERPRETATION OF LINEAR PROGRAMMING

A.1 Introduction

A simple linear problem is presented to show by example how constraints and optimizing functions beh‿ve.

A.2 Problem 1

Consider the problem of baking cookies to generate weekly revenue. There are two types of cookies for which you have the major ingredients. Consider Table A.1 which introduces two types of cookies which have been shown in the past to sell quite easily.

Table A.1 Cookie Samples

Batch	Raisins	Chocolate Chips	Baking Time	Selling Price
A	3 kg	2 kg	40 minutes	$12
B	1 kg	3 kg	30 minutes	$10

Due to the spoiling of raisins you must use at least 60 kg a week. While the raisin supply is unlimited, the chocolate chip stock is restricted to 120 kg per week.

If the selling price is \$12 per batch of type A and only \$10 of type B, how many batches of each would you bake to make the most money?

Solution

Let A be the number of batches of type A required and B be the number of B batches. We want to optimize the total income during one week of operation. The optimizing function would look like

$$f = 12A + 10B = \text{Income} , \qquad \text{A.1}$$

since we want to maximize total revenue in one week.

The raisin constraint would be

$$3A + 1B \geq 60 , \qquad \text{A.2}$$

since 3 kg. of raisins are used in batch A and only one is required for batch B but their sum must be greater or equal to 60 kg. to prevent spoiling. Figure A.1 illustrates the region of two dimensional space that this constraint includes.
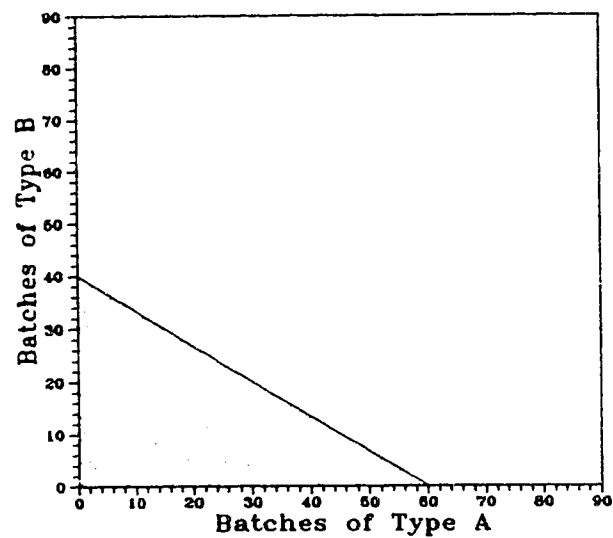
The chocolate chip constraint is

$$2A + 3B \leq 120 . \qquad \text{A.3}$$

This stock is limited to 120 kg and must be less than or equal to this value. Figure A.2 shows how this constraint limits the 2D plane.

Time is another constraint that must be taken into consideration. Since there are 2400 minutes in a work week and to bake cookies it takes 40 and 30 minutes respectively
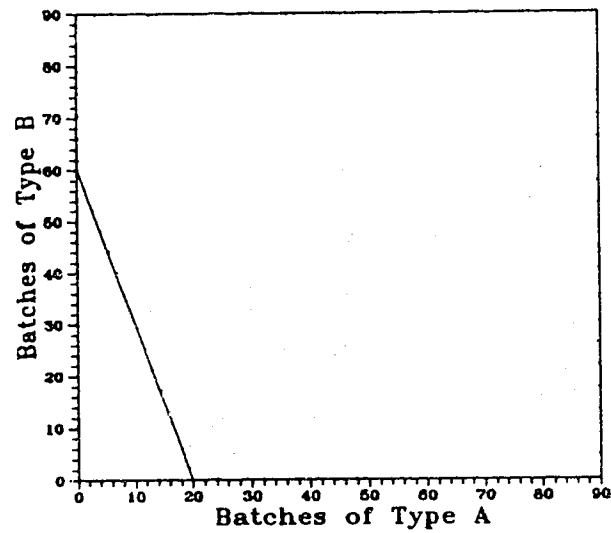
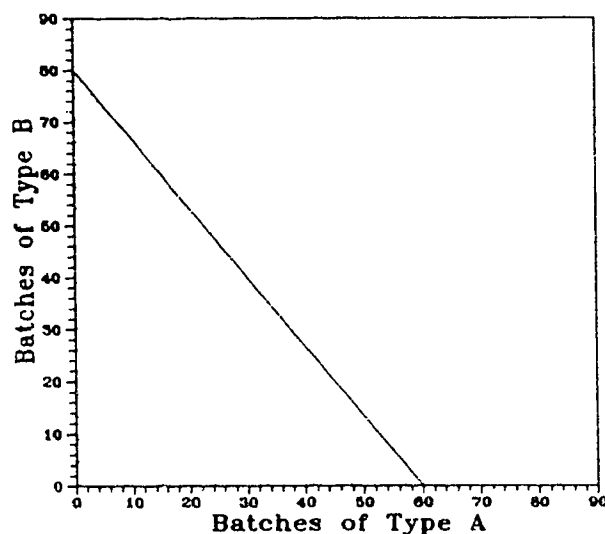**Figure A.1** Raisin Constraint

Figure A.2 Chocolate Chip Constraint

to bake a batch of A and B type cookies, the time constraint equation would look like

$$40A + 30B \leq 2400 .$$
<div align="right">A.4</div>

One week would isolate the shaded area shown in Figure A.3.

Figure A.3 Time Constraint

The number of batches must be greater or equal to zero since both variables represent physical quantities. These additional constraints are Equations A.5 and A.6. Only the first quadrant is drawn for this reason.

$$A \geq 0 .$$
<div align="right">A.5</div>
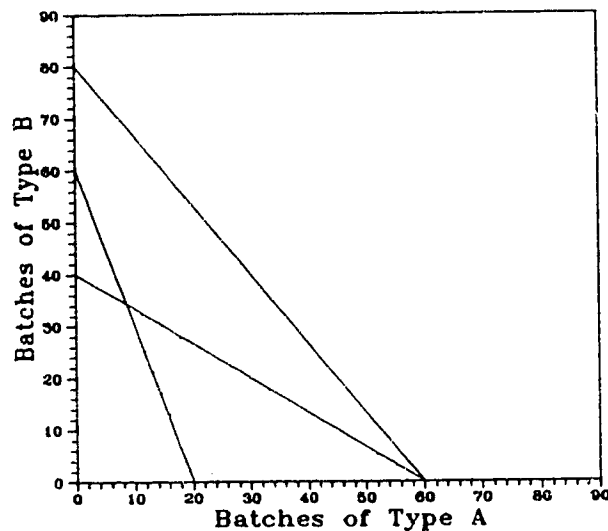
$$B \geq 0 .$$
<div align="right">A.6</div>

Figures A.1 through A.3 illustrate that each constraint confines an area in the 2D plane. The overlapping of these regions, demonstrated in Figure A.4, exposes the range of plausible values. The region is described by a triangle with the corners at

(20,0),(60,0), and the intercept (8.57,34.29). The optimum value, maximum income for one week of operation, will be in this region.

Figure A.4 Area Enclosed by Constraints

As lines of constant profit are swept across the triangle in Figure A.5 it is easily found that the coordinate (60,0) is the point of maximum revenue. Baking 60 batches of Type A cookie and not baking *any* Type B cookies would generate the most weekly income. This would be $720 with the chocolate chip stock and time being exhausted.
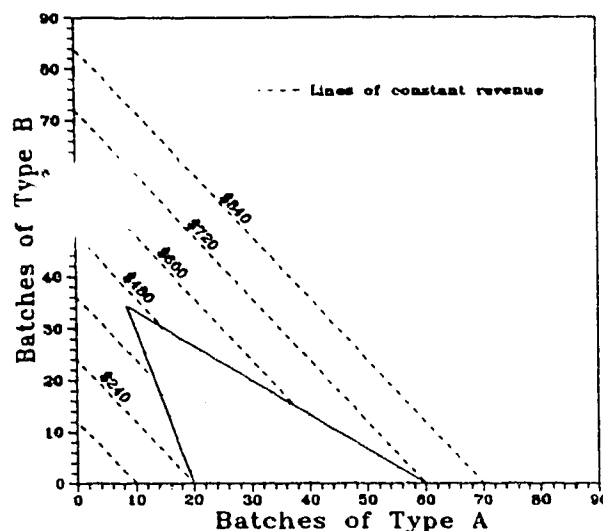
Figure A.5 Income lines

A.3   Problem 2

Let's now change the problem to show how a constraint would affect the problem. Suppose that we are going to dedicate three quarters of the week to cookie baking and the remainder baking cakes. How can we generate the most cookie income in this time interval?
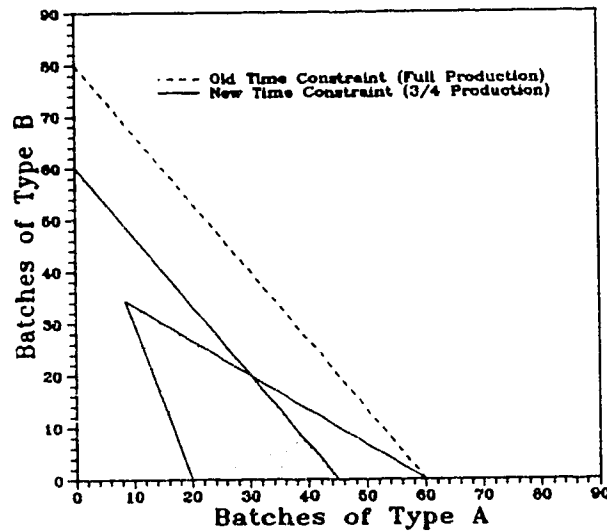
Solution

Only the time constraint would change. We no longer have 2400 minutes to bake cookies, rather we only would like to use 1800 minutes on cookie baking and the remaining 600 minutes on baking cakes. The other constraints would be unchanged since the prices and stock system are identical to the original problem. The new time constraint would look like

$$40A + 30B \leq 1800 \ .$$

Figure A.6 shows the shifting effect of the new constraint. This line translates

Figure A.6 Time constraint shifting

towards the origin reducing the feasible area for a solution.

A new optimal point is achieved if the lines of constant revenue are again swept across the polygon created by the constraints. The intersection point, (30,20), shown in Figure A.7 represents that if 30 batches of Type A cookie and 20 batches of Type B cookie are baked a total of $560 can be made in 1800 minutes of baking time. The ingredients are not the limiting factor, rather, time prevents the accumulation of more revenue.
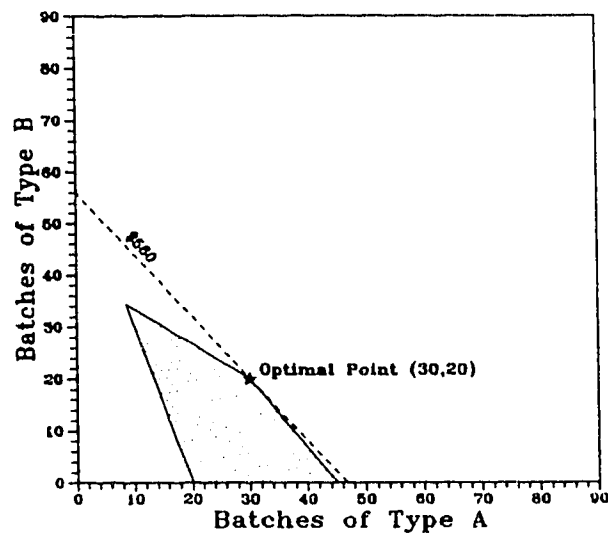
Figure A.7 New Optimal Operating
Point for 75% cookie baking minutes

A.4   Summary

This linear programming example illustrated a simple graphical analysis used in

problems with only two variables. It was shown how constraints limit the plausible range

for a solution. If the constraint changes, the line will move to its new location possibly

reducing the effective solution area. This was displayed by this small cookie baking

company for two different time periods.The objective function was shown to sweep lines

of constant revenue across the plane. This function could be maximized by choosing the

correct income potential.

MUSCLE DATA DERIVATION FOR LINEAR PROGRAMMING MODELS

B.1   Introduction

G.J. Pruim et al. [1980] used seven male subjects to predict the maximum possible muscle tensions during forceful bilateral occlusion. A two dimensional model originating from a symmetric three dimensional system was used to find the muscle forces given muscle EMG data and measured bite forces. A significant portion of the muscle data used in this study is derived from Pruim's data. Some of Pruim's work refers to the Schumacher [1961] investigation.

B.2   Muscle Force Prediction

The subject's bite force was measured at three locations, the first premolar and first and second molars, by two steel wedge transducers used previously by Pruim [1978]. Simultaneous measurement of integrated EMG data was obtained at the superficial masseter, anterior and posterior temporalis, and the opening muscles with four pair of surface electrodes. Using these measured results and predicted physiological muscle areas from Schumacher [1961], Pruim found that it was possible to determine a

relationship between the integrated EMG data and muscle force with the two dimensional static model of the TMJ.

The model required spatial data of the subjects which was obtained from lateral and frontal cephalogram. Once the origin and insert of each muscle or muscle group could be determined, the mandible could be loaded. The bite force, which is known, would act as the force initiator while the muscles and condylar reactions would balance this. Pruim's major results for muscle areas chosen and predicted muscle tensions are shown below in Table B.1. Also shown is the muscular stress which was calculated by dividing the muscle tension by its corresponding area. These results will be used later in this appendix.

Table B.1 Muscular Data from Pruim's Investigation

Muscle Group	Physiological Crossectional Area (cm²)	Maximum Average Muscle Tension (N)	Muscular Stress σ (MPa)
Masseter / Medial Pterygoid	5.3	639.5	1.208
Anterior Temporalis	2.6	362.0	1.392
Posterior Temporalis	1.6	197.5	1.238
Digastric (Opening)	1.0	115.0	1.150
Lateral Pterygoid	2.1	378.5	1.805

Seven male subjects were used to determine the average maximum possible muscle force in each of the above muscle groups.

B.3 Present Muscle Data

The model chosen for the present investigation does not have the same muscular divisions as chosen by Pruim. It is for this reason that the following separation of the muscle groups was done. To approximate the biological system of the TMJ, it was suggested that the muscle groups be broken into smaller more independent components to allow the models more flexibility and versatility.

The masseter/medial pterygoid sling used in Pruim's analysis was separated. Schumacher's original data that was conglomerated for Pruim's model was segregated into their original values. The masseter muscle is usually described as two portions, deep and superficial. Due to the nature of integrated EMG sampling, it is unlikely that accurate readings for each of the two masseters was achieved or even possible. From Faulkner et al. [1986], the Type I muscle data that used only ratios of muscle areas to predict muscle force was used to divide the masseter. A ratio of 1.34 (10.3 / 7.7), for the deep to superficial masseter areas would be used to separate this muscle group. Its muscular stress, 1.208 Mpa, is assumed to be the same. The largest muscle, the temporalis, was divided into three portions creating a middle temporalis. To do this, one third of each of the anterior and posterior temporalis muscles were added together to generate the third portion, termed the middle following McEvoy [1989]. The muscular stress, dissimilar for both anterior and posterior components, was taken as an average of these two values to estimate the stress in the middle temporalis.

The following table, Table B.2, presents the muscular data used in this thesis. The muscular stress was used to determine the maximum possible muscle tensions in the new muscle groupings and are used in each of the linear programming models. They provide biological barriers which mathematically prevents overloading of the muscles. They also furnish a realistic influence which each model must have if it is to mimic th actual system.

The *inferior* belly of the lateral pterygoid muscle is active during clenching while the superior portion is active only upon opening of the mouth [McNamara, 1970]. An area distinction between these heads of the lateral pterygoid was done by Schumacher [1961]. 16 adult cadavers were investigated to determine their physiological crossectional areas. The average area of the lateral pterygoid muscle was 1.525 cm^2; 0.37 cm^2 and 1.155 cm^2 for the superior and inferior bellies respectively. Using Pruim's more recent data for muscle areas and Schumacher's ratio of a new area was determined for only the inferior head of the lateral pterygoid.

Table B.2 Revised Muscle Group Data

Muscle Group	Physiological Crossectional Area (cm^2)	Maximum Stress σ_{max} (Mpa)	Maximum Force $F_{saturation}$ (N)
Deep Masseter	1.950	1.208	235.56
Superficial Masseter	1.450	1.208	175.16
Medial Pterygoid	1.900	1.208	229.52
Anterior Temporalis	1.733	1.392	241.23
Middle Temporalis	1.400	1.315	184.10
Posterior Temporalis	1.067	1.238	132.09
Lateral Pterygoid	1.590	1.805	287.00